NATIONAL ADVISORY COMMITTEE FOR AERONAUTICS

TECHNICAL NOTE 2357

METHOD FOR CALCULATION OF RAM-JET PERFORMANCE

By John R. Henry and J. Buel Bennett

Langley Aeronautical Laboratory
Langley Field, Va.

Washington
June 1951

NATIONAL ADVISORY COMMITTEE FOR AERONAUTICS

TECHNICAL NOTE 2357

METHOD FOR CALCULATION OF RAM-JET PERFORMANCE

By John R. Henry and J. Buel Bennett

SUMMARY

A method utilizing precalculated solutions graphically presented for calculating subsonic or supersonic ram-jet performance parameters is presented with the associated equations and graphs. By assuming constant values of specific-heat ratio and gas constant equal to those of standard air, the thrust-coefficient calculation has been reduced to a few simple operations. Correction methods are presented to account for variations in specific-heat ratio and gas constant. The correction to the thrust coefficient for a typical set of operating conditions may be of the order of 5 to 10 percent.

INTRODUCTION

A convenient index to ram-jet engine performance is the thrust coefficient, which is defined as the thrust force per unit flight dynamic pressure per unit reference cross-sectional area. For a given set of operating conditions, the thrust coefficient can be compared with the drag coefficient to determine whether the propelled body will accelerate, decelerate, or maintain a constant flight speed. The thrust coefficient also provides the engine designer or research worker with a useful performance indicator which, to a certain extent, can be considered without regard to the propelled-body configuration. For given engine performance, flight conditions, and fuel properties, the maximum theoretical thrust coefficient can be calculated and compared with the actual value. From this comparison, the shortcomings of the engine can be determined and the direction of further developmental work fixed.

The flight-thrust-coefficient calculation from performance data, from estimates for the individual components of the engine, or from performance data taken in directly connected duct tests can be most laborious and time consuming, the amount of labor depending on the amount of accuracy attempted and the methods used. Extremely high accuracy is difficult to obtain conveniently because of the problems

involved in treating three-dimensional flows, the trial and error processes and assumptions used in determining the change in gas properties with temperature and chemical reactions, and the general lack of precise data on the performances of the ram-jet engine components; however, thrust-coefficient calculations based on one-dimensional theory and frequently on standard values of specific heats and gas constant are sufficiently accurate for most purposes. The error introduced by assuming one-dimensional flow will vary according to the ram-jet design; for example, most ram-jet burners produce transverse temperature variations in the combustion zone that produce deviations from one-dimensional flow.

Through use of the momentum equation, the general energy equation, the continuity equation, the simple gas law, and the one-dimensional theory, it is possible to estimate the conditions at each station in the ram jet for a given flight condition, intake diffuser efficiency, combustion-chamber performance, and exhaust-nozzle efficiency. The obvious calculating procedure is to start at the diffuser inlet and make a station-to-station analysis leading up to the determination of the exhaust-nozzle exit velocity and the gas mass flow. When these quantities are known, the thrust coefficient can be determined directly. An example of this type of calculation which has been appreciably simplified by the use of graphical solutions is presented in reference 1.

The previously outlined procedure can be appreciably shortened by eliminating all intermediate steps and proceeding directly from values of basic variables to the thrust coefficient. Expressing the thrust coefficient in terms of basic variables leads to an unwieldy equation; however, grouping variables and making use of precalculated solutions graphically presented reduces the calculation to a few simple operations. The purpose of this paper is to present such a calculation method, as well as graphical solutions, algebraic derivations, and associated equations for the determination of other significant quantities.

The calculations are presented as charts covering variable ranges of flight Mach numbers from 0 to 4.0, combustion-chamber inlet Mach number from 0 to 0.5, combustion-chamber temperature rise extending somewhat beyond that obtainable with gasoline and air mixtures, and all possible values of diffuser total-pressure-recovery ratio and combustion-chamber and exhaust-nozzle total-pressure ratio. Combustion-chamber inlet Mach number was limited to 0.5 because higher values do not appear practical with a ram-jet combustion chamber where the flow is confined, since at this value an appreciable total-temperature rise will cause thermal choking.

SYMBOLS

a	speed of sound
A	area, square feet
C_{F_I}	thrust coefficient
$C_{F_{II}}$	internal-force coefficient
$\bar{c}_p$	arithmetic average of specific heats at constant pressure corresponding to static and total temperatures
D_e	external drag, pounds
f	fuel-air ratio
F	force, pounds
g	standard acceleration due to gravity, feet per second per second
I	specific impulse, seconds
J	mechanical equivalent of heat
K	friction coefficient
M	Mach number
p	absolute static pressure, pounds per square foot
p_t	absolute total pressure, pounds per square foot
q	dynamic pressure; one-half momentum flux per unit area, pounds per square foot
R	universal gas constant, foot-pounds per pound per ^oF
T	absolute static temperature, ^oR
T_t	absolute total temperature, ^oR
ΔT_{t2-3}	total temperature increase across combustion chamber, ^oF
V	velocity

W	air weight flow
α	mass-flow parameter
β	heat-addition parameter
γ	ratio of specific heat at constant pressure to specific heat at constant volume
$\overline{\gamma}$	arithmetic average of specific-heat ratios corresponding to static and total temperatures
δ	angle of inclination of external surface of body to thrust axis
η	ratio of downstream to upstream absolute total pressure for a particular engine component
θ	pressure-loss parameter for method I
λ	pressure-loss parameter for method II
ρ	specific mass density

Subscripts:

0 to 5	conditions at corresponding stations indicated in figure 1
a	adjusted value
b	body
d	intake diffuser
e	external
i	internal
n	nozzle
t	total
x	segment of cross-sectional area
β	heat-addition parameter
θ	pressure-loss parameter for method I
I, II	calculation methods

ANALYSIS

Theory

The conventional expression for net thrust on a ducted body in flight is discussed in this section of the paper for the purpose of identifying the pertinent forces, in particular the forces which are to be classified as drag and subtracted from the gross thrust to obtain the net thrust. Figure 1 is a sketch of a body suitable for this discussion. In relation to the terms force, thrust, and drag in this discussion, an algebraic sense has been adopted that a force acting from right to left in figure 1 is positive and that a force acting from left to right is negative. The following expression for the net force on the body is the sum of the momentum changes of the internal and external flows between initial and final stations located in regions of free-stream static pressure; thus,

$$F_b = \left[\int_0^{A_{5_i}} V_{5ix}(\rho V)_{5ix}\, dA - \left(\frac{W}{g}\right)_i V_0\right] + \left[\int_0^{A_{5_e}} V_{5ex}(\rho V)_{5ex}\, dA - \left(\frac{W}{g}\right)_e V_0\right] \quad (1)$$

where the subscripts i and e refer to internal and external flow, respectively. The subscript x refers to the particular segment of cross-sectional area dA at station 5 (fig. 1). The first bracketed term of equation (1) may be a positive or negative quantity depending on whether the body contains a thrusting engine or a drag-producing object such as an air-cooled heat exchanger. The second bracketed term will never be a positive quantity since the external flow is always subjected to an over-all momentum loss due to energy losses associated with flow over the body. Integral expressions have been used to make the equation more general; however, the internal flow at station 5 is frequently expressed one-dimensionally so that equation (1) is reduced to the following:

$$F_b = \left(\frac{W}{g}\right)_i (V_{5_i} - V_0) + \left[\int_0^{A_{5_e}} V_{5ex}(\rho V)_{5ex}\, dA - \left(\frac{W}{g}\right)_e V_0\right] \quad (2)$$

For isentropic external flow, no change occurs in external-flow momentum between stations 0 and 5 so that equation (2) reduces to

$$F_b = \left(\frac{W}{g}\right)_i (V_{5_i} - V_0) \tag{3}$$

Equation (3), in addition to being the expression for the net force on the body for isentropic external flow, or zero external drag, is also the commonly used definition of the gross thrust force due to the engine contained within the body under conditions of nonisentropic external flow. Equation (3) is the gross-thrust expression utilized in the calculation method identified herein as method I.

The term $\int_0^{A_{5e}} V_{5ex}(\rho V)_{5ex}\, dA - \left(\frac{W}{g}\right)_e V_0$ of equation (1) or (2) is defined as external drag. As defined, external drag arises from any process to which the external flow is subjected which leads to total-pressure losses or deficiencies. Such items as skin friction, separation of the flow or turbulence, and shock waves fall in this classification.

At this point a discussion of the analytical and experimental determination of various terms of equations (1) and (2) is desirable. The terms associated with the internal flow can, in most cases, be calculated from the given conditions for the problem. One notable exception occurs for certain supersonic flight cases and is discussed subsequently. The group of external-flow terms or the external drag is not calculable in many instances. For subsonic flight speeds, such is generally the case and drag must be determined experimentally for a given body under the desired operating conditions or estimated from test results of a similar body. The several methods for determining drag experimentally generally involve use of one or more of the following items: wake-survey measurements, wind-tunnel balance measurements, and external-force determination through the use of surface-static-pressure measurements and friction-force estimates.

Inspection of equations (1) or (2) and figure 1 indicates that the obvious method for determining drag experimentally is to measure the momentum of the external flow at stations 0 and 4, provided that the static pressure at station 4 is equal to that of the free stream. If the static pressure at station 4 is not equal to that of the free stream, for subsonic flow it is still possible to estimate drag from momentum measurements. The momentum of the internal flow at station 5 can be estimated from measurements at station 4 on the assumption of no losses between stations 4 and 5. From measurements of the momentum of the combined flows at station 5, the external-flow momentum can be determined

and the external drag evaluated. For supersonic flow this procedure is not convenient because of the presence of shock and expansion waves between stations 4 and 5 when p_{4i} is not equal to p_0.

Since equation (1) is the expression for the net force on the body, this equation represents the thrust or drag force that would be measured by a wind-tunnel balance. From internal-flow-momentum measurements, mentioned previously, and the balance readings, the external drag can be determined.

Through use of surface-static-pressure measurements taken on the part of the body surface wetted by the external flow and estimates of the skin-friction coefficient, the force parallel to the thrust axis on the outside surface of the body can be computed as follows:

$$F_{eb} = -\int_0^{A_{eb}} (\cos \delta) K q_e \, dA_{eb} - \int_0^{A_{eb}} (\sin \delta) p_e \, dA_{eb} \qquad (4)$$

where the subscript eb refers to external body surface. The first term of equation (4) expresses the friction-drag force as being proportional to the product of the cosine of the angle of inclination of the external surface to the thrust axis, a friction coefficient K, the local dynamic pressure, and the external-surface area. The integral is taken over the entire external-surface area. The second term is the external-pressure-drag force in terms of the components of the external-surface-pressure forces parallel to the thrust axis. The internal force on the body can be determined through use of internal-flow measurements at stations 1 and 4 and the following equation:

$$F_{ib} = \left(\frac{W}{g}\right)_i (V_{4i} - V_{1i}) + p_{4i}A_{4i} - p_{1i}A_{1i} \qquad (5)$$

Since

$$F_b = F_{ib} + F_{eb} \qquad (6)$$

equation (2) is equivalent to equation (6), and the two are solvable for the drag term as follows:

$$D_e = \int_0^{A_{5e}} V_{5ex}(\rho V)_{5ex} \, dA - \left(\frac{W}{g}\right)_e V_0$$

$$= F_{ib} + F_{eb} - \left(\frac{W}{g}\right)_i (V_{5_i} - V_0) \qquad (7)$$

An inspection of equations (4) to (7) shows that the numerical value of drag is independent of the pressure reference; therefore, to determine the drag the pressures may be referenced to free-stream or to absolute zero pressure as shown. Unlike thrust and drag expressions, the absolute force expressions of equations (4) and (5) do not become zero for the no-flow condition.

At supersonic flight speeds for certain cases, equations (1) and (2) have practical application with regard to analytical calculations. For internal air flow, if, through use of a suitably designed exhaust nozzle, free-stream static pressure is obtained at the nozzle exit (station 4), V_4 is equal to V_5 and is calculable. However, when an under- or over-expanded exhaust nozzle is present, the determination of the velocity at station 5 is likely to be impractical because of the series of expansion and compression waves present between stations 4 and 5.

The calculation of the external drag for supersonic flow requires, according to equations (7) and (4), that the external-flow dynamic and static pressures be calculable at all points on the external surface, which is generally possible for supersonic inlets operating at design conditions; however, if the diffuser back pressure is large enough, a normal shock wave will be present upstream from the inlet lip. The presence of the normal shock introduces a region of subsonic flow in front of the inlet in both the internal and external flows, which precludes ordinary calculation methods. Some special methods are available for calculating these flow conditions such as that presented in reference 2. Generally, supplementary experimental data are required.

The operating condition described in the preceding paragraph, that is, operation with a standing normal shock in front of the inlet, requires that the internal-flow stream tube diverge in the region of mixed subsonic and supersonic flow between the normal shock and inlet lip. A divergence of the internal-flow stream tube is also obtained in the purely supersonic case for an inlet with spike-type center body operating with the oblique shock ahead of the inlet lip. Since a diverging stream tube in these cases indicates that external compression is taking place, a pressure-drag force on the external surface of the stream tube and an equal and opposite force in the thrust direction on the internal surface are introduced. If the net force on the body is determined by adding algebraically the conventional gross thrust expression of equation (3) and the external drag and if the external drag is determined from a summation of external-surface pressure forces and friction estimates, the pressure-drag force on the stream tube must be added to the external forces on the body to determine total external drag, because the conventional gross-thrust expression includes the thrust force on the stream tube. For this reason the pressure-drag force on the stream tube is frequently referred to as additive drag. Additive drag occurs only for supersonic inlet diffusers which compress

externally because the streamlines to the diffuser lip are parallel in the absence of external compression.

As previously mentioned, the analytical evaluation of V_5 is not practical for supersonic flow if the exhaust-nozzle-exit static pressure is not equal to free-stream static pressure. For application to this case, a second calculation method, method II, is presented, which leads to the evaluation of an "internal-force coefficient." If the internal flow from stations 0 to 4 (fig. 1) is considered to be contained within a stream tube, the internal-force coefficient evaluates the summation of the absolute forces exerted by the internal flow on the walls of the stream tube. For the design in which free-stream conditions exist immediately upstream of the intake-diffuser lip, the walls of the internal-flow stream tube between stations 0 and 1 become parallel so that any forces on this segment of the tube parallel to the thrust axis are eliminated; therefore, the internal-force coefficient, in this case, evaluates the absolute force on the inside surface of the ram-jet body. The expression for the internal force of calculation method II is as follows:

$$F_{0\text{-}4i} = \left(\frac{W}{g}\right)_i (V_{4i} - V_0) + p_{4i}A_{4i} - p_0A_{0i} \tag{8}$$

where static pressures are absolute quantities.

In order to obtain the net force on the ram-jet body, the absolute force on the external surface of the ram jet plus the absolute force exerted by the external flow on the stream tube between stations 0 and 1 must be added algebraically to the expression of equation (8). The external-force quantity to be added algebraically to equation (8) is as follows:

$$F_{0\text{-}4e} = -\left\{\left[p_{1i}A_{1i} + \left(\frac{W}{g}\right)_i V_{1i}\right] - \left[p_0A_{0i} + \left(\frac{W}{g}\right)_i V_0\right]\right\} + F_{eb} \tag{9}$$

where the static pressures are also absolute quantities. The fact should be noted that, when the walls of the stream tube are parallel between stations 0 and 1, the external-force quantity $F_{0\text{-}4e}$ becomes equal to the absolute force on the external surface of the ram-jet body F_{eb}. All the conditions pertaining to the feasibility of drag calculations also apply to the external-force calculation of method II.

Application of Theory to Calculation Methods

Method I is based on the expression for the conventional thrust coefficient, which includes the thrust quantity of equation (3):

$$C_{F_I} = \frac{W_2}{g} \frac{V_5(1 + f) - V_0}{A_2 q_0} \tag{10}$$

The fuel is assumed to be introduced between stations 0 and 5; hence, the term (1 + f) is used to correct the mass flow at station 5 to the sum of the fuel and air. Adiabatic processes are assumed between stations 0 and 2. The reference cross-sectional area is taken to be that of station 2. By use of the perfect gas law, Bernoulli's compressible-flow equation, and the aforementioned assumptions, equation (10) reduces to

$$C_{F_I} = \eta_d \alpha \sqrt{\frac{\gamma_2 R_0}{\gamma_0 R_2}} \left[\sqrt{\frac{R_5 \overline{\gamma}_5}{R_0 \gamma_0}} \beta\theta(1 + f) - M_0 \right] \tag{11}$$

where

$$\eta_d = \frac{p_{t2}}{p_{t0}} \tag{12}$$

$$\alpha = \frac{2\left(1 + \frac{\overline{\gamma}_0 - 1}{2} M_0^2 \frac{\gamma_0}{\overline{\gamma}_0}\right)^{\frac{\overline{\gamma}_0 + 1}{2(\overline{\gamma}_0 - 1)}}}{M_0^2 \left(1 + \frac{\overline{\gamma}_2 - 1}{2} M_2^2 \frac{\gamma_2}{\overline{\gamma}_2}\right)^{\frac{\overline{\gamma}_2 + 1}{2(\overline{\gamma}_2 - 1)}}} \tag{13}$$

$$\beta = \sqrt{\frac{2}{\overline{\gamma}_5 - 1}} \sqrt{1 + \frac{\overline{\gamma}_0 - 1}{2} M_0^2 \frac{\gamma_0}{\overline{\gamma}_0} + \frac{\Delta T_{t2-3}}{T_0}} \tag{14}$$

$$\theta = \sqrt{1 - \left(\frac{1}{1 + \frac{\overline{\gamma}_0 - 1}{2} M_0^2 \frac{\gamma_0}{\overline{\gamma}_0}}\right)^{\frac{\overline{\gamma}_0(\overline{\gamma}_5-1)}{\overline{\gamma}_5(\overline{\gamma}_0-1)}} \left(\frac{1}{\eta_d} \frac{1}{\eta_n} \frac{1}{\frac{p_{t3}}{p_{t2}}}\right)^{\frac{\overline{\gamma}_5-1}{\overline{\gamma}_5}}} \tag{15}$$

and

$$\eta_n = \frac{p_{t5}}{p_{t4}} \tag{16}$$

The appendix contains a complete derivation of the preceding equations, as well as expressions for p_{t5}/p_0, T_{t5}/T_0, T_5/T_0, A_5/A_2, I, and M_5.

Equation (11) is of the same general form as equation (10), but the term V_0 has been replaced with M_0 and the rest of the terms replaced with the parameters α, β, and θ, the gas properties, and the diffuser total-pressure-recovery ratio. The mass flow is directly proportional to α, a function of combustion-chamber-inlet Mach number, flight Mach number, and gas properties. The exhaust velocity V_5 is directly proportional to the product of β and θ. Flight Mach number, the ratio of combustion total-temperature rise to free-stream static temperature, and gas properties determine β; whereas θ is a function of flight Mach number, total-pressure ratio through the ram jet from free-stream to free-stream conditions, and gas properties. The parameters α, β, and θ can be designated, roughly, as the mass flow, heat-addition, and pressure-loss parameters, respectively. The parameters α, β, and θ are interrelated to a certain extent because they are functions of M_2, ΔT_{t2-3}, and p_{t3}/p_{t2}, respectively, all of which are associated with the combustion-chamber performance. For a given combustion-chamber geometry, the values of all the following variables are determined by fixing two: Mach number before and after combustion, total-temperature ratio through the combustion chamber, and total-pressure ratio through the combustion chamber.

The second calculation method is based on the following equation for internal-force coefficient which includes the force expression of equation (8):

$$C_{F_{II}} = \frac{W_2}{g} \frac{V_4(1 + f) - V_0}{A_2 q_0} + \frac{p_4 A_4}{A_2 q_0} - \frac{p_0 A_0}{A_2 q_0} \tag{17}$$

where the static pressure at station 4 may be greater or less than

atmospheric static pressure as previously discussed. If procedures similar to those of method I are used, the force-coefficient expression of equation (17) can be reduced to:

$$C_{F_{II}} = \eta_d \alpha \sqrt{\frac{\gamma_2 R_0}{\gamma_0 R_2}} \left[\sqrt{\frac{R_4 \bar{\gamma}_4}{R_0 \gamma_0}} \beta \lambda (1 + f) - M_0 - \frac{1}{\gamma_0 M_0} \right] \tag{18}$$

where

$$\lambda = \frac{1 + \dfrac{1}{\gamma_4 M_4^2}}{\sqrt{1 + \dfrac{2\bar{\gamma}_4}{\left(\bar{\gamma}_4 - 1\right)\gamma_4 M_4^2}}} \tag{19}$$

The appendix contains a complete derivation of the preceding equations as well as expressions for T_{t4}/T_0, p_4/p_0, T_4/T_0, M_4, and p_{t4}/p_4.

Equation (18) differs from equation (11) in that, in order to account for the pressure-area terms, θ has been replaced by λ and another flight Mach number term introduced. Although λ is a function of gas properties and the Mach number at station 4, it can still be considered a pressure-loss parameter similar to θ since the Mach number at station 4 is dependent on the pressure losses up to that station.

The methods of calculation can be adapted to any engine in which continuous-flow air processed in the thermodynamic cycle is employed for propulsion. The required modifications to the ram-jet application are that, for the combustion parameter β, the term ΔT_{t2-3} must be the algebraic sum of all total-temperature changes from the free stream to the nozzle exit and, for the pressure-loss parameter θ, the group of total-pressure-ratio terms must be an expression of the total-pressure ratio from the free stream to the nozzle exit. Additional terms introduced by these two modifications can be expressed in terms of efficiencies and other fundamental parameters associated with the added engine components.

GRAPHICAL PRESENTATION OF SOLUTIONS

Calculation Based on Standard-Air Properties

An examination of equations (11) and (18) indicates that the main problem in the determination of the thrust coefficient is the evaluation of the mass-flow parameter α, the heat-addition parameter β, and one of the two pressure-loss parameters θ or λ. A close approximation to these quantities can be obtained directly by assuming standard-air values for the ratio of specific heats γ at all stations. Plots of equations (13), (14), (15), and (19) are presented on this basis in figures 2 to 5. (Each figure has been broken down into several page-size plots for the purposes of accuracy and convenience; however, the first figure in each group covers the entire range of variables and can be used to determine the appropriate plot for particular values of the variables.)

The thrust-coefficient expressions which are appropriate to use with values taken from these figures are as follows:

$$C_{F_I}' = \eta_d \alpha' \left[\beta' \theta' (1 + f) - M_0 \right] \tag{20}$$

$$C_{F_{II}}' = \eta_d \alpha' \left[\beta' \lambda' (1 + f) - M_0 - \frac{1}{1.4 M_0} \right] \tag{21}$$

Values based on standard-air specific-heat ratio and gas constant have been designated as primed values. As is indicated in the discussion of the numerical example, thrust coefficients calculated on this basis for conditions representative of typical ram-jet operation are on the order of 5 to 10 percent low. This discrepancy, however, varies according to the given conditions and is mainly a function of the total-temperature levels in the engine and the fuel properties.

An inspection of the preceding equations indicates that, with one exception, the thrust coefficient and associated parameters involve only basic variables such as flight Mach number, diffuser total-pressure-recovery ratio, combustion-chamber characteristics, exhaust-nozzle total-pressure-recovery ratio, which would be either given or measured. The one exception is the pressure-loss parameter λ, which is a function of the Mach number at the exhaust-nozzle exit (station 4), which in turn is a function of the Mach number at the end of the combustion chamber (station 3), the nozzle-area contraction, and any total-pressure and

temperature changes between stations 3 and 4. The Mach number at station 3 is obtainable directly from the basic combustion-chamber variables, provided that the calculated or measured performance is available in a form similar to that of figure 6, which is a plot of the characteristics of a combustion chamber with low friction and turbulence-pressure losses. Additional information on this subject is available in reference 3, in which theoretical relations concerning combustion-chamber performance are presented. The Mach number at station 4 can be evaluated by use of the expression

$$\frac{M}{\left(1 + \frac{\overline{\gamma} - 1}{2} M^2 \frac{\gamma}{\overline{\gamma}}\right)^{\frac{\overline{\gamma}+1}{2(\overline{\gamma}-1)}}} = \sqrt{\frac{gRT_t}{\gamma}} \frac{\frac{W}{g}(1 + f)}{Ap_t} \tag{22}$$

derived from the presentation in reference 4 and plotted in figure 7. The exhaust-nozzle Mach number is evaluated from figure 7 by obtaining the ordinate corresponding to M_3, multiplying it by the factor

$$\frac{A_4}{A_3} \frac{p_{t4}}{p_{t3}} \sqrt{\frac{\gamma_4}{\gamma_3} \frac{R_3}{R_4} \frac{T_{t3}}{T_{t4}}},$$

and reading M_4 corresponding to the new ordinate. The term $\gamma/\overline{\gamma}$ is negligible up to a Mach number of approximately 3.0 and has been neglected in this range. Figure 7(e) presents a correction factor for use when $\gamma/\overline{\gamma}$ deviates from a value of 1.0 in the range of Mach number from 3.0 to 4.0.

The value of fuel-air ratio of equations (20) and (21) depends on the type of fuel used, the desired combustion-chamber total-temperature rise, the total temperature before combustion, and the burner efficiency. As an aid to evaluating this quantity, the theoretical variation of fuel-air ratio with total-temperature rise and the initial total temperature has been calculated for the combustion of n-octane and air through use of references 5 to 11 and plotted in figure 8. All effects due to dissociation were accounted for in the calculations by using the assumption that equilibrium conditions are attained. The fuel-air ratio plotted is an effective value or one based on 100-percent burner efficiency. The value substituted in equations (20) and (21) should be the effective value modified to compensate for the burner inefficiency.

For simplicity of presentation, sample problems have been calculated by both methods for the same conditions at a supersonic flight Mach number of 2.0. The combustion of n-octane and air at 100-percent burner efficiency has been assumed. In order to illustrate the calculation procedures in more detail, an outline of a numerical example is presented in table I.

Calculation Accounting for Variation of Specific-Heat Ratio and Gas Constant

For more precise answers, additional charts and information have been supplied to correct α', β', θ', and λ' to correspond to equilibrium values of the specific-heat ratios. The mass-flow-parameter correction factor $\frac{\alpha}{\alpha'}$ is plotted in figure 9. The assumption was made that the average of the specific-heat ratios corresponding to total and static temperatures $\overline{\gamma}_0$ is equal to the average of the standard air value, 1.400, and the value γ_{t0} corresponding to free-stream total temperature. This assumption holds as long as the free-stream static temperature of the air is not appreciably in excess of 500° R. The assumption was also made that terms involving the combustion-chamber-inlet Mach number M_2 are insignificant. This assumption holds within the limits of $M_2 = 0$ to 0.5 fixed in this paper. The expression

$$\frac{\alpha}{\alpha'} = \frac{\left[1 + \frac{0.7\,\gamma_{t0} - 0.6}{\gamma_{t0} + 1.4} M_0^2\right]^{\frac{\gamma_{t0}+3.4}{2(\gamma_{t0}-0.6)}}}{\left(1 + \frac{M_0^2}{5}\right)^{3.0}} \tag{23}$$

which is plotted in figure 9, was derived from equation (13).

The heat-addition-parameter correction of β' to β is obtained in a different manner. First, an intermediate value of β', designated β'', is determined. An adjusted value of M_0, $M_{0a\beta}$, corresponding to corrected values of the specific-heat ratios at station 0, is obtained and is substituted in the β' charts (fig. 3) to obtain β''. The relation between $M_{0a\beta}$ and M_0

$$M_{0a\beta} = M_0\sqrt{\frac{3.5(\gamma_{t0} - 0.6)}{\gamma_{t0} + 1.4}} \tag{24}$$

was obtained by setting the term involving M_0 in equation (14) equal to a similar term in which $M_{0a\beta}$ and standard-air values of the specific-heat ratio were used. Equation (24) is plotted in figure 10. Second, in order to correct the heat-addition parameter β'' to β, equation (14) indicates that

$$\beta = \beta''\sqrt{\frac{0.40}{\overline{\gamma}_5 - 1}} \tag{25}$$

The correction of the pressure-loss parameter θ' to θ is achieved in the same manner as the correction of β' to β''. Two steps are necessary, since both M_0 and the total-pressure-ratio terms of equation (15) are complicated by the specific-heat ratio. Using the term involving M_0 in equation (15) gives the expression for $M_{0a\theta}$:

$$M_{0a\theta} = \sqrt{5\left\{\left[1 + \frac{0.7(\gamma_{t0} - 0.6)}{\gamma_{t0} + 1.4} M_0^2\right]^{\frac{(\gamma_{t0}+1.4)(\overline{\gamma}_5-1)}{\overline{\gamma}_5(\gamma_{t0}-0.6)}} - 1\right\}} \tag{26}$$

This equation is plotted in figure 11. This adjusted value of M_0 can be used in the θ' charts to obtain θ''. By the same procedure,

$$\left(\frac{1}{\eta_d}\frac{1}{\eta_n}\frac{1}{p_{t3}/p_{t2}}\right)_a = \left(\frac{1}{\eta_d}\frac{1}{\eta_n}\frac{1}{p_{t3}/p_{t2}}\right)^{\frac{3.5(\overline{\gamma}_5-1)}{\overline{\gamma}_5}} \tag{27}$$

which is plotted in figure 12. Using values obtained in figures 11 and 12 to substitute in the charts for θ' (fig. 4) results in the corrected value θ.

The procedure for correcting the pressure-loss parameter λ' is similar to that used for α' except that two steps are again necessary. First, λ' is corrected to λ'' which is a value based on the assumption

that $\overline{\gamma}_4$ is equal to γ_4. The following expression, which is plotted in figure 13(a), is obtained from equation (19):

$$\frac{\lambda''}{\lambda'} = \frac{M_4^2 + \frac{1}{\overline{\gamma}_4}}{M_4^2 + \frac{1}{1.4}} \sqrt{\frac{M_4^2 + 5}{M_4^2 + \frac{2}{\overline{\gamma}_4 - 1}}} \tag{28}$$

Second, λ'' is corrected to λ through use of the following expression:

$$\frac{\lambda}{\lambda''} = \frac{M_4^2 + \frac{1}{\overline{\gamma}_4}\frac{\overline{\gamma}_4}{\gamma_4}}{M_4^2 + \frac{1}{\overline{\gamma}_4}} \sqrt{\frac{M_4^2 + \frac{2}{\overline{\gamma}_4 - 1}}{M_4^2 + \frac{2}{\overline{\gamma}_4 - 1}\frac{\overline{\gamma}_4}{\gamma_4}}} \tag{29}$$

which is plotted in figure 13(b). The effect of changes in $\overline{\gamma}_4$ is negligible in the preceding expression and is neglected in the plot.

In order to determine the specific-heat ratios γ, γ_t, and $\overline{\gamma}$ to use in the preceding corrections, it is necessary to know the effective fuel-air ratio, the temperatures appropriate to the particular specific-heat ratio, and the relation between γ, temperature, and fuel-air ratio for the particular gas. The aforementioned gas properties have been calculated, for the combustion of n-octane and air, by use of references 5 to 11. All effects due to dissociation were accounted for in the calculations by using the assumption that equilibrium conditions are attained. Plots of combustion total-temperature rise as a function of fuel-air ratio and initial temperature and the instantaneous value of the ratio of specific heats and the gas constant as functions of temperature and fuel-air ratio are presented in figures 8, 14, and 15, respectively. Use of the effective fuel-air ratio is equivalent to assuming that the unburned fuel has a negligible effect on these values, as is true for reasonable combustion efficiencies. Figures 8, 14, and 15 were calculated on the assumption of 1 atmosphere pressure. Reference 5 indicates the effect of pressure to be very small; for instance, an increase in pressure of 5 atmospheres produced a maximum of 0.25 percent change in temperature rise.

The variation of the ratio of specific heats (fig. 14) is quite marked with temperature increases up to 2500° R. From 2500° R to 5000° R

the variation with temperature is much less significant than the composition or fuel-air-ratio effect, which is approximately constant over the temperature range up to the point where dissociation takes place. The effects of dissociation are to break down the water, the carbon dioxide, and the nitrogen into elements and compounds in such a way that the ratio of specific heats of the mixture becomes more similar to that of air. These effects tend to reduce the spread between the curves of constant fuel-air ratio in figure 14 as the temperature is increased above 3500° to 4000° R.

In the determination of the various parameters involved in the calculation of thrust coefficient, small changes in the ratio of specific heats γ will produce large changes in the values of the parameters because the difference between γ and 1 appears in exponents and multiplying factors in equations (13), (14), (15), and (19). On the other hand, small changes in gas constant have little effect on the value of thrust coefficient since the gas constant appears only as a square root multiplying factor in equations (11) and (18). The gas constant (fig. 15) varies only with the composition of the gas. This variation is less than 1 percent up to temperatures at which dissociation takes place. At 5000° R the spread in values of gas constant between air and a stoichiometric fuel-air ratio is approximately 5 percent.

In order to evaluate the correction factor α/α', it is necessary to determine the free-stream total temperature T_{t0} for use in figure 14. The temperature can be determined through a trial and error solution of the following equation:

$$\frac{T_{t0}}{T_0} = 1 + \frac{0.7(\gamma_{t0} - 0.6)}{\gamma_{t0} + 1.4} M_0^2 \qquad (30)$$

derived from the value of T_{t0}/T_0 given in the appendix. The tables of reference 12 will be found useful in performing the first step of this calculation. Generally, only two steps are necessary since the effect of changes in γ is small in this case.

The corrections to β' and θ' must be calculated concurrently since the static temperature at station 5, T_5, is a function of both β and θ. Correcting β' and θ' to β'' and θ'', respectively, which accounts for deviation of the free-stream specific-heat ratios from standard values, is a straightforward process using γ_{t0} in combination with figures 3, 4, 10, and 11. Corrections from β'' to β and from θ'' to θ are more complicated as they require a trial-and-error process.

The expression for T_{t5}/T_0 as derived in the appendix is

$$\frac{T_{t5}}{T_0} = \frac{\overline{\gamma}_5 - 1}{2} \beta^2$$

This equation combined with equation (25) gives

$$T_{t5} = \frac{T_0}{5} \beta''^2 \tag{31}$$

The adjusted pressure-ratio term, and thus θ, can be approximated by using γ_{t5} corresponding to T_{t5} and figure 12. Then from equation (25) and the expression for T_5/T_0 as given in the appendix:

$$T_5 = \frac{T_0}{5} \beta''^2 \left(1 - \theta^2\right) \tag{32}$$

which is plotted in figure 16. From the approximate T_5, γ_5 can be evaluated by using figure 14. At this point a revised value of γ_{t5} should be determined provided that T_5 is within the region where dissociation takes place, as indicated in figure 14. This value is obtained by starting at a point corresponding to γ_5 and T_5 and moving up to T_{t5} along a line parallel to the curves corresponding to specific-heat ratios for no dissociation. This procedure produces a specific-heat ratio corresponding to T_{t5} for a gas of the same composition of exhaust products as at T_5. If γ_{t5} were taken at the correct temperature and fuel-air ratio for dissociated mixtures, there would be a discrepancy between γ_5 and γ_{t5} in that the gas would have changed composition between the two temperatures. Since the total temperature in this case does not exist physically in the gas but is a mathematical concept, the composition at the static temperature is taken as being correct. After re-evaluating the average specific-heat ratio $\overline{\gamma}_5$ the process for calculation of the static temperature T_5 can be repeated until the values converge. Usually the main part of the correction is accomplished by using specific-heat-ratio values based on the total temperature so that the trial-and-error processes produce only second-order corrections. The final value of the combustion parameter β can be evaluated by using equation (25).

In order to calculate the thrust coefficient from equation (11), in addition to the parameters previously discussed, R_5, R_2, γ_2, R_0, and γ_0 have to be determined. The evaluation of R_5 can be made directly by using T_5, the effective fuel-air ratio, and figure 15. The terms R_2 and γ_2 can be assumed to correspond to zero fuel-air ratio and T_{t0}; therefore, γ_2 equals γ_{t0}. Standard values can be used for R_0 and γ_0.

The determination of the appropriate temperatures and specific-heat ratios for the correction of the pressure-loss parameter λ' is similar to that of θ'. As derived in the appendix,

$$\frac{T_{t4}}{T_0} = \frac{\overline{\gamma}_4 - 1}{2} \beta^2$$

From this expression and equation (25),

$$\frac{T_{t4}}{T_0} = \frac{\beta''^2}{5} \tag{33}$$

A first approximation of T_4 is obtained by using the following equation:

$$\frac{T_4'}{T_0} = \frac{\beta''^2}{M_4^2 + 5} \tag{34}$$

This approximate value, based on the standard-air value of the specific-heat ratio, is related to the corrected static temperature by the following expression derived from the equation for T_4/T_0 (see appendix) and equation (25):

$$\frac{T_4}{T_4'} = \frac{\dfrac{0.4}{\overline{\gamma}_4 - 1} \dfrac{\overline{\gamma}_4}{\gamma_4} \left(M_4^2 + 5 \right)}{M_4^2 + \dfrac{2}{\overline{\gamma}_4 - 1} \dfrac{\overline{\gamma}_4}{\gamma_4}} \tag{35}$$

Equation (35) has been plotted in figure 17. By first substituting in equation (35) the specific-heat ratio corresponding to T_4', T_4 can be evaluated by trial and error. Once T_4 is obtained $\overline{\gamma}_4$ can be evaluated and the pressure-loss parameter λ can be determined directly from figure 13.

An outline of the calculations necessary to correct the numerical examples in the preceding section for deviation of the specific-heat ratios and gas constants from standard-air values is presented in table II.

In order to illustrate the general method, the numerical examples presented include all the detailed corrections for deviation of γ and R from standard-air values. However, thrust coefficients for the conditions of the example presented have been calculated by assuming no deviation from standard-air values except at stations 4 and 5, where $\overline{\gamma}$, γ, and R were assumed to correspond to total-temperature values, so that all trial-and-error processes are eliminated. The answers arrived at by use of these assumptions agreed with those presented in steps 36 and 46 of table II within less than 1 percent. If for a particular problem an appreciable number of calculations are to be made by using corrected values of specific-heat ratio and gas constant, the number of steps generally can be considerably reduced in a manner similar to that described.

CONCLUDING REMARKS

A method utilizing graphical presentations of precalculated solutions for calculating ram-jet thrust coefficient and other important quantities has been presented with the associated equations and graphs. By use of the assumption of constant values of specific-heat ratio and gas constant equal to those of standard air, the calculation procedure permits in a few simple operations the direct determination of thrust coefficient from values of basic variables. Additional procedures are presented for correcting for deviations of specific-heat ratio γ and gas constant R from standard values. An examination of the differences between the corrected and uncorrected values of the calculated thrust coefficients in the numerical examples indicates that the values based on standard specific-heat ratio and gas constant are 6 or 7 percent low. These differences are believed to represent fairly typical accuracy for ram-jet performance calculations in current use. Inasmuch as the assumption of one-dimensional flow may introduce errors of similar magnitude, the aforementioned discrepancies are probably permissible for most calculations.

In cases where it is desired to correct for specific-heat-ratio and gas-constant variation, a number of the less significant corrections described in the general calculation procedure can usually be omitted without appreciable loss of accuracy. Short cuts of this nature, applicable to the conditions set up in the numerical example, have been previously discussed.

The variation of specific-heat ratio γ throughout the thermodynamic cycle is more important than the gas constant because the quantity $\gamma - 1$ appears as an exponent and also as a multiplying factor in a number of equations; whereas the gas constant appears only as a square-root multiplying factor. Variations in the value of γ result from changes in temperature and fuel-air ratio and from dissociation effects. The variation with temperature reduces with rise in temperature and becomes less important than variation with fuel-air ratio above 2500° R. The effect of increasing amounts of dissociation is to reduce the effect of changes in fuel-air ratio. The variation in values of gas constant with fuel-air ratio is less than 1 percent up to temperatures where dissociation occurs. At 5000° R the spread in values of gas constant over the fuel-air-ratio range up to stoichiometric fuel-air ratios is 5 percent.

Langley Aeronautical Laboratory
National Advisory Committee for Aeronautics
Langley Field, Va., December 8, 1950

APPENDIX

DERIVATION OF THRUST- AND INTERNAL-FORCE-COEFFICIENT EXPRESSIONS AND ASSOCIATED RELATIONS

Thrust Coefficient and Related Parameters Obtained by Method I

The conventional thrust-coefficient expression for ram jets (see fig. 1) is:

$$C_{F_I} = \frac{\frac{W}{g}\left[V_5(1 + f) - V_0\right]}{A_2 q_0}$$

The following expression gives Bernoulli's application to compressible flow:

$$T_{t5} - T_5 = \frac{V_5^2}{2Jg\bar{c}_{p5}} \tag{A1}$$

For isentropic flow,

$$T_5 = T_{t5}\left(\frac{p_5}{p_{t5}}\right)^{\frac{\bar{\gamma}_5 - 1}{\bar{\gamma}_5}} \tag{A2}$$

Substituting equation (A2) in equation (A1) gives

$$T_{t5}\left[1 - \left(\frac{p_5}{p_{t5}}\right)^{\frac{\bar{\gamma}_5 - 1}{\bar{\gamma}_5}}\right] = \frac{V_5^2}{2gR_5\left(\frac{\bar{\gamma}_5}{\bar{\gamma}_5 - 1}\right)} \tag{A3}$$

Expanding p_5/p_{t5} into the product of several pressure ratios and substituting p_0 for p_5 yields

$$\frac{T_{t5}}{T_0}\left[1 - \left(\frac{p_0}{p_{t0}}\right)^{\frac{\bar{\gamma}_5-1}{\bar{\gamma}_5}}\left(\frac{p_{t0}}{p_{t2}}\frac{p_{t2}}{p_{t3}}\frac{p_{t3}}{p_{t5}}\right)^{\frac{\bar{\gamma}_5-1}{\bar{\gamma}_5}}\right] = \frac{V_5^2}{2gR_5T_0\frac{\bar{\gamma}_5}{\bar{\gamma}_5 - 1}} \tag{A4}$$

Substituting the expression for Mach number and the speed of sound in equation (A1) as applied to station 0 gives

$$\frac{T_{t0}}{T_0} = 1 + \frac{\bar{\gamma}_0 - 1}{2} M_0^2 \frac{\gamma_0}{\bar{\gamma}_0} \tag{A5}$$

Converting equation (A5) to a pressure ratio by using an isentropic relationship

$$\left(\frac{p_0}{p_{t0}}\right)^{\frac{\bar{\gamma}_5-1}{\bar{\gamma}_5}} = \left(\frac{1}{1 + \frac{\bar{\gamma}_0 - 1}{2} M_0^2 \frac{\gamma_0}{\bar{\gamma}_0}}\right)^{\frac{\bar{\gamma}_0(\bar{\gamma}_5-1)}{\bar{\gamma}_5(\bar{\gamma}_0-1)}} \tag{A6}$$

The expression T_{t5}/T_0 may be written as follows by use of equation (A5)

$$\frac{T_{t5}}{T_0} = \frac{T_{t0} + \Delta T_{t2-3}}{T_0} = 1 + \frac{\bar{\gamma}_0 - 1}{2} M_0^2 \frac{\gamma_0}{\bar{\gamma}_0} + \frac{\Delta T_{t2-3}}{T_0} \tag{A7}$$

Substituting equations (A7) and (A6) in equation (A4), η_d for p_{t2}/p_{t0}, η_n for p_{t5}/p_{t3}, and solving for V_5 gives

$$V_5 = \sqrt{\frac{2gR_5\bar{\gamma}_5}{\bar{\gamma}_5 - 1} T_0 \left(1 + \frac{\bar{\gamma}_0 - 1}{2.} M_0^2 \frac{\gamma_0}{\bar{\gamma}_0} + \frac{\Delta T_{t2-3}}{T}\right)\left[1 - \left(\frac{1}{1 + \frac{\bar{\gamma}_0 - 1}{2} M_0^2 \frac{\gamma_0}{\bar{\gamma}_0}}\right)^{\frac{\bar{\gamma}_0(\bar{\gamma}_5-1)}{\bar{\gamma}_5(\bar{\gamma}_0-1)}} \left(\frac{1}{\eta_d} \frac{1}{\eta_n} \frac{1}{p_{t3}/p_{t2}}\right)^{\frac{\bar{\gamma}_5-1}{\bar{\gamma}_5}}\right]} \tag{A8}$$

Let

$$\beta = \sqrt{\frac{2}{\bar{\gamma}_5 - 1}} \sqrt{1 + \frac{\bar{\gamma}_0 - 1}{2} M_0^2 \frac{\gamma_0}{\bar{\gamma}_0} + \frac{\Delta T_{t2-3}}{T_0}} \tag{A9}$$

and

$$\theta = \sqrt{1 - \left(\frac{1}{1 + \frac{\bar{\gamma}_0 - 1}{2} M_0^2 \frac{\gamma_0}{\bar{\gamma}_0}}\right)^{\frac{\bar{\gamma}_0(\bar{\gamma}_5-1)}{\bar{\gamma}_5(\bar{\gamma}_0-1)}} \left(\frac{1}{\eta_d} \frac{1}{\eta_n} \frac{1}{p_{t3}/p_{t2}}\right)^{\frac{\bar{\gamma}_5-1}{\bar{\gamma}_5}}} \tag{A10}$$

Then, substitute equations (A9) and (A10) in equation (A8) to obtain

$$V_5 = \beta\theta\sqrt{gR_5\bar{\gamma}_5 T_0} \tag{A11}$$

The perfect gas law and the expressions for Mach number and the speed of sound can be used to write an equation for mass flow as follows:

$$\frac{W}{g} = \rho_2 A_2 V_2 = \frac{p_2}{gR_2T_2}\, a_2 M_2 A_2 = \frac{p_2}{\sqrt{T_2}}\sqrt{\frac{\gamma_2}{gR_2}}\, A_2 M_2 \tag{A12}$$

Equations similar to equations (A5) and (A6) substituted in equation (A12) produce

$$\frac{W}{g} = \sqrt{\frac{\gamma_2}{gR_2}}\, \frac{p_{t2} A_2 M_2}{\sqrt{T_{t2}}\left(1 + \frac{\overline{\gamma}_2 - 1}{2} M_2^2 \frac{\gamma_2}{\overline{\gamma}_2}\right)^{\frac{\overline{\gamma}_2+1}{2(\overline{\gamma}_2-1)}}} \tag{A13}$$

$$\frac{W}{g} = \sqrt{\frac{\gamma_2}{gR_2}}\, \frac{\eta_d p_0 A_2 M_2 \left(1 + \frac{\overline{\gamma}_0 - 1}{2} M_0^2 \frac{\gamma_0}{\overline{\gamma}_0}\right)^{\frac{\overline{\gamma}_0+1}{2(\overline{\gamma}_0-1)}}}{\sqrt{T_0}\left(1 + \frac{\overline{\gamma}_2 - 1}{2} M_2^2 \frac{\gamma_2}{\overline{\gamma}_2}\right)^{\frac{\overline{\gamma}_2+1}{2(\overline{\gamma}_2-1)}}} \tag{A14}$$

Let

$$\alpha = \frac{2\left(1 + \frac{\overline{\gamma}_0 - 1}{2} M_0^2 \frac{\gamma_0}{\overline{\gamma}_0}\right)^{\frac{\overline{\gamma}_0+1}{2(\overline{\gamma}_0-1)}} M_2}{M_0^2 \left(1 + \frac{\overline{\gamma}_2 - 1}{2} M_2^2 \frac{\gamma_2}{\overline{\gamma}_2}\right)^{\frac{\overline{\gamma}_2+1}{2(\overline{\gamma}_2-1)}}} \tag{A15}$$

Equation (A14) then can be simplified to

$$\frac{W}{g} = \sqrt{\frac{\gamma_2}{gR_2}} \frac{\eta_d p_0 A_2}{\sqrt{T_0}} \frac{M_0^2}{2} \alpha \tag{A16}$$

From the definition of Mach number,

$$V_0 = a_0 M_0 = M_0 \sqrt{\gamma_0 g R_0 T_0} \tag{A17}$$

Flight dynamic pressure may be expressed by the perfect gas law and the expression for the speed of sound as

$$q_0 = \frac{1}{2} \rho_0 a_0^2 M_0^2 = \frac{\gamma_0}{2} p_0 M_0^2 \tag{A18}$$

Equations (A16), (A11), (A17), and (A18) may be used in the expression for thrust coefficient to produce

$$C_{F_I} = \eta_d \alpha \sqrt{\frac{\gamma_2 R_0}{\gamma_0 R_2}} \left[\sqrt{\frac{R_5 \bar{\gamma}_5}{R_0 \gamma_0}} \beta\theta(1 + f) - M_0 \right] \tag{A19}$$

Other parameters at station 5 can be derived in terms of α, β, and θ. From equations (A1), (A11), (A7), and (A9), it follows that

$$\frac{T_5}{T_0} = \frac{\beta^2 \left(\bar{\gamma}_5 - 1 \right)}{2} \left(1 - \theta^2 \right) \tag{A20}$$

Substituting the relations of the perfect gas law, and equations (A20), (A11), and (A16) in the expression

$$A_5 = \frac{W(1 + f)}{g \rho_5 V_5}$$

produces

$$\frac{A_5}{A_2} = \frac{1}{4}\sqrt{\frac{\gamma_2 R_5}{\bar{\gamma}_5 R_2}}\left(\bar{\gamma}_5 - 1\right)\alpha\beta\,\frac{1 - \theta^2}{\theta}\,\eta_d M_0^2(1 + f) \tag{A21}$$

From the expression for Mach number and the speed of sound, equations (A11), and (A20), it follows that

$$M_5 = \sqrt{\frac{2\bar{\gamma}_5}{\left(\bar{\gamma}_5 - 1\right)\gamma_5}}\sqrt{\frac{\theta^2}{1 - \theta^2}} \tag{A22}$$

From equations (A7) and (A9)

$$\frac{T_{t5}}{T_0} = \frac{\bar{\gamma}_5 - 1}{2}\,\beta^2 \tag{A23}$$

From equations (A2), (A20), and (A23)

$$\frac{p_{t5}}{p_0} = \left(\frac{1}{1 - \theta^2}\right)^{\frac{\bar{\gamma}_5}{\bar{\gamma}_5 - 1}} \tag{A24}$$

The expression for specific impulse (pounds thrust per pound fuel per second) is

$$I = \frac{V_5(1 + f) - V_0}{gf} \tag{A25}$$

Substituting from equations (A11) and (A17) in (A25) produces

$$I_I = \frac{a_0}{gf}\left[\sqrt{\frac{\bar{\gamma}_5 R_5}{\gamma_0 R_0}}\,\beta\theta(1 + f) - M_0\right] \tag{A26}$$

Internal-Force Coefficient and Related Parameters Obtained by Method II

The internal-force-coefficient expression (see fig. 1) is

$$C_{F_{II}} = \frac{\frac{W}{g}\left[V_4(1 + f) - V_0\right] + p_4A_4 - p_0A_0}{A_2q_0}$$

The derivation used in obtaining equation (A3) may be applied to station 4 to give the expression

$$T_{t4}\left[1 - \left(\frac{p_4}{p_{t4}}\right)^{\frac{\overline{\gamma}_4 - 1}{\overline{\gamma}_4}}\right] = \frac{V_4^2}{\frac{2gR_4\overline{\gamma}_4}{\overline{\gamma}_4 - 1}} \tag{A27}$$

Substituting from equations similar to (A2) and (A5) as applied to station 4 in equation (A27) produces

$$T_{t4}\left[\frac{1}{1 + \frac{2\overline{\gamma}_4}{(\overline{\gamma}_4 - 1)M_4^2\gamma_4}}\right] = \frac{V_4^2}{\frac{2gR_4\overline{\gamma}_4}{\overline{\gamma}_4 - 1}} \tag{A28}$$

Solving for V_4 yields

$$V_4 = \sqrt{\frac{2gR_4\overline{\gamma}_4T_0}{\overline{\gamma}_4 - 1}\frac{T_{t4}}{T_0}\frac{1}{1 + \frac{2\overline{\gamma}_4}{(\overline{\gamma}_4 - 1)M_4^2\gamma_4}}} \tag{A29}$$

An equation similar to equation (A7) may be used for (T_{t4}/T_0) in equation (A29) to obtain

$$V_4 = \sqrt{2g \frac{R_4\overline{\gamma}_4}{\overline{\gamma}_4 - 1} T_0 \left(1 + \frac{\overline{\gamma}_0 - 1}{2} M_0^2 \frac{\gamma_0}{\overline{\gamma}_0} + \frac{\Delta T_{t2-3}}{T_0}\right) \frac{1}{1 + \frac{2\overline{\gamma}_4}{\left(\overline{\gamma}_4 - 1\right) M_4^2 \gamma_4}}} \tag{A30}$$

Let

$$\lambda = \frac{1 + \frac{1}{\gamma_4 M_4^2}}{\sqrt{1 + \frac{2\overline{\gamma}_4}{\left(\overline{\gamma}_4 - 1\right)\gamma_4 M_4^2}}} \tag{A31}$$

Substituting from equation (A9) and (A31) reduces equation (A30) to

$$V_4 = \sqrt{gR_4\overline{\gamma}_4 T_0} \frac{\beta\lambda}{1 + \frac{1}{\gamma_4 M_4^2}} \tag{A32}$$

Equations (A32), (A16), (A17), and (A18) substituted in the internal-force-coefficient expression gives

$$C_{F_{II}} = \eta_d \alpha \sqrt{\frac{\gamma_2 R_0}{\gamma_0 R_2}} \left(\sqrt{\frac{R_4\overline{\gamma}_4}{R_0\gamma_0}} \frac{\beta\lambda(1 + f)}{1 + \frac{1}{\gamma_4 M_4^2}} - M_0 \right) + \frac{p_4 A_4}{q_0 A_2} - \frac{p_0 A_0}{q_0 A_2} \tag{A33}$$

Equation (A9) may be used in an equation similar to equation (A7) for station 4 to give

$$\frac{T_{t4}}{T_0} = \frac{\overline{\gamma}_4 - 1}{2} \beta^2 \tag{A34}$$

Equations (A32) and (A34) may be substituted in equation (A1) as applied to station 4 to obtain

$$\frac{T_4}{T_0} = \beta^2 \frac{\overline{\gamma}_4 - 1}{2}\left[1 - \frac{\lambda^2}{\left(1 + \frac{1}{\gamma_4 M_4^2}\right)^2}\right] \tag{A35}$$

Substituting the perfect-gas relationship and equations (A35), (A32), and (A16) in the expression

$$A_4 = \frac{W(1 + f)}{g\rho_4 V_4} \tag{A36}$$

produces

$$\frac{p_4}{p_0} = \sqrt{\frac{\gamma_2 R_4}{R_2 \overline{\gamma}_4}} \frac{\overline{\gamma}_4 - 1}{2} \frac{A_2}{A_4} \frac{M_0^2}{2} \eta_d \alpha\beta \left(\frac{1 + \frac{1}{\gamma_4 M_4^2}}{\lambda} - \frac{\lambda}{1 + \frac{1}{\gamma_4 M_4^2}}\right)(1 + f) \tag{A37}$$

$$\frac{p_4 A_4}{q_0 A_2} = \frac{p_4}{p_0} \frac{p_0}{q_0} \frac{A_4}{A_2} \tag{A38}$$

Combining equations (A18), (A37), and (A38) yields

$$\frac{p_4 A_4}{q_0 A_2} = \sqrt{\frac{\gamma_2 R_0}{\gamma_0 R_2}} \eta_d \alpha\beta \sqrt{\frac{R_4 \overline{\gamma}_4}{R_0 \gamma_0}} \frac{\overline{\gamma}_4 - 1}{2\overline{\gamma}_4} \left(\frac{1 + \frac{1}{\gamma_4 M_4^2}}{\lambda} - \frac{\lambda}{1 + \frac{1}{\gamma_4 M_4^2}}\right)(1 + f) \tag{A39}$$

Solution of equations (A39), (A31), and (A33) gives

$$C_{F_{II}} = \sqrt{\frac{\gamma_2 R_0}{\gamma_0 R_2}}\,\eta_d \alpha \left[\sqrt{\frac{R_4 \bar{\gamma}_4}{R_0 \gamma_0}}\,\beta\lambda(1 + f) - M_0\right] - \frac{p_0 A_0}{q_0 A_2} \tag{A40}$$

Substituting equation (A18) and the continuity equation between stations 0 and 2 in $\frac{p_0 A_0}{q_0 A_2}$ produces

$$\frac{p_0 A_0}{q_0 A_2} = \frac{2}{\gamma_0 M_0^2}\,\frac{\rho_2 V_2}{\rho_0 V_0} \tag{A41}$$

Equation (A41) may be expressed in terms of the perfect gas law and the relationships for Mach number and the speed of sound as follows:

$$\frac{p_0 A_0}{q_0 A_2} = \frac{2}{\gamma_0 M_0^2}\,\frac{p_2}{p_0}\,\frac{M_2}{M_0}\sqrt{\frac{\gamma_2 R_0 T_0}{\gamma_0 R_2 T_2}} \tag{A42}$$

Substituting expressions similar to equations (A5) and (A6) for stations 0 and 2 produces

$$\frac{p_0 A_0}{q_0 A_2} = \frac{2}{\gamma_0 M_0^2}\,\frac{M_2}{M_0}\sqrt{\frac{\gamma_2 R_0}{\gamma_0 R_2}}\,\frac{p_{t2}}{p_{t0}}\,\frac{\left(1 + \frac{\bar{\gamma}_0 - 1}{2} M_0^2\,\frac{\gamma_0}{\bar{\gamma}_0}\right)^{\frac{\bar{\gamma}_0 + 1}{2(\bar{\gamma}_0 - 1)}}}{\left(1 + \frac{\bar{\gamma}_2 - 1}{2} M_2^2\,\frac{\gamma_2}{\bar{\gamma}_2}\right)^{\frac{\bar{\gamma}_2 + 1}{2(\bar{\gamma}_2 - 1)}}} \tag{A43}$$

Substituting equation (A15) in equation (A43)

$$\frac{p_0 A_0}{q_0 A_2} = \sqrt{\frac{R_0 \gamma_2}{R_2 \gamma_0}}\,\frac{1}{\gamma_0 M_0}\,\eta_d \alpha \tag{A44}$$

From equations (A44) and (A40),

$$C_{F_{II}} = \eta_d \sqrt{\frac{\gamma_2 R_0}{\gamma_0 R_2}}\, \alpha \left[\sqrt{\frac{R_4 \bar{\gamma}_4}{R_0 \gamma_0}}\, \beta\lambda(1 + f) - M_0 - \frac{1}{\gamma_0 M_0} \right] \tag{A45}$$

Expressions for the total-temperature ratio and static-pressure ratio for station 4 are given by equations (A34) and (A37), respectively.

Substituting equation (A31) in equation (A35) produces

$$\frac{T_4}{T_0} = \frac{\beta^2}{\frac{\gamma_4}{\bar{\gamma}_4} M_4^2 + \frac{2}{\bar{\gamma}_4 - 1}} \tag{A46}$$

Equation (A31) can be solved for Mach number as follows:

$$M_4 = \sqrt{\frac{-\left[\bar{\gamma}_4(\lambda^2 - 1) + 1\right] \pm \lambda \sqrt{(\bar{\gamma}_4)^2(\lambda^2 - 1) + 1}}{\gamma_4(\lambda^2 - 1)(\bar{\gamma}_4 - 1)}} \tag{A47}$$

Through use of an equation similar to equation (A2) but written for station 4 and equations (A34), (A35), and (A37), it follows that

$$\frac{p_{t4}}{p_0} = \sqrt{\frac{\gamma_2 R_4}{R_2 \bar{\gamma}_4}}\, \frac{\bar{\gamma}_4 - 1}{2}\, \frac{A_2}{A_4}\, \frac{M_0^2}{2}\, \eta_d\, \frac{\alpha\beta}{\lambda}\, \frac{\left(1 + \frac{1}{\gamma_4 M_4^2}\right)^{\frac{\bar{\gamma}_4 + 1}{\bar{\gamma}_4 - 1}} (1 + f)}{\left[\left(1 + \frac{1}{\gamma_4 M_4^2}\right)^2 - \lambda^2\right]^{\frac{1}{\bar{\gamma}_4 - 1}}} \tag{A48}$$

REFERENCES

1. Hall, Newman A.: Ramjet Performance Method. Naval Ordnance Lab. Memo. 9962, Dec. 15, 1948.

2. Ferri, Antonio: Method for Evaluating from Shadow or Schlieren Photographs the Pressure Drag in Two-Dimensional or Axially Symmetrical Flow Phenomena with Detached Shock. NACA TN 1808, 1949.

3. Foa, Joseph V., and Rudinger, George: On the Addition of Heat to a Gas Flowing in a Pipe at Subsonic Speed. Jour. Aero. Sci., vol. 16, no. 2, Feb. 1949, pp. 84-94.

4. Taylor, G. I., and Maccoll, J. W.: The Mechanics of Compressible Fluids. Two-Dimensional Flow at Speeds Less than That of Sound. Vol. III of Aerodynamic Theory, div. H, ch. III, W. F. Durand, ed., Julius Springer (Berlin), 1935, pp. 229-234.

5. Mulready, Richard C.: The Ideal Temperature Rise Due to the Constant Pressure Combustion of Hydrocarbon Fuels. Meteor Rep. UAC-9, United Aircraft Corp., Res. Dept., July 1947.

6. Hodgman, Charles D., and Holmes, Harry N., eds.: Handbook of Chemistry and Physics, Twenty-fourth ed., Chemical Rubber Publishing Co., 1940.

7. Lutz, Otto: Technical Thermodynamics of Dissociating Gas Mixtures. AAF translation No. F-TS-997-RE, Air Materiel Command, Wright Field, Dayton, Ohio, Jan. 1948.

8. Prosen, Edward J., and Rossini, Frederick D.: Heats of Combustion and Formation of the Paraffin Hydrocarbons at 25° C. Res. Paper No. RP1642, Nat. Bur. Standards Jour. Res., vol. 34, no. 3, March 1945, pp. 263-269.

9. Huff, Vearl N., and Calvert, Clyde S.: Charts for the Computation of Equilibrium Composition of Chemical Reactions in the Carbon-Hydrogen-Oxygen-Nitrogen System at Temperatures from 2000° to 5000° K. NACA TN 1653, 1948.

10. Heck, Robert C. H.: The New Specific Heats. Mech. Eng., vol. 62, no. 1, Jan. 1940, p. 10.

11. Keenan, Joseph H., and Kaye, Joseph: A Table of Thermodynamic Properties of Air. Jour. Appl. Mech. vol. 10, no. 3, Sept. 1943, pp. A-123 - A-130.

12. Burcher, Marie A.: Compressible Flow Tables for Air. NACA TN 1592, 1948.

TABLE I.- ILLUSTRATIVE EXAMPLE FOR

STANDARD-AIR CONDITIONS

Step	Variable	Value	Source
		Method I.- Thrust coefficient	
1	M_0	2.00	Given
2	η_d	.80	Do.
3	T_0, $^\circ R$	520	Do.
4	M_2	.20	Do.
5	ΔT_{t2-3}, $^\circ F$	3000	Do.
6	p_{t3}/p_{t2}	.876	Do.
7	M_3	.501	Do.
8	η_n	1.000	Do.
9	$T_{t0}' = T_{t2}'$	.936	Steps 1 and 3 and equation (A5)
10	$\Delta T_{t2-3}/T_0$	5.769	Steps 3 and 5
11	$\eta_d(p_{t3}/p_{t2})\eta_n$	.701	Steps 2, 6, and 8
12	f	.0538	Steps 5 and 9 and figure 8(d)
13	α'	.5690	Steps 1 and 4 and figure 2(j)
14	β'	6.154	Steps 1 and 10 and figure 3(d)
15	θ'	.6196	Steps 1 and 11 and figure 4(f)
16	C_{F_I}'	.9186	Steps 1, 2, 12, 13, 14, and 15 and equation (20)
		Method II.- Internal-force coefficient	
17	λ'	0.6998 (M_4 assumed = 1.0)	Figure 5(a)
18	$C_{F_{II}}'$	.9928	Steps 1, 2, 12, 13, 14, and 17 and equation (21)

TABLE II.- ILLUSTRATIVE EXAMPLE FOR CONDITIONS CORRECTED TO ACCOUNT FOR VARIABLE SPECIFIC-HEAT RATIO AND GAS CONSTANT

[Other steps are given in table I]

Step	Variable	Value	Source
	Method I.- Thrust coefficient		
[a]19	$\gamma_{t0} = \gamma_2$	1.3843	Step 20 and figure 14(a)
20	$T_{t0} = T_{t2}$	930	Steps 1, 3, and 19 and equation (30)
21	f	.0538	Steps 5 and 20 and figure 8(d)
22	α/α'	1.008	Steps 1 and 19 and figure 9
23	α	.575	Steps 13 and 22
24	T_{t5}	3930	Steps 5 and 20
25	$M_{0a\beta}$	1.988	Steps 1 and 19 and figure 10
26	β''	6.152	Steps 10 and 25 and figure 3(d)
27	γ_{t5}	1.2569	Steps 21 and 24 and figure 14(d)
[b]28	T_5	2797	Steps 3, 26, and 34 and figure 16(a)
29	γ_5	1.2724	Steps 21 and 28 and figure 14(c)
30	$\overline{\gamma}_5$	1.2646	Steps 27 and 29
31	$M_{0a\theta}$	1.635	Steps 1, 19, and 30 and figure 11(c)
32	$\left[\left(p_{t3}/p_{t2}\right)\eta_d\eta_n\right]^a$	.772	Steps 11 and 30 and figure 12
33	β	7.560	Steps 26 and 30 and equation (25)
34	θ	.546	Steps 31 and 32 and figure 4(d)
35	R_5	53.72	Steps 21 and 28 and figure 15
36	C_{F_I}	.9836	Steps 1, 2, 19, 21, 23, 30, 33, 34, and 35 and equation (11)
	Method II.- Internal-force coefficient		
37	T_4'	3285	Steps 3 and 26 and equation (34)
[c]38	T_4/T_4'	1.062	Step 41 and figure 17
39	T_4	3489	Steps 37 and 38
40	γ_4	1.2615	Steps 21 and 39 and figure 14(d)
41	$\overline{\gamma}_4$	1.2592	Steps 27 and 40
42	λ''/λ'	.869	Step 41 and figure 13(a)
43	λ/λ''	1.000	Steps 40 and 41 and figure 13(b)
44	λ	.608	Steps 17, 42, and 43
45	β	7.644	Steps 26 and 41 and equation (25)
46	$C_{F_{II}}$	1.054	Steps 1, 2, 19, 21, 23, 35, 41, 44, and 45 and equation (18)

[a]Value of $\gamma = 1.4$ is assumed as a first approximation in trial-and-error process.

[b]Note that T_5 depends on θ (step 34), which can be first approximated by using γ_{t5} (step 27) in place of $\overline{\gamma}_5$ (step 30) to obtain step 31 and 32.

[c]Note that T_4/T_4' (step 38) depends on $\overline{\gamma}_4$ (step 41), which can be first approximated by using γ_{t4} (step 27).

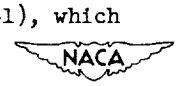

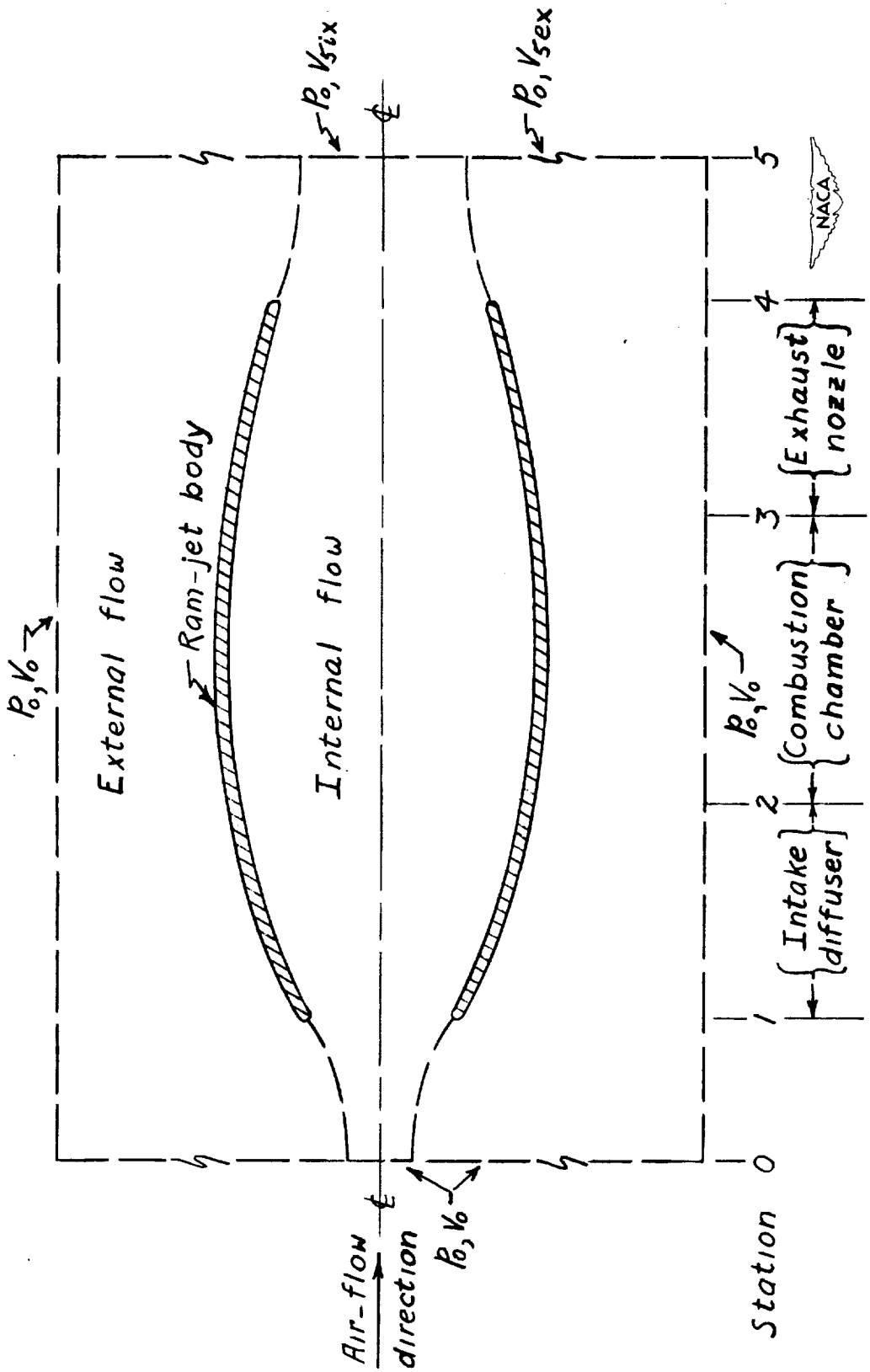

Figure 1.- Sketch of configuration used in analysis.

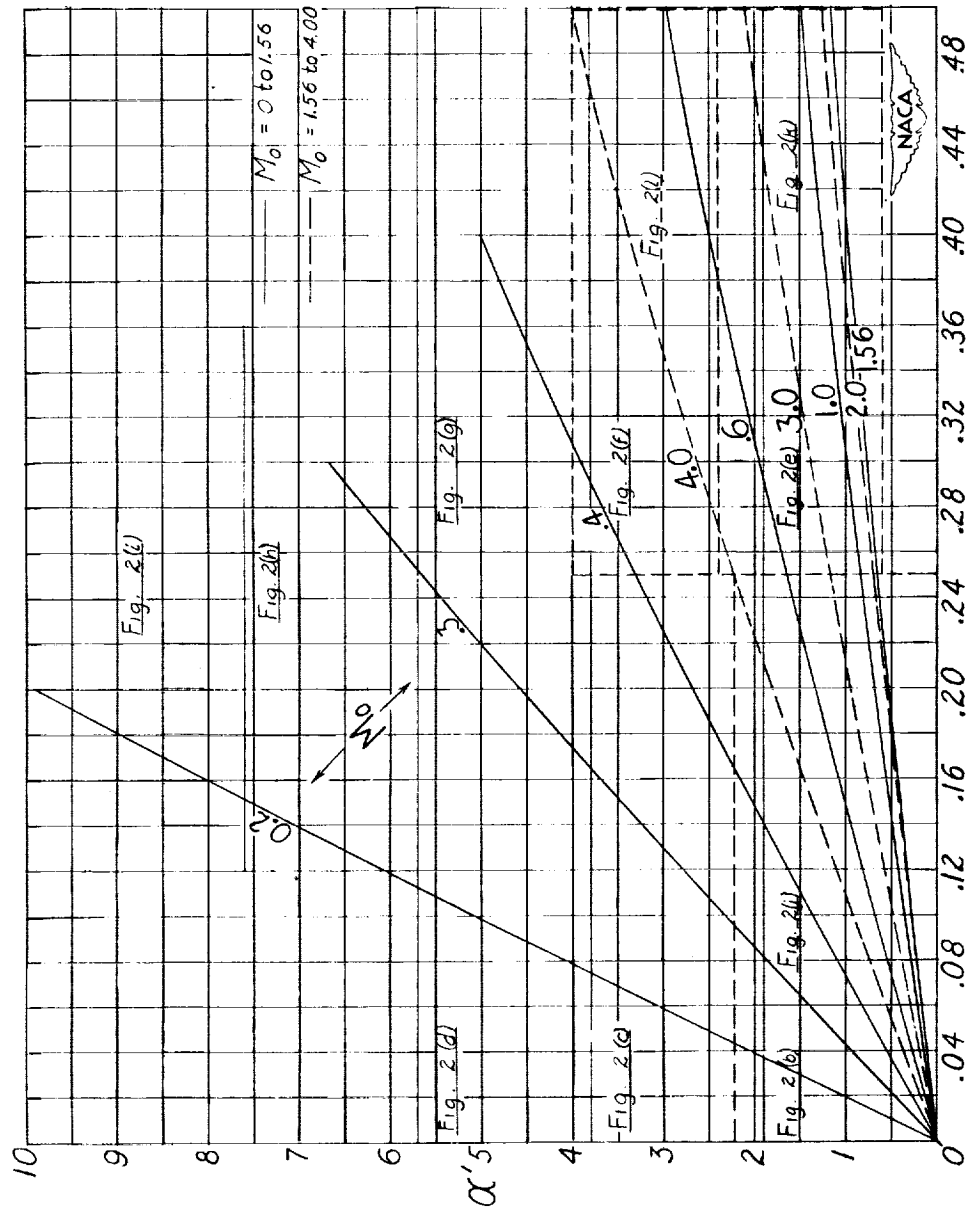

(a) Master plot.

Figure 2.- Mass-flow parameter α'.

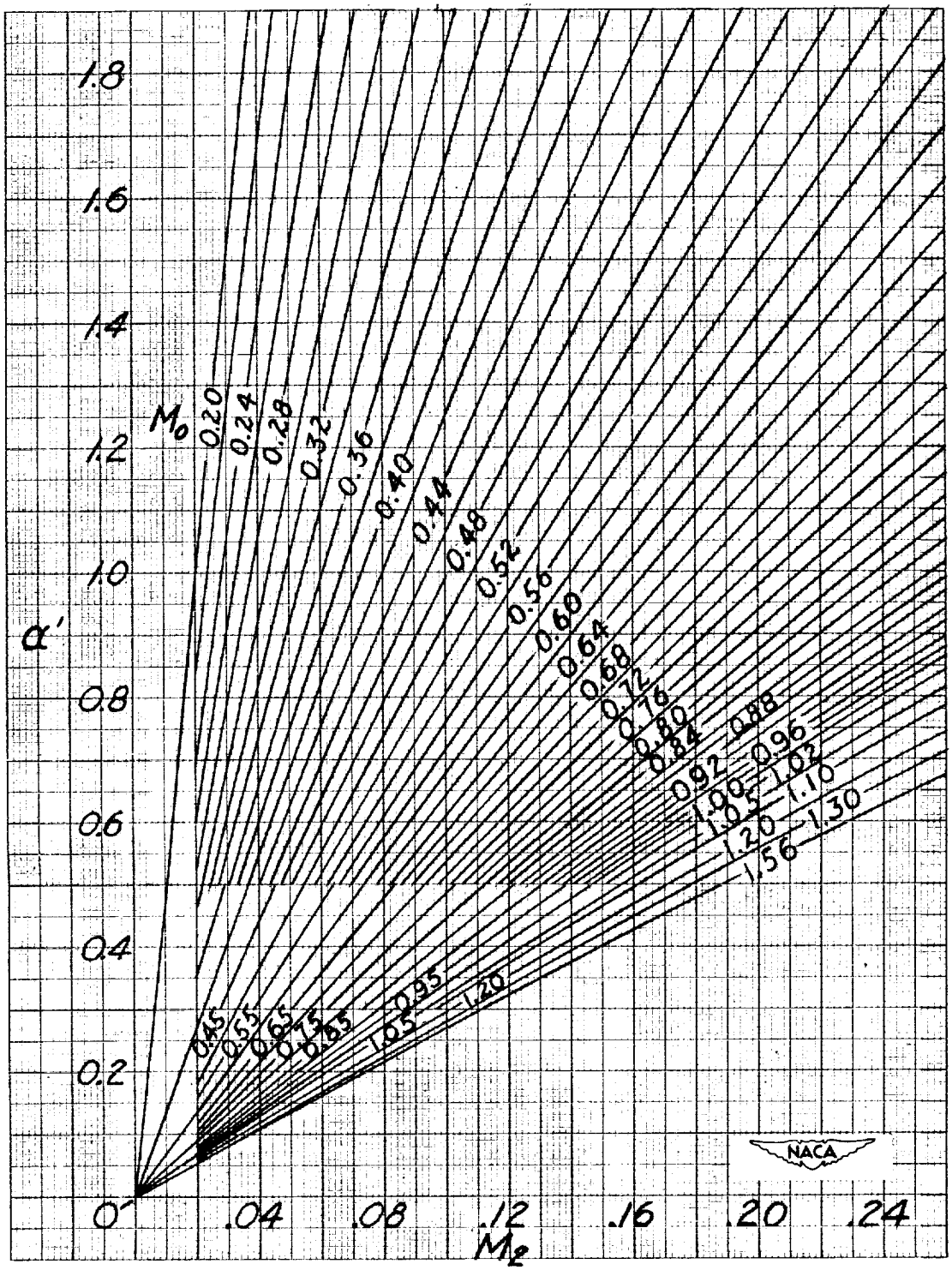

(b) M_0 = 0 to 1.56; M_2 = 0 to 0.25; α' = 0 to 1.90.

Figure 2.- Continued.

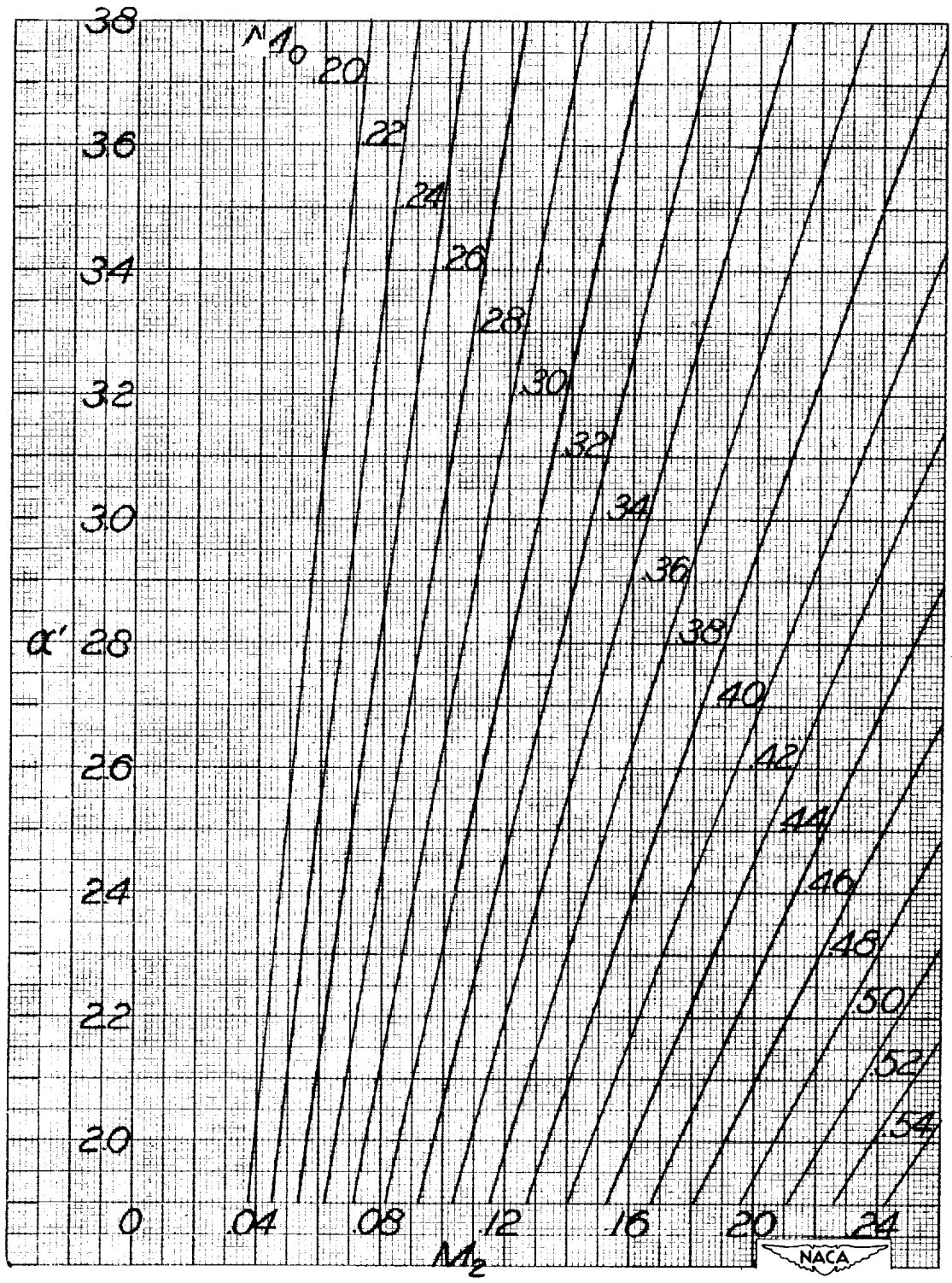

(c) M_0 = 0 to 0.54; M_2 = 0 to 0.25; α' = 1.90 to 3.80.

Figure 2.- Continued.

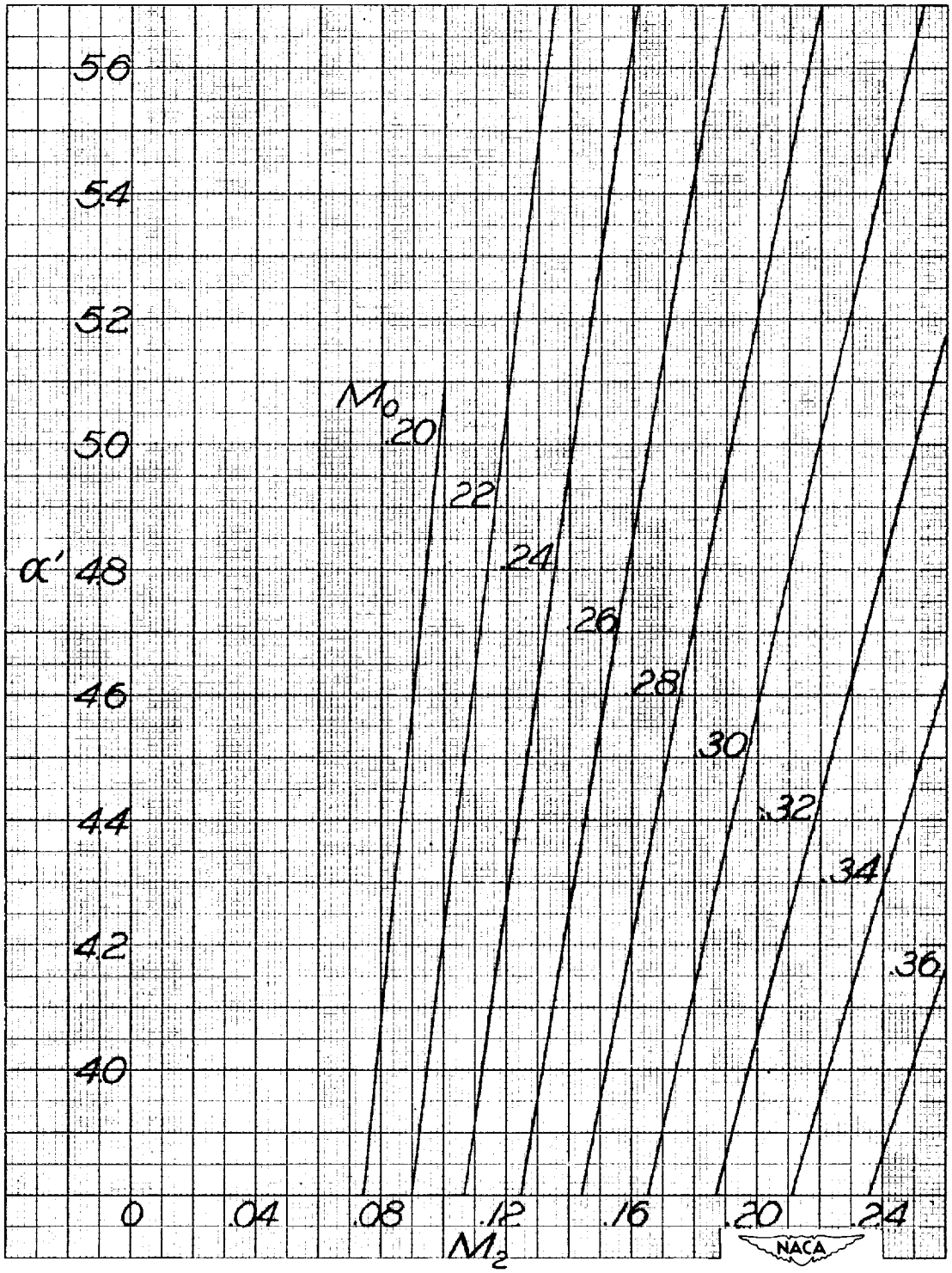

(d) M_0 = 0 to 0.36; M_2 = 0 to 0.25; α' = 3.80 to 5.70.

Figure 2.- Continued.

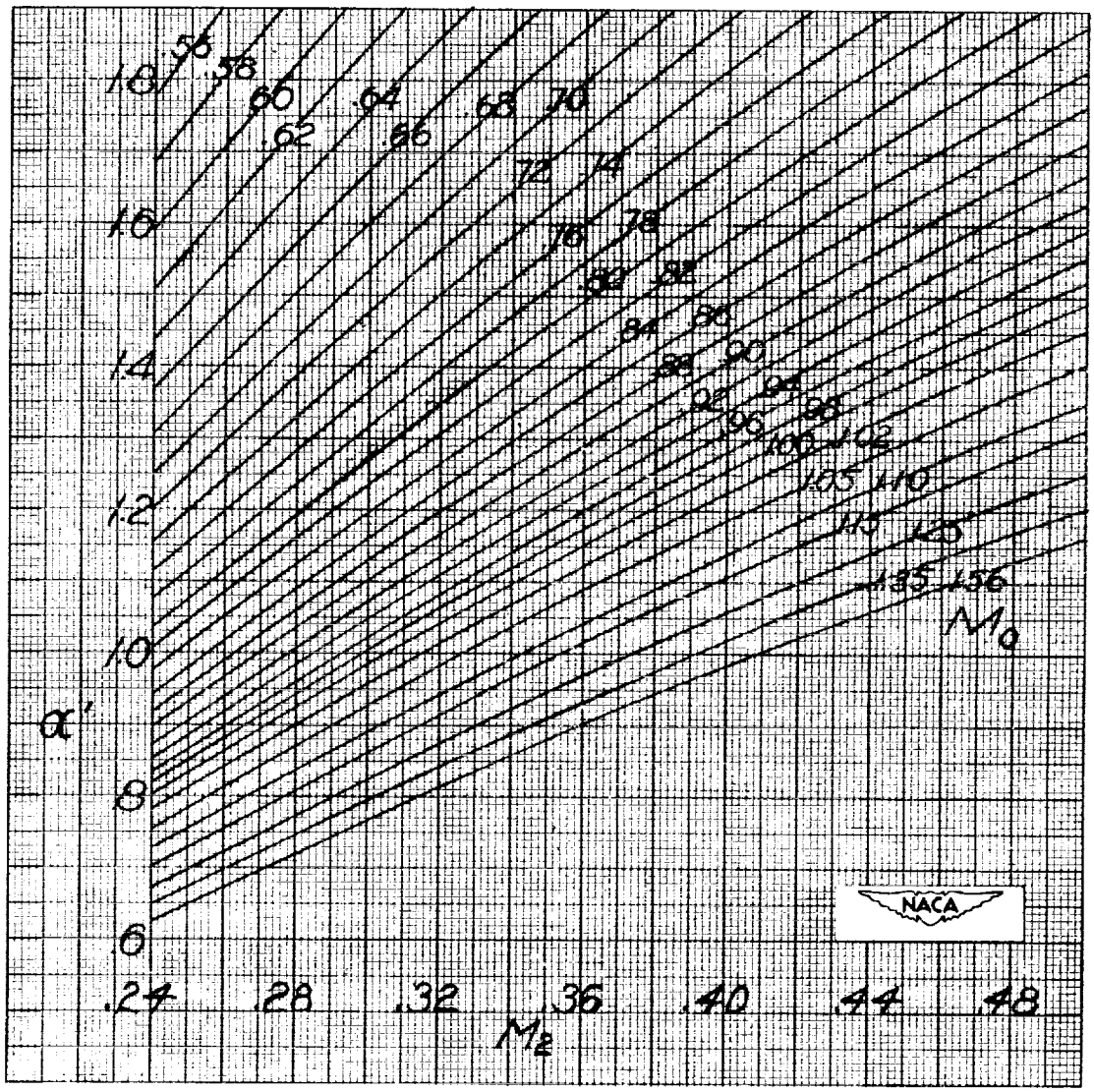

(e) M_0 = 0.56 to 1.56; M_2 = 0.24 to 0.50; α' = 0 to 1.90.

Figure 2.- Continued.

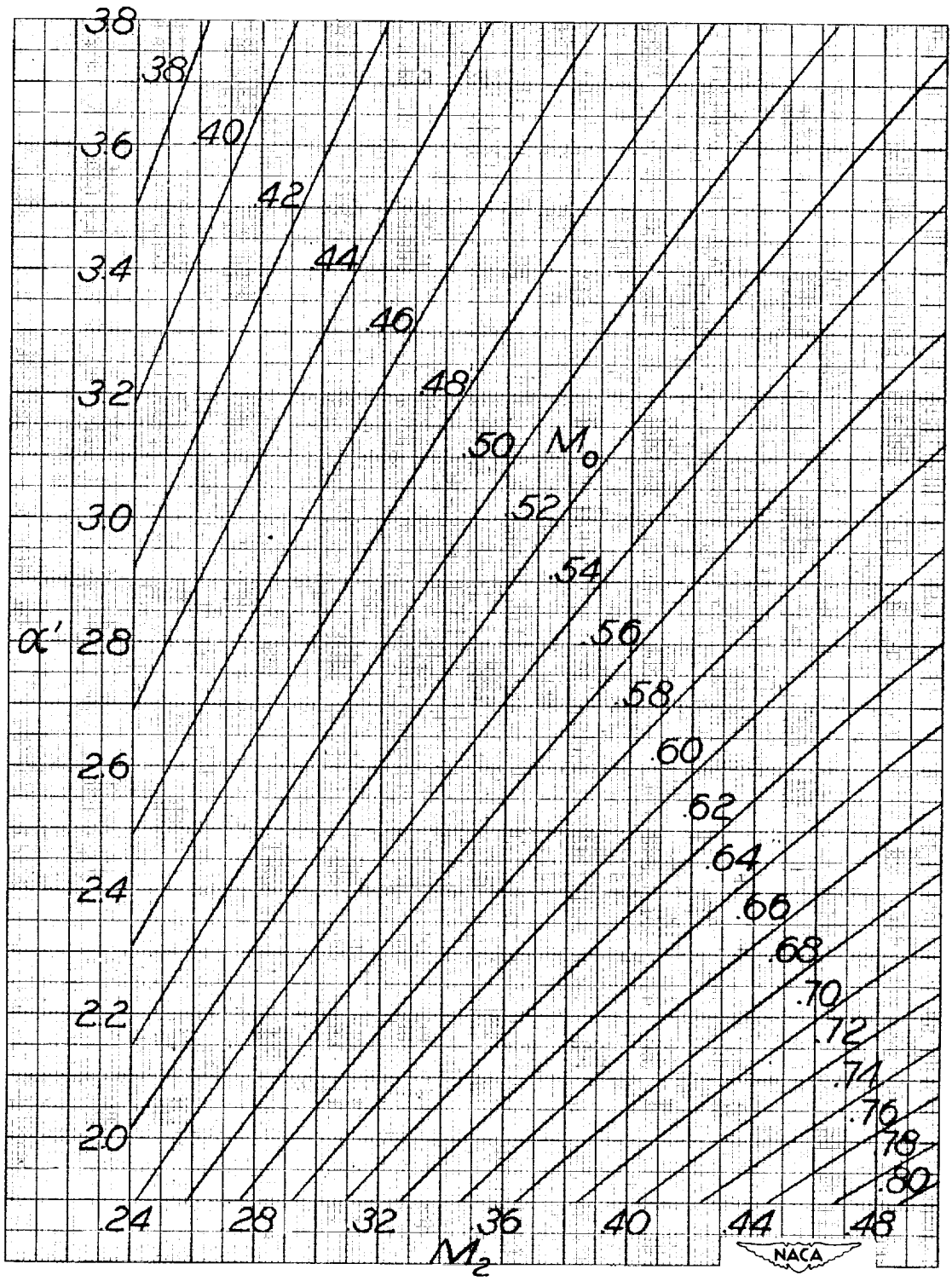

(f) M_0 = 0.38 to 0.80; M_2 = 0.24 to 0.50; α' = 1.90 to 3.80.

Figure 2.- Continued.

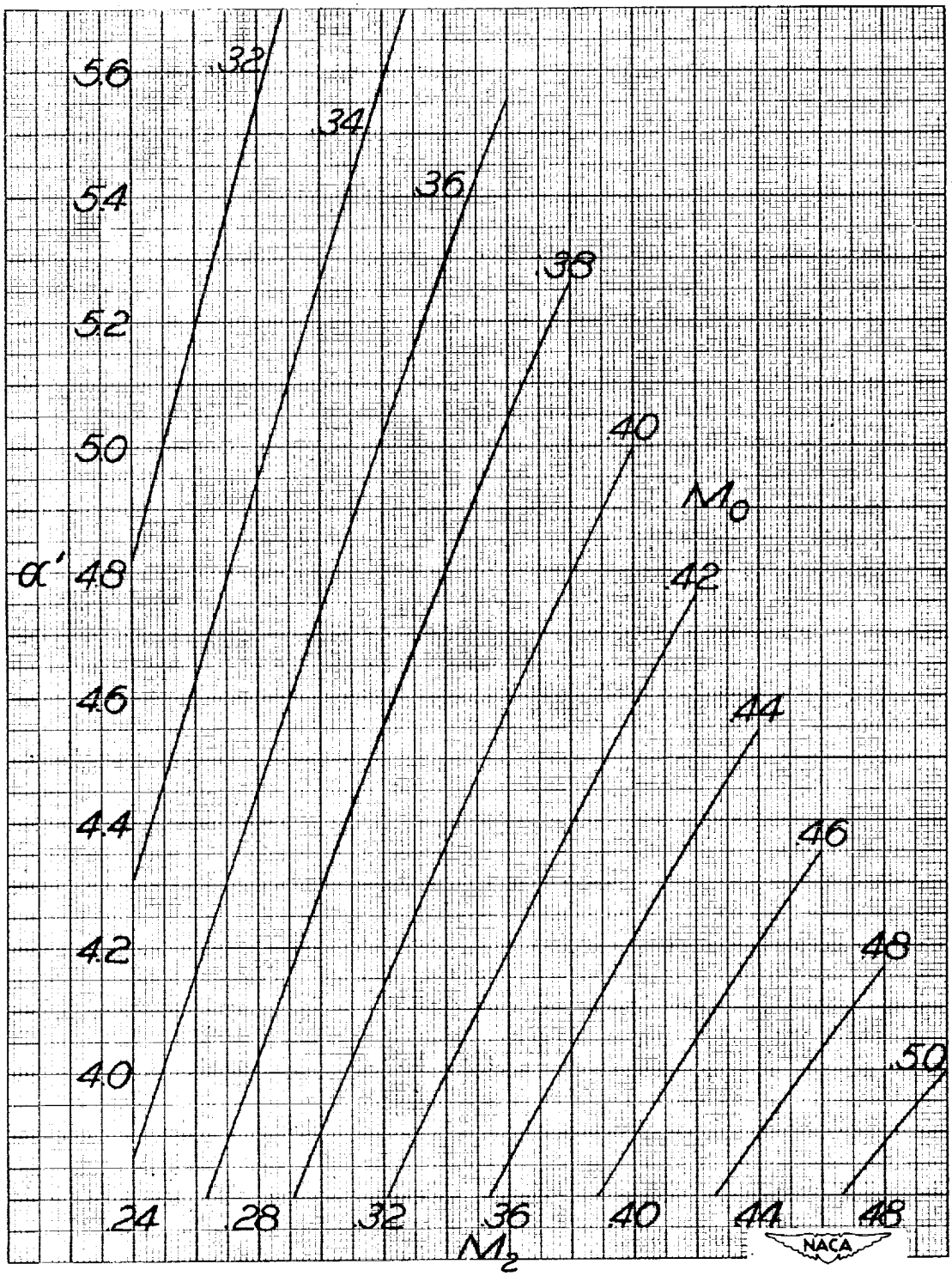

(g) M_0 = 0.32 to 0.50; M_2 = 0.24 to 0.50; α' = 3.80 to 5.70.

Figure 2.- Continued.

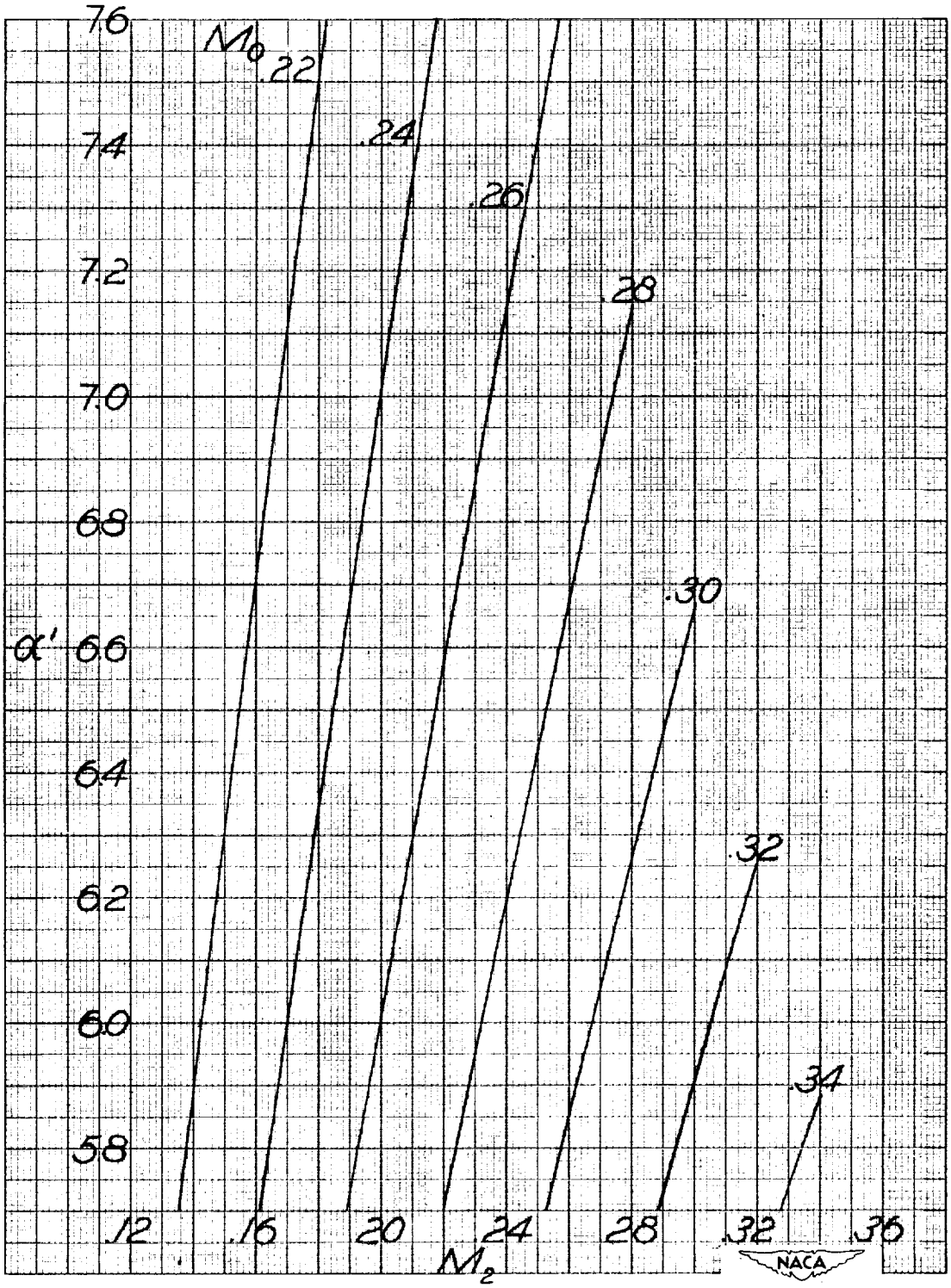

(h) M_0 = 0.22 to 0.34; M_2 = 0.12 to 0.36; α' = 5.70 to 7.60.

Figure 2.- Continued.

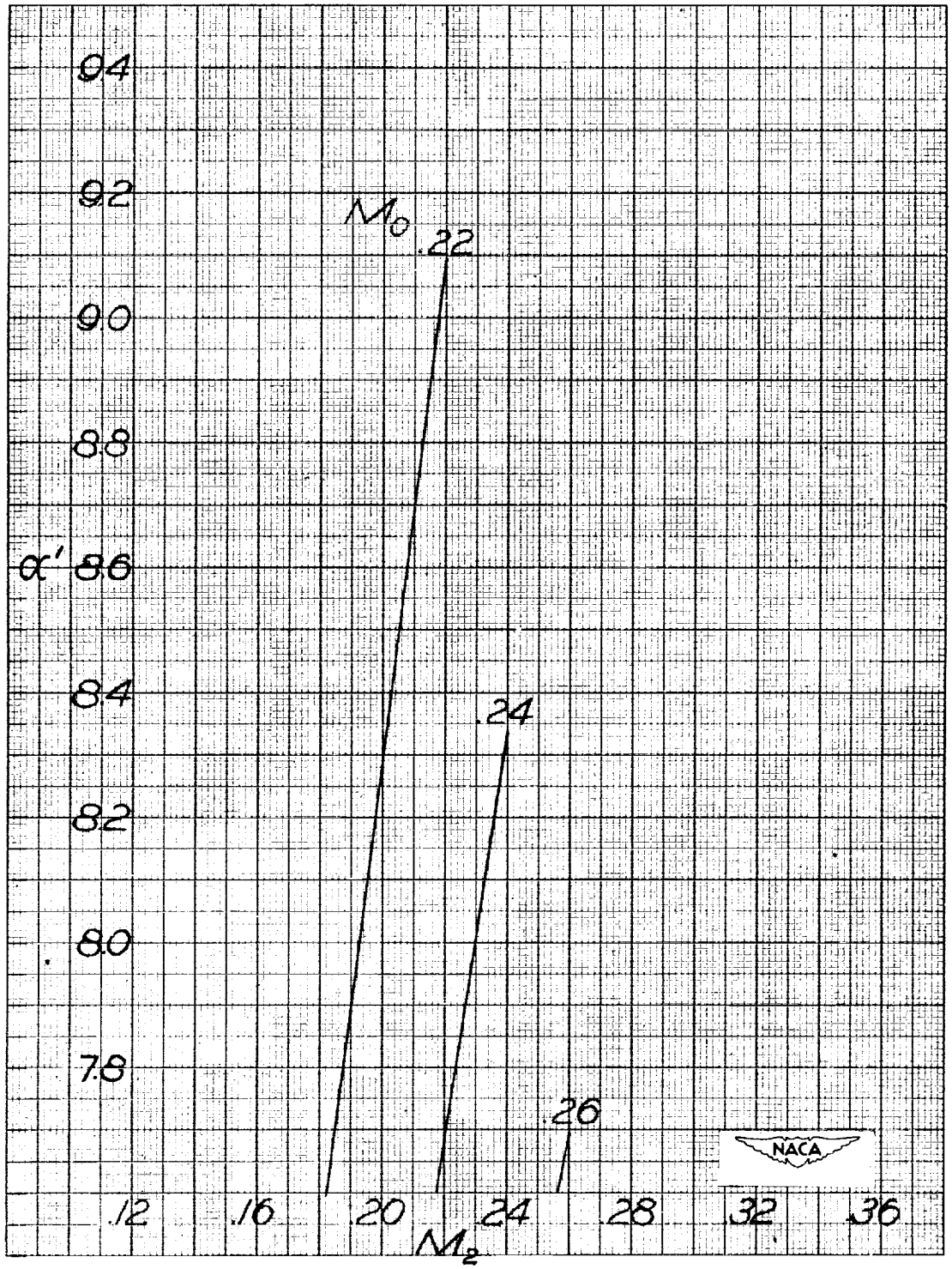

(i) M_0 = 0.22 to 0.26; M_2 = 0.12 to 0.36; α' = 7.60 to 9.40.

Figure 2.- Continued.

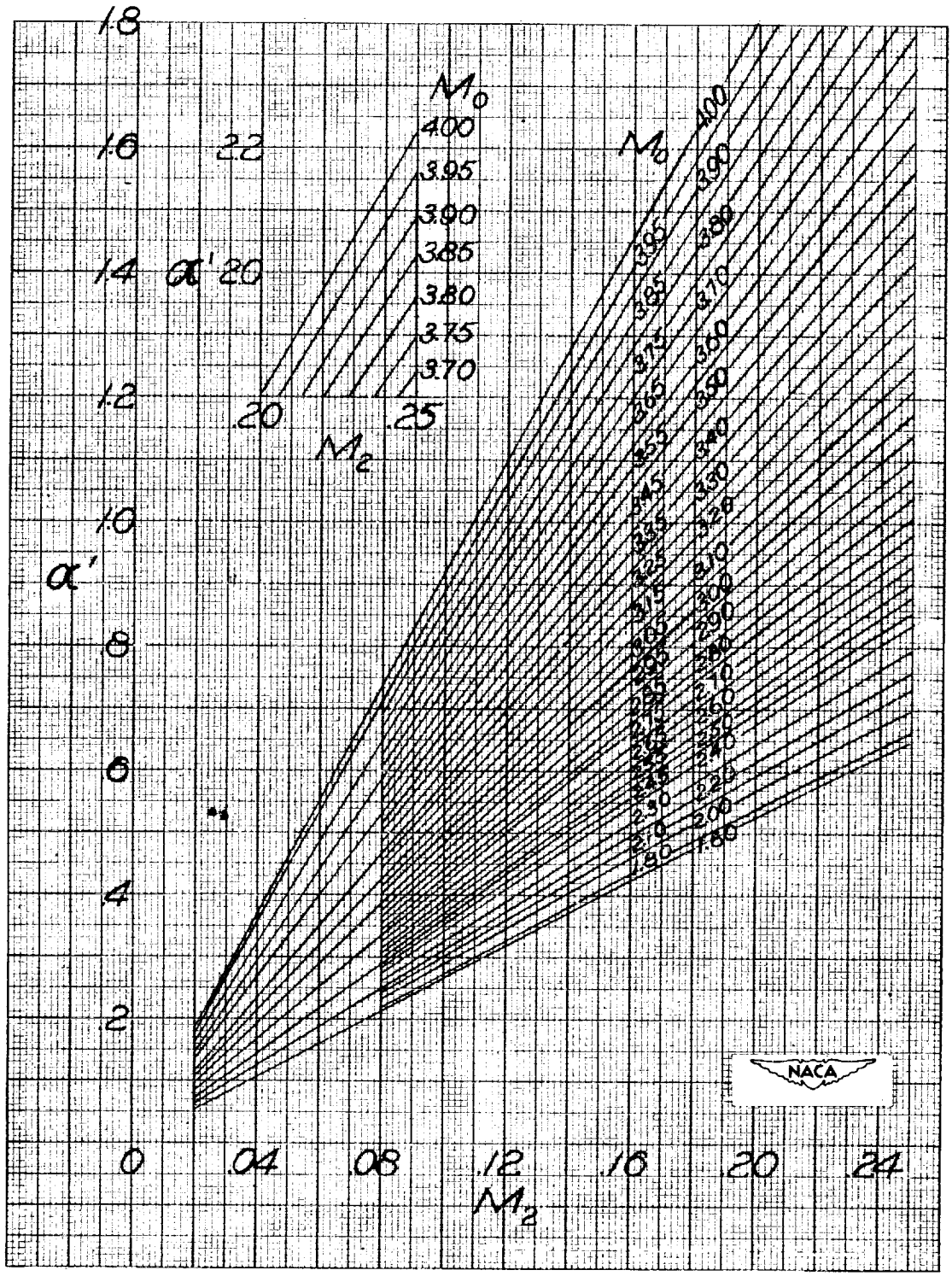

(j) M_0 = 1.60 to 4.00; M_2 = 0 to 0.25; α' = 0 to 2.20.

Figure 2.- Continued.

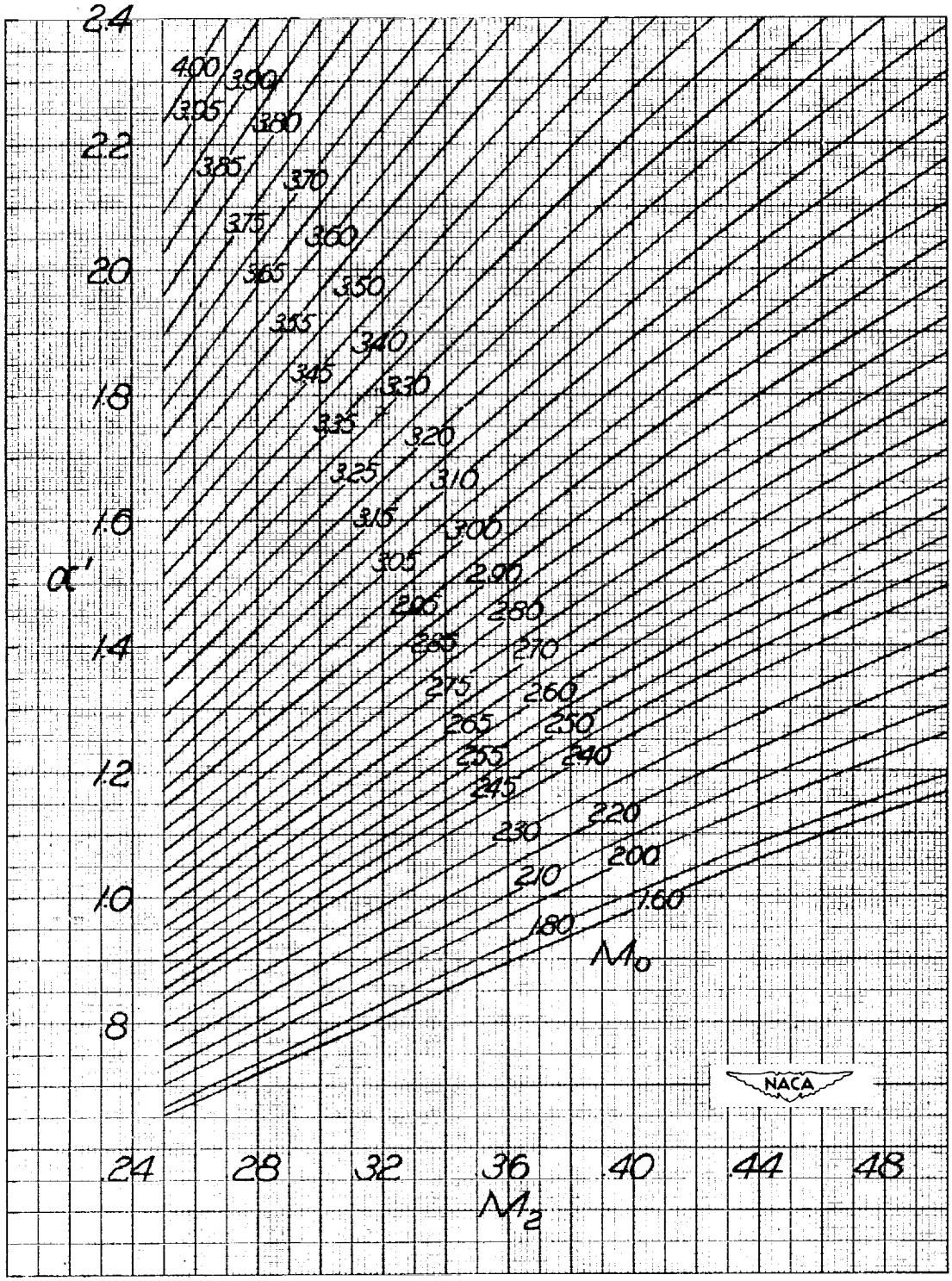

(k) M_0 = 1.60 to 4.00; M_2 = 0.25 to 0.50; α' = 0.60 to 2.40.

Figure 2.- Continued.

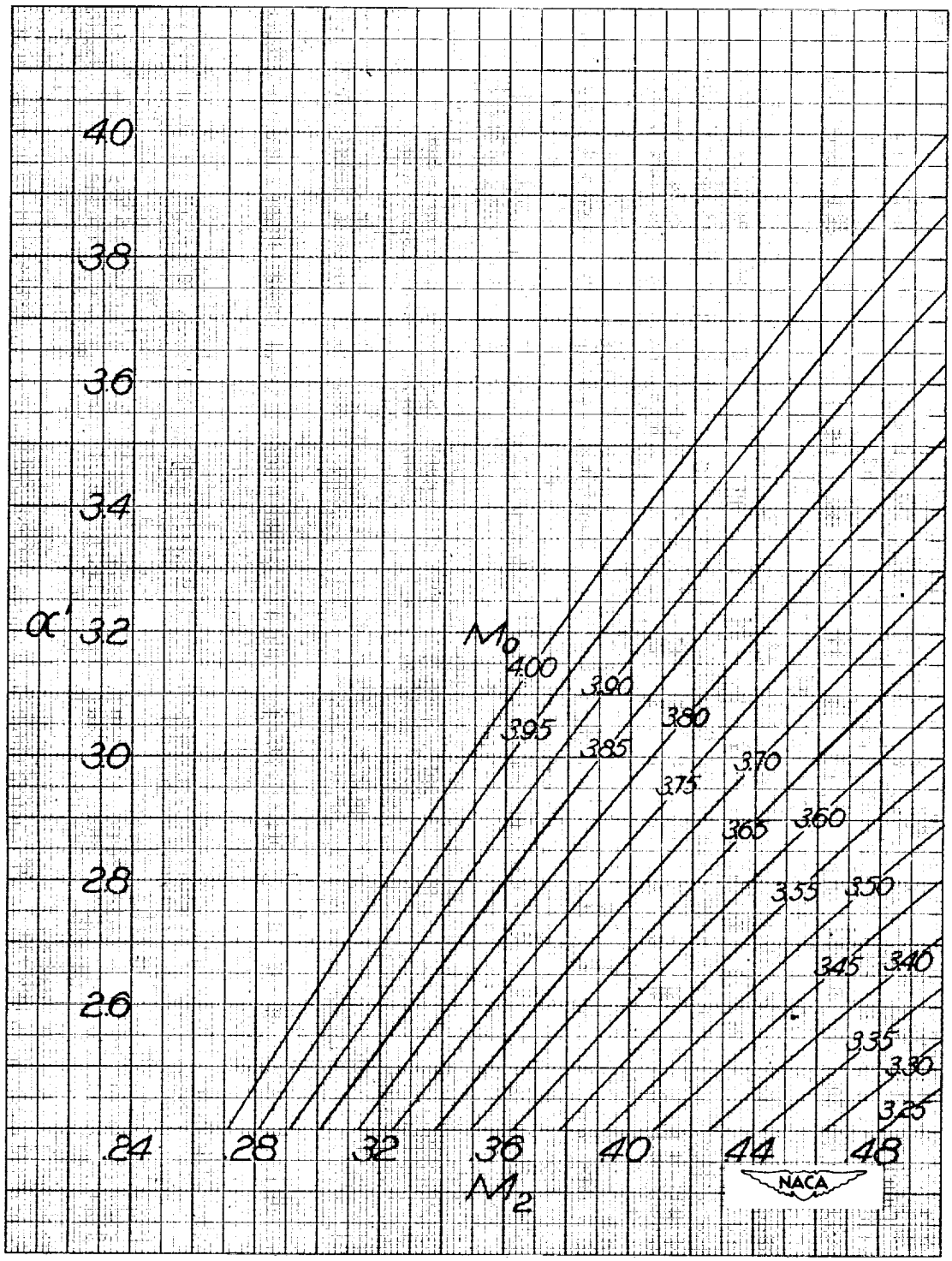

(l) M_0 = 3.25 to 4.00; M_2 = 0.25 to 0.50; α' = 2.40 to 4.00.

Figure 2.- Concluded.

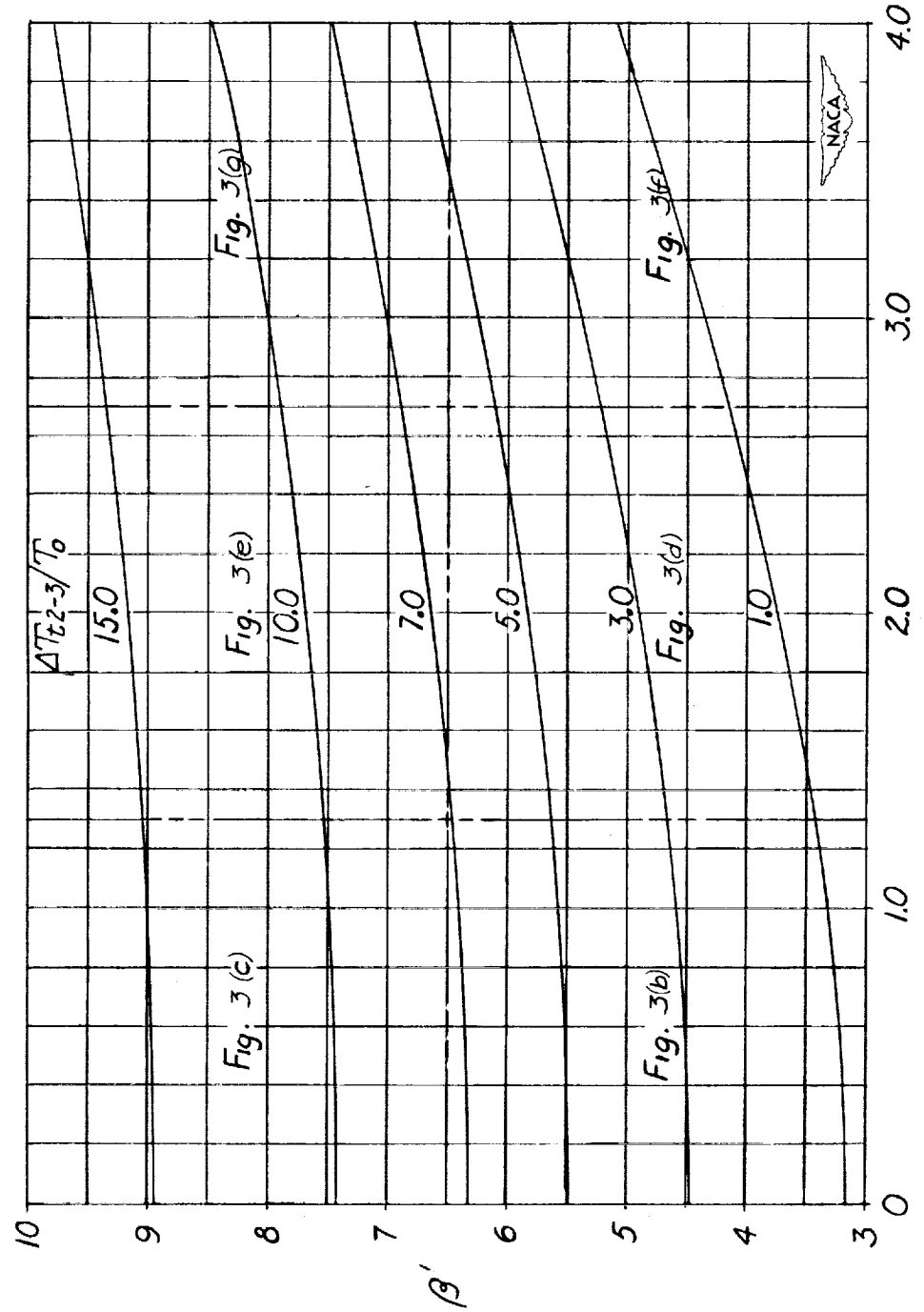

(a) Master plot.

Figure 3.- Heat-addition parameter β'.

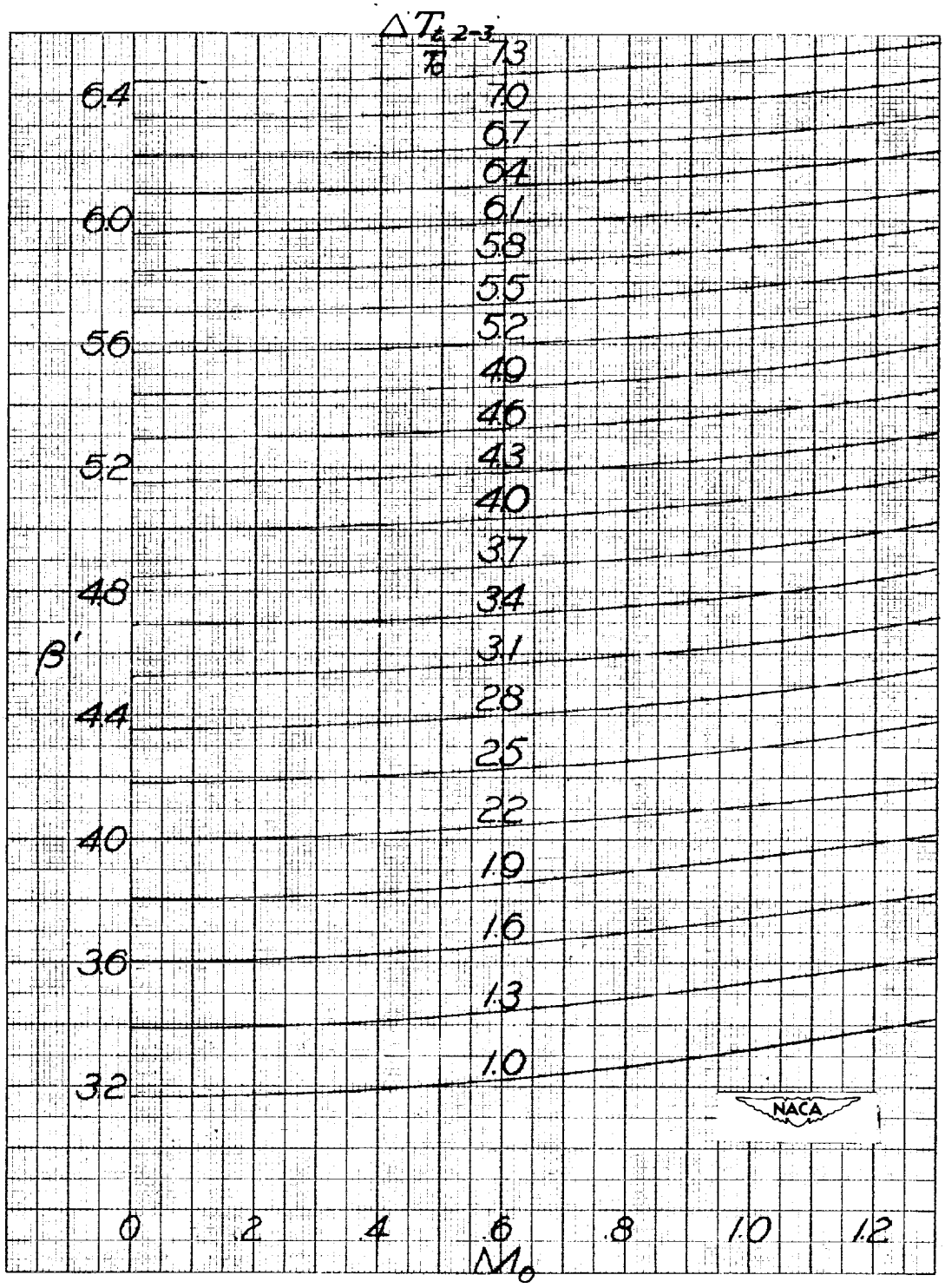

(b) M_0 = 0 to 1.30; $\frac{\Delta T_{t2-3}}{T_0}$ = 1.00 to 7.30; β' = 2.80 to 6.60.

Figure 3.- Continued.

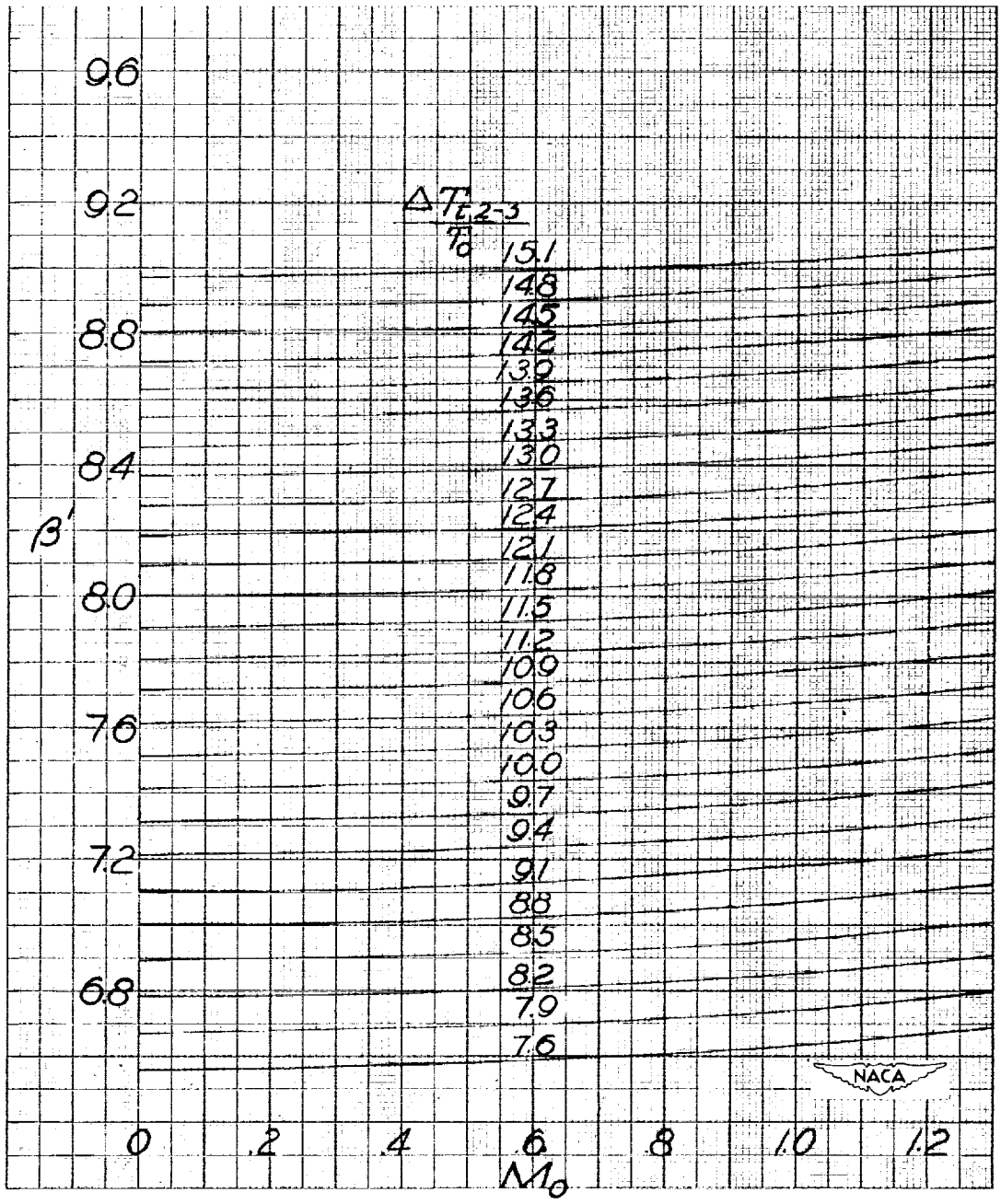

(c) M_0 = 0 to 1.30; $\frac{\Delta T_{t2-3}}{T_0}$ = 7.6 to 15.1; β' = 6.40 to 9.20.

Figure 3.- Continued.

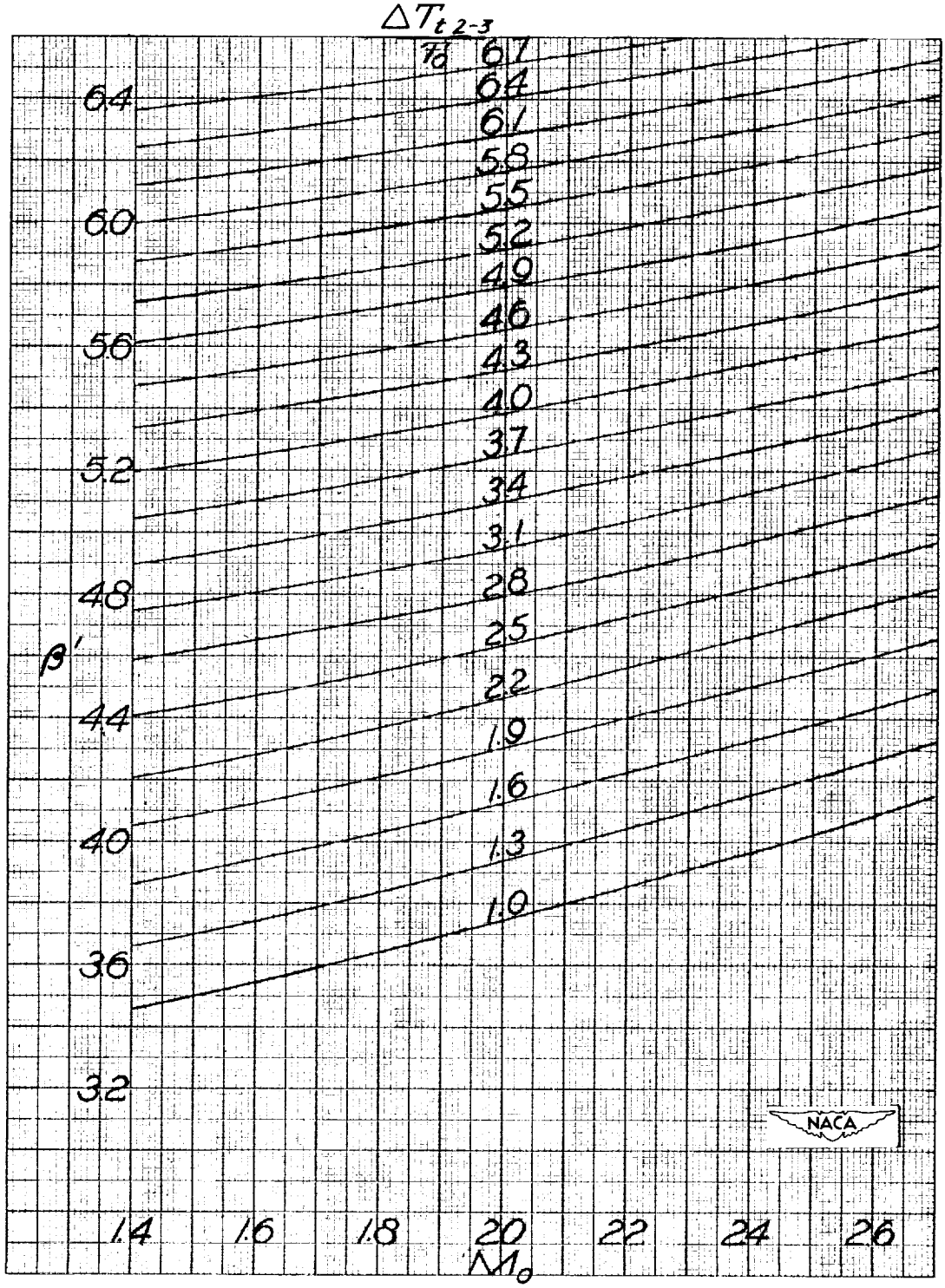

(d) M_0 = 1.40 to 2.70; $\frac{\Delta T_{t2-3}}{T_0}$ = 1.00 to 6.70; β' = 3.40 to 6.60.

Figure 3.- Continued.

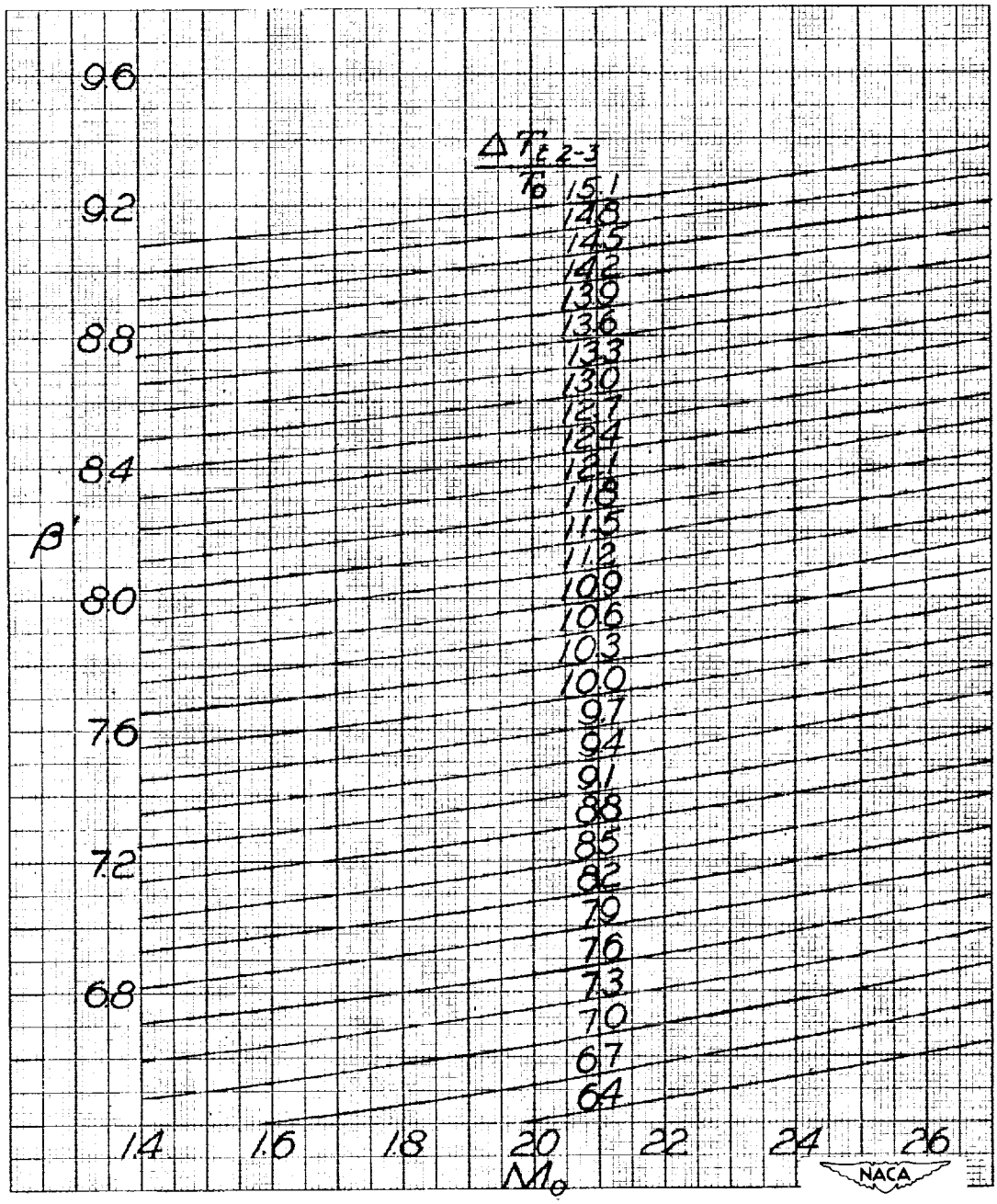

(e) M_0 = 1.40 to 2.70; $\frac{\Delta T_{t2-3}}{T_0}$ = 6.40 to 15.10; β' = 6.40 to 9.40.

Figure 3.- Continued.

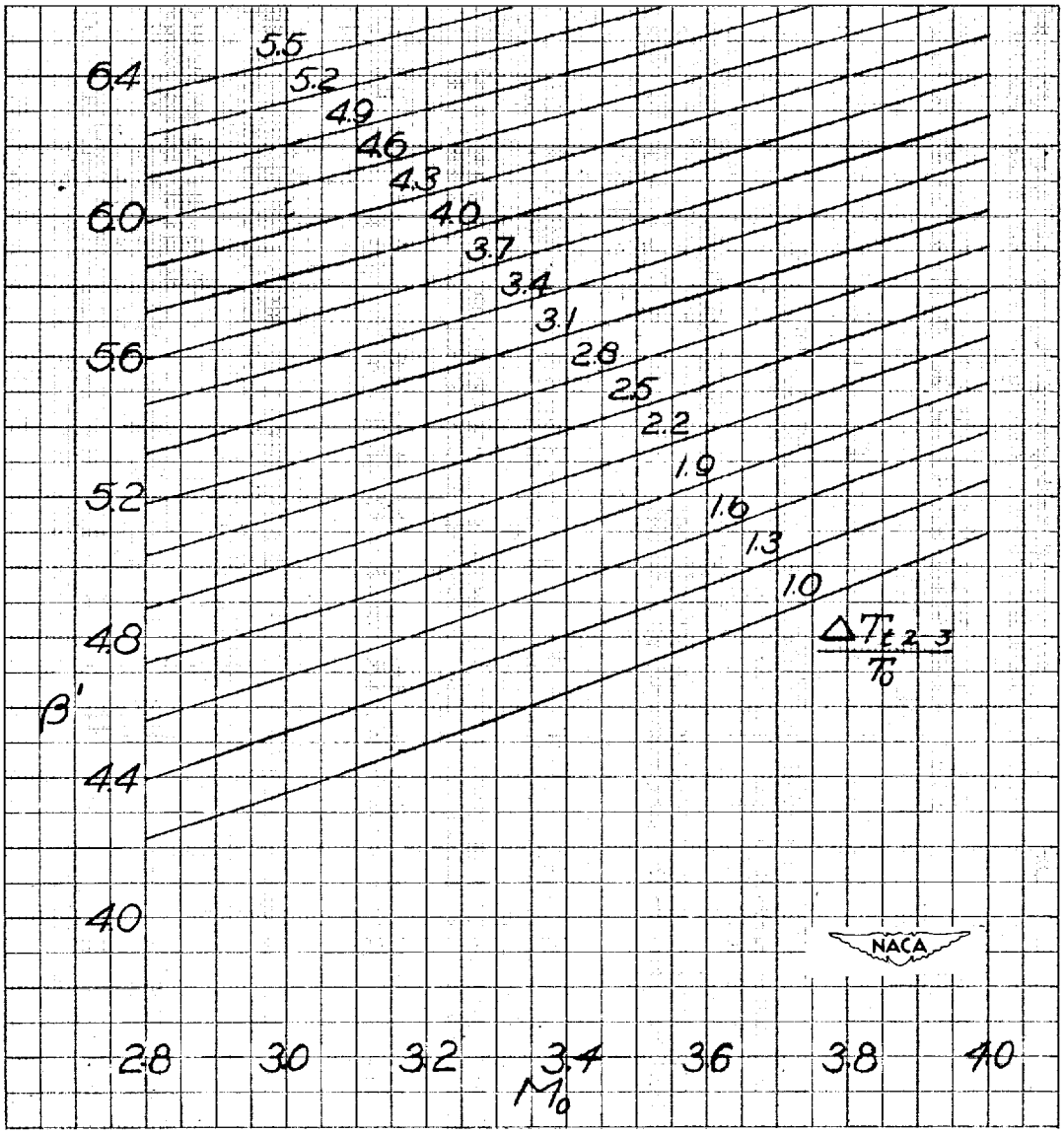

(f) M_0 = 2.80 to 4.00; $\frac{\Delta T_{t2-3}}{T_0}$ = 1.00 to 5.50; β' = 4.00 to 6.60.

Figure 3.- Continued.

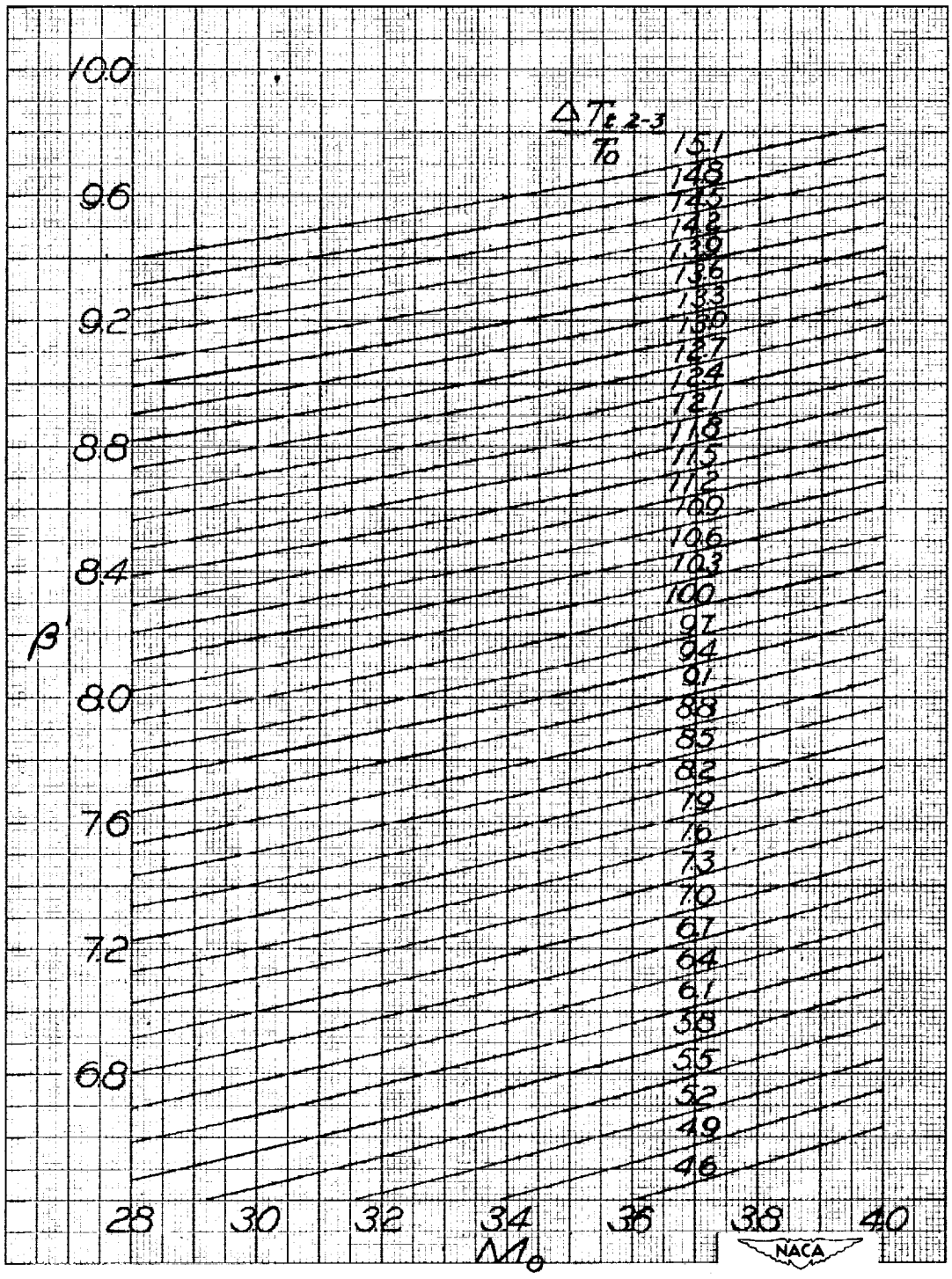

(g) M_0 = 2.80 to 4.00; $\frac{\Delta T_{t2-3}}{T_0}$ = 4.60 to 15.10; β' = 6.40 to 10.00.

Figure 3.- Concluded.

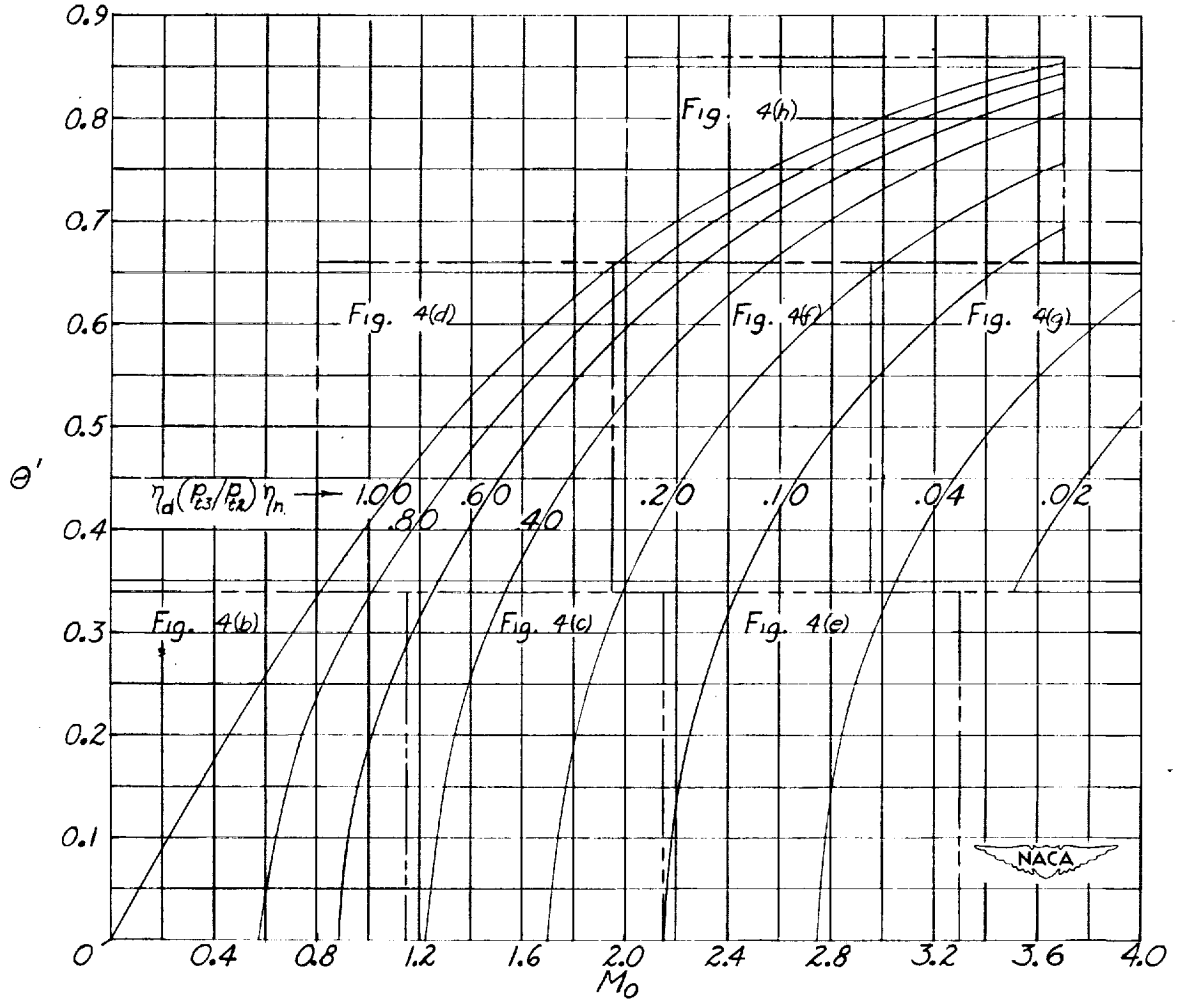

(a) Master plot.

Figure 4.- Pressure-loss parameter θ'.

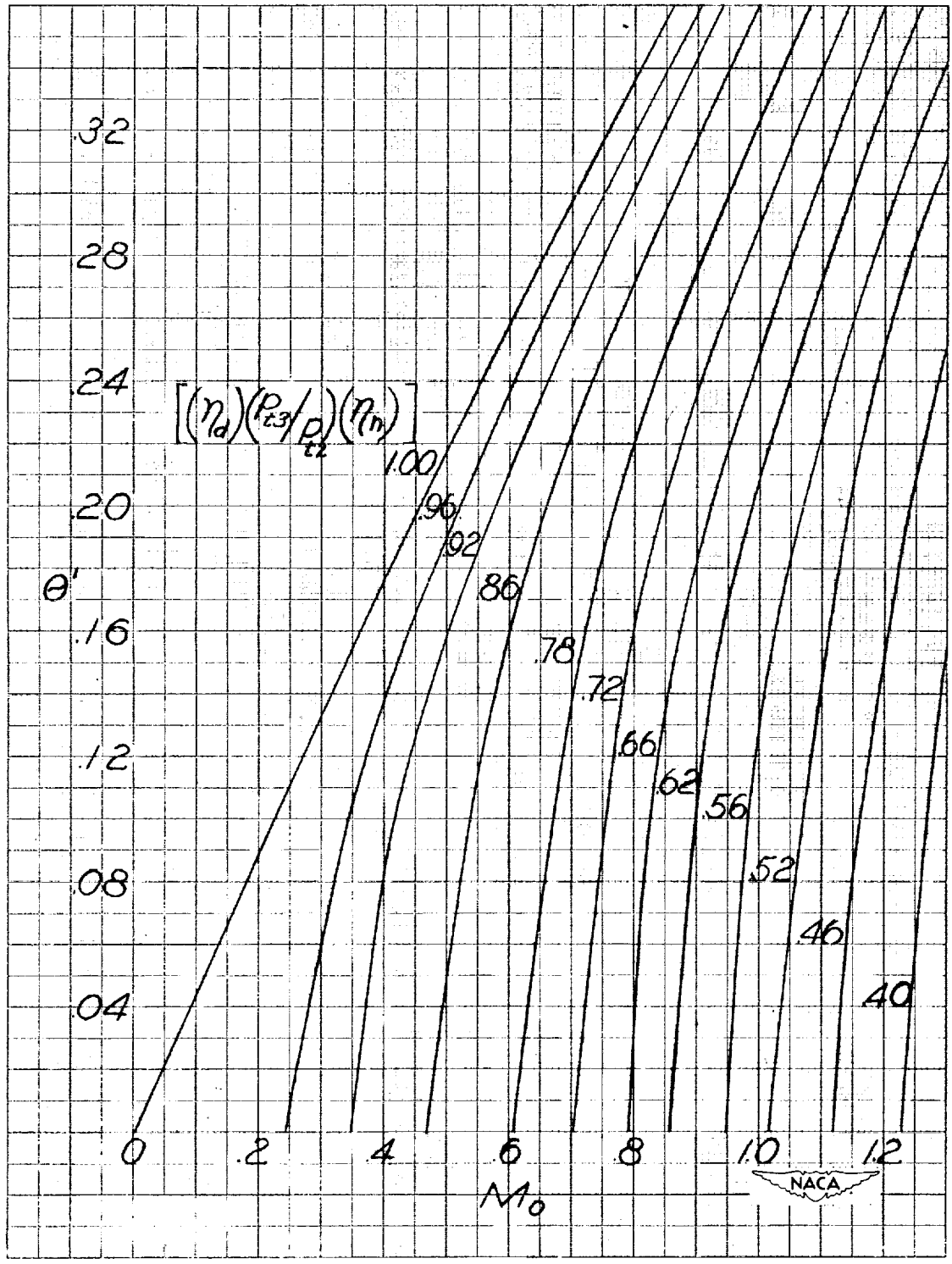

(b) M_0 = 0 to 1.30; $\eta_d \left(\frac{p_{t3}}{p_{t2}}\right) \eta_n$ = 0.40 to 1.00; θ' = 0 to 0.36.

Figure 4.- Continued.

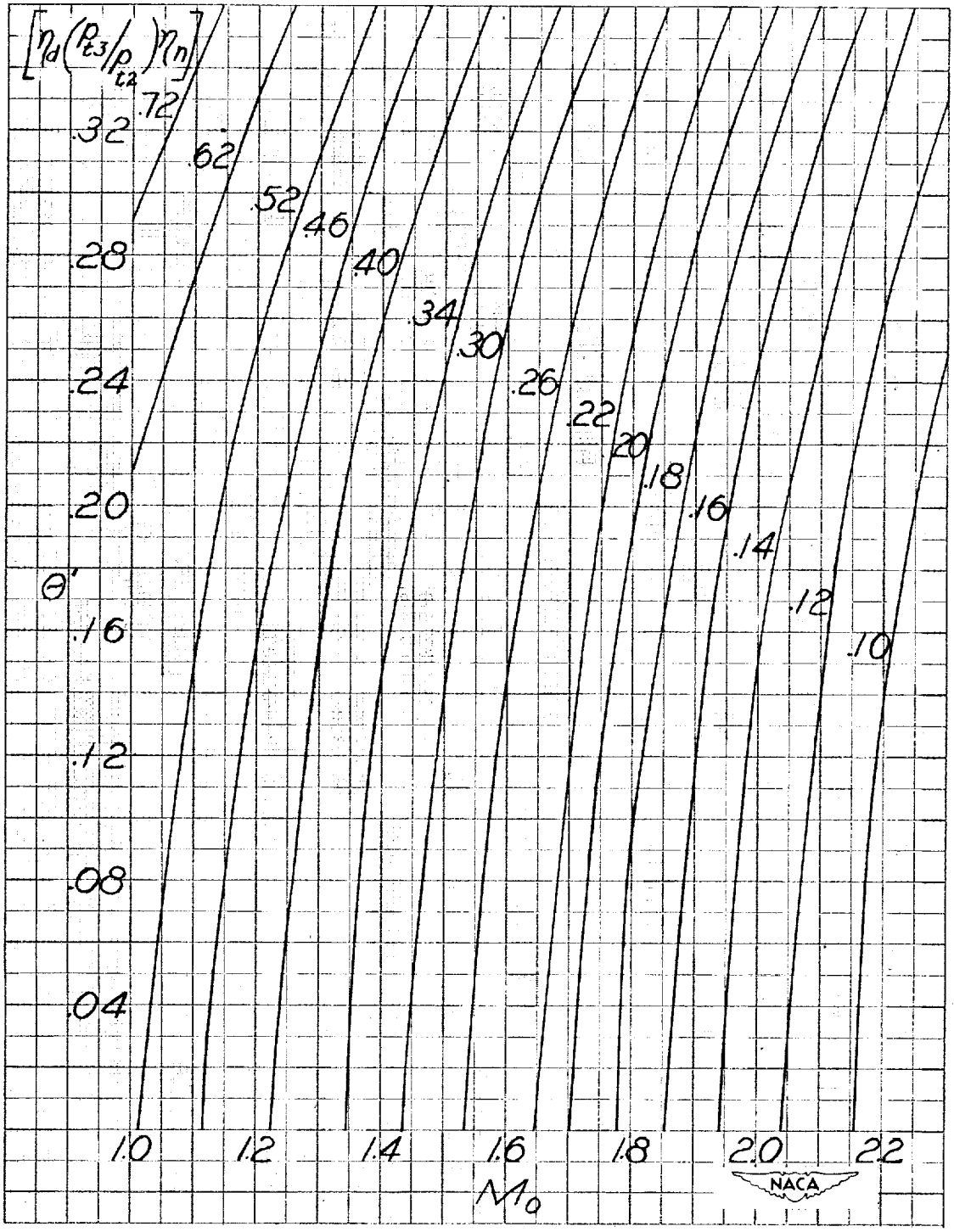

(c) M_0 = 1.00 to 2.30; $\eta_d \left(\frac{p_{t3}}{p_{t2}}\right) \eta_n$ = 0.10 to 0.72; θ' = 0 to 0.36.

Figure 4.- Continued.

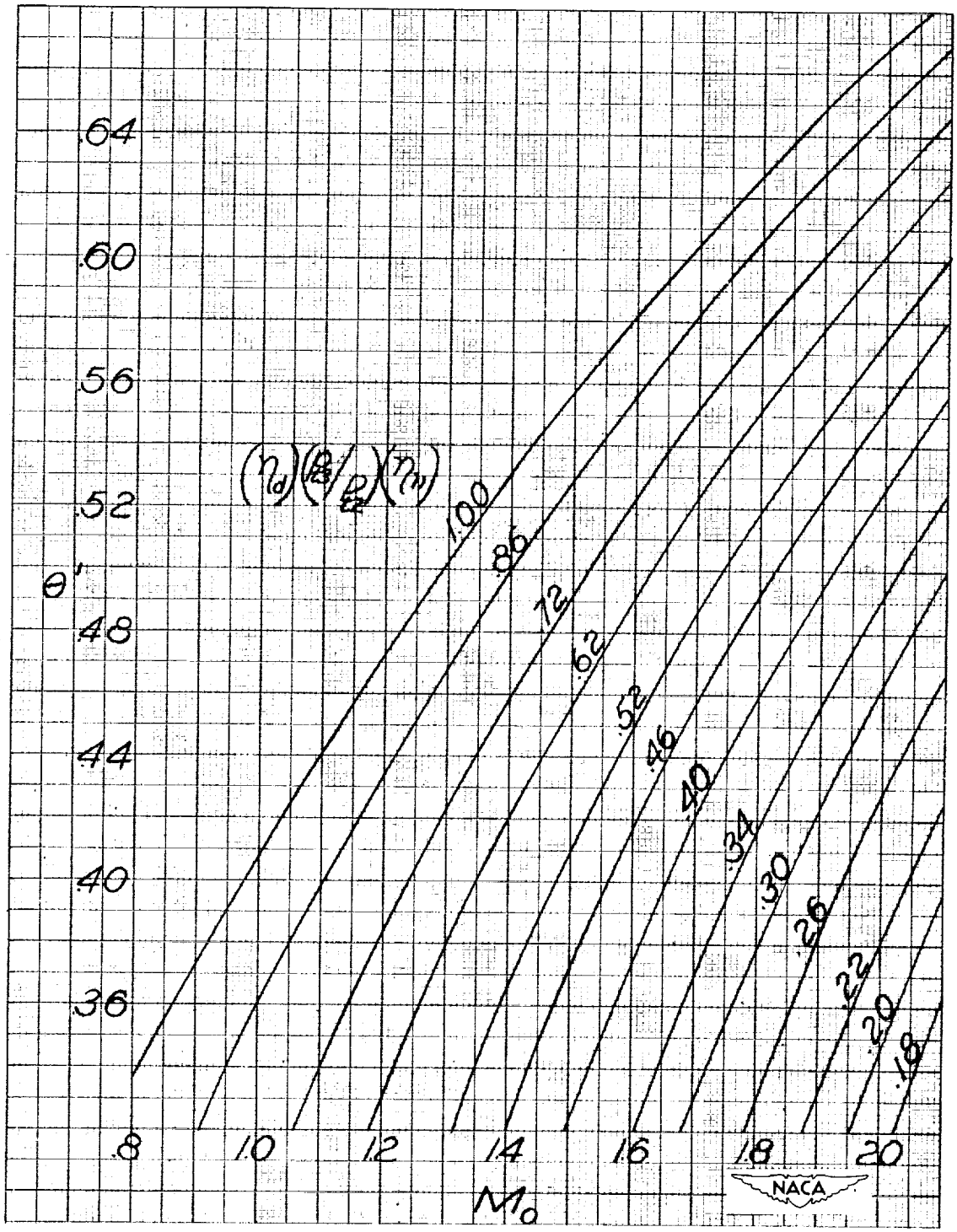

(d) M_0 = 0.80 to 2.10; $\eta_d \left(\frac{p_{t3}}{p_{t2}}\right) \eta_n$ = 0.18 to 1.00; θ' = 0.32 to 0.68.

Figure 4.- Continued.

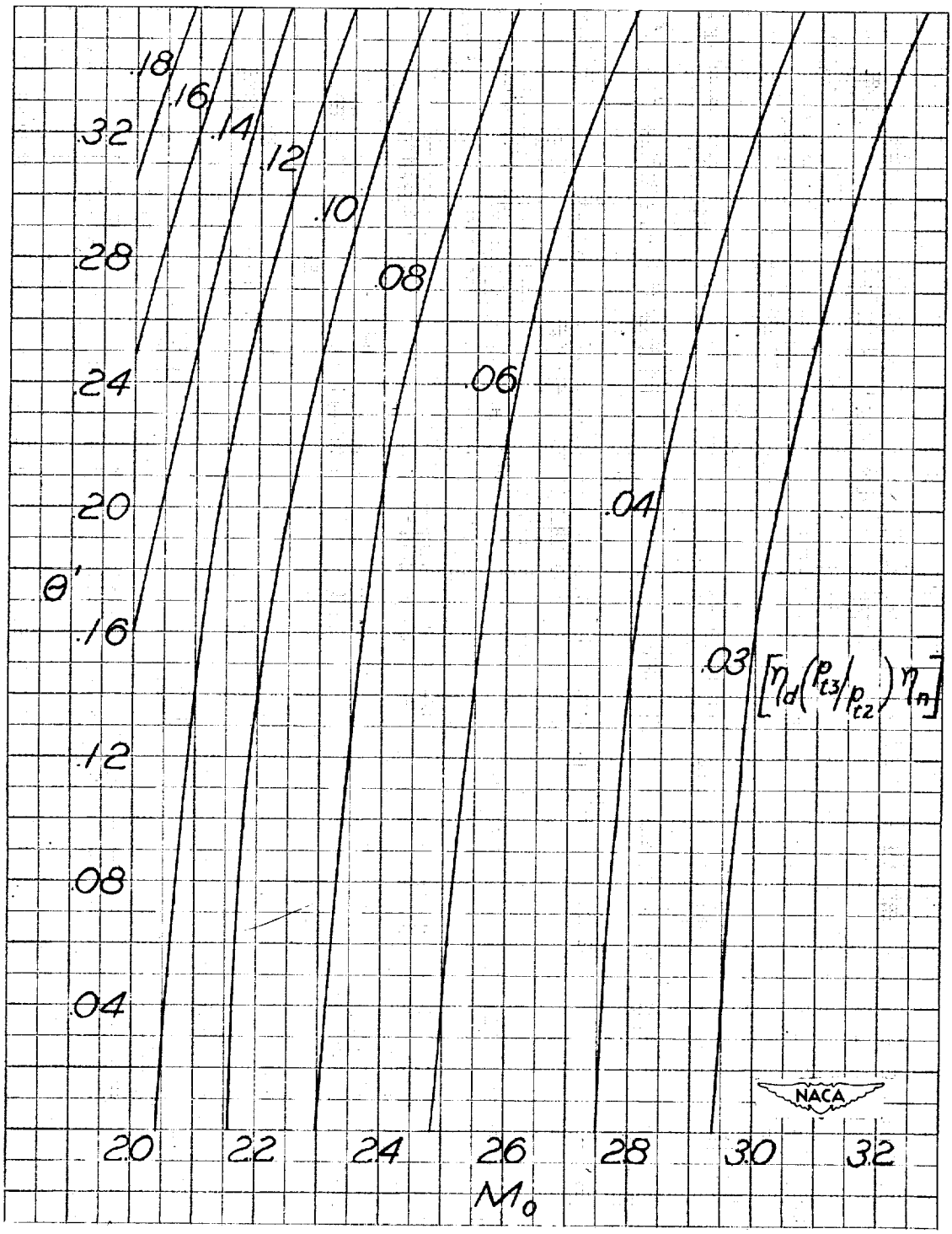

(e) M_0 = 2.00 to 3.30; $\eta_d \left(\frac{p_{t3}}{p_{t2}}\right) \eta_n$ = 0.03 to 0.18; θ' = 0 to 0.36.

Figure 4.- Continued.

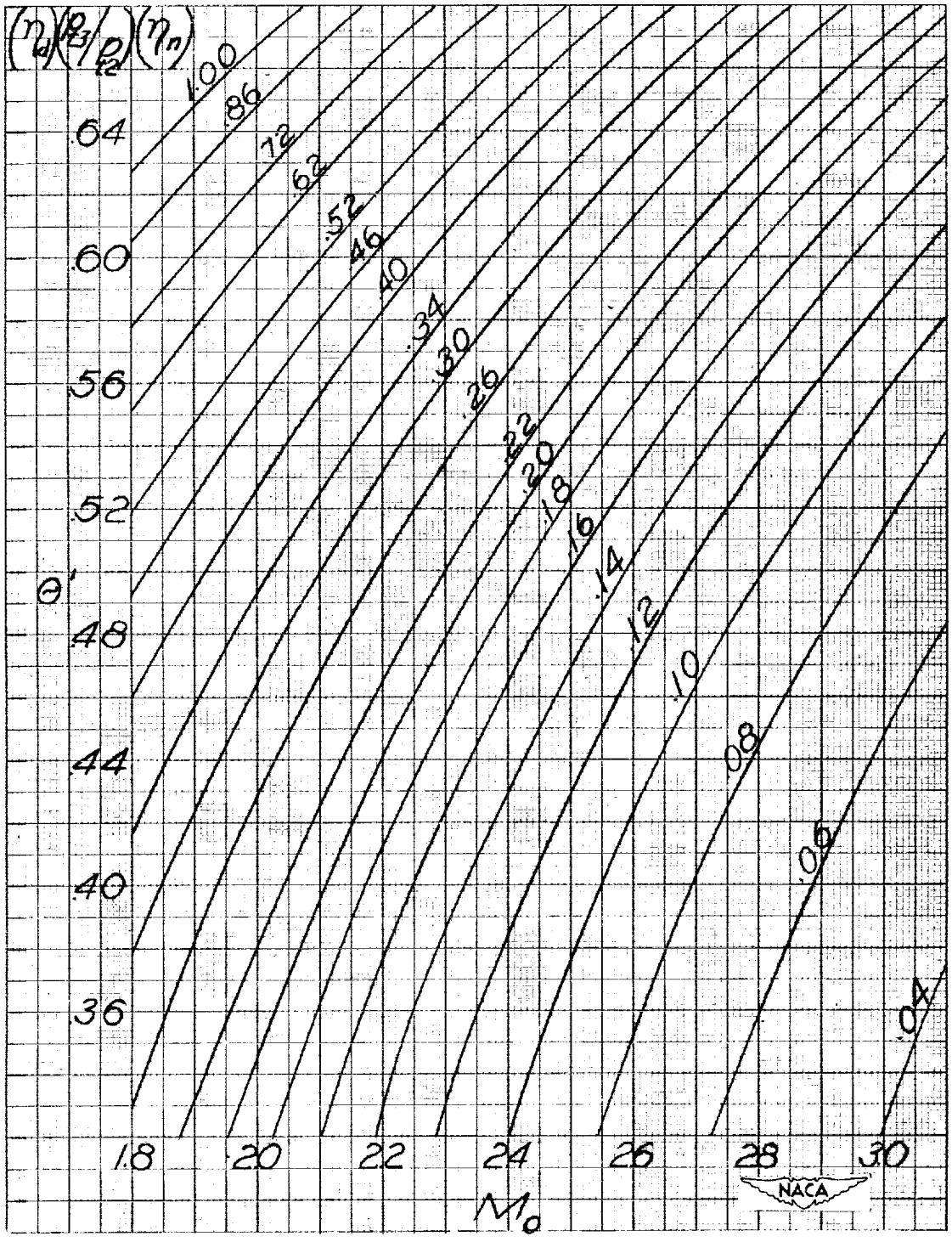

(f) M_0 = 1.80 to 3.10; $\eta_d \left(\frac{p_{t3}}{p_{t2}}\right) \eta_n$ = 0.04 to 1.00; θ' = 0.32 to 0.68.

Figure 4.- Continued.

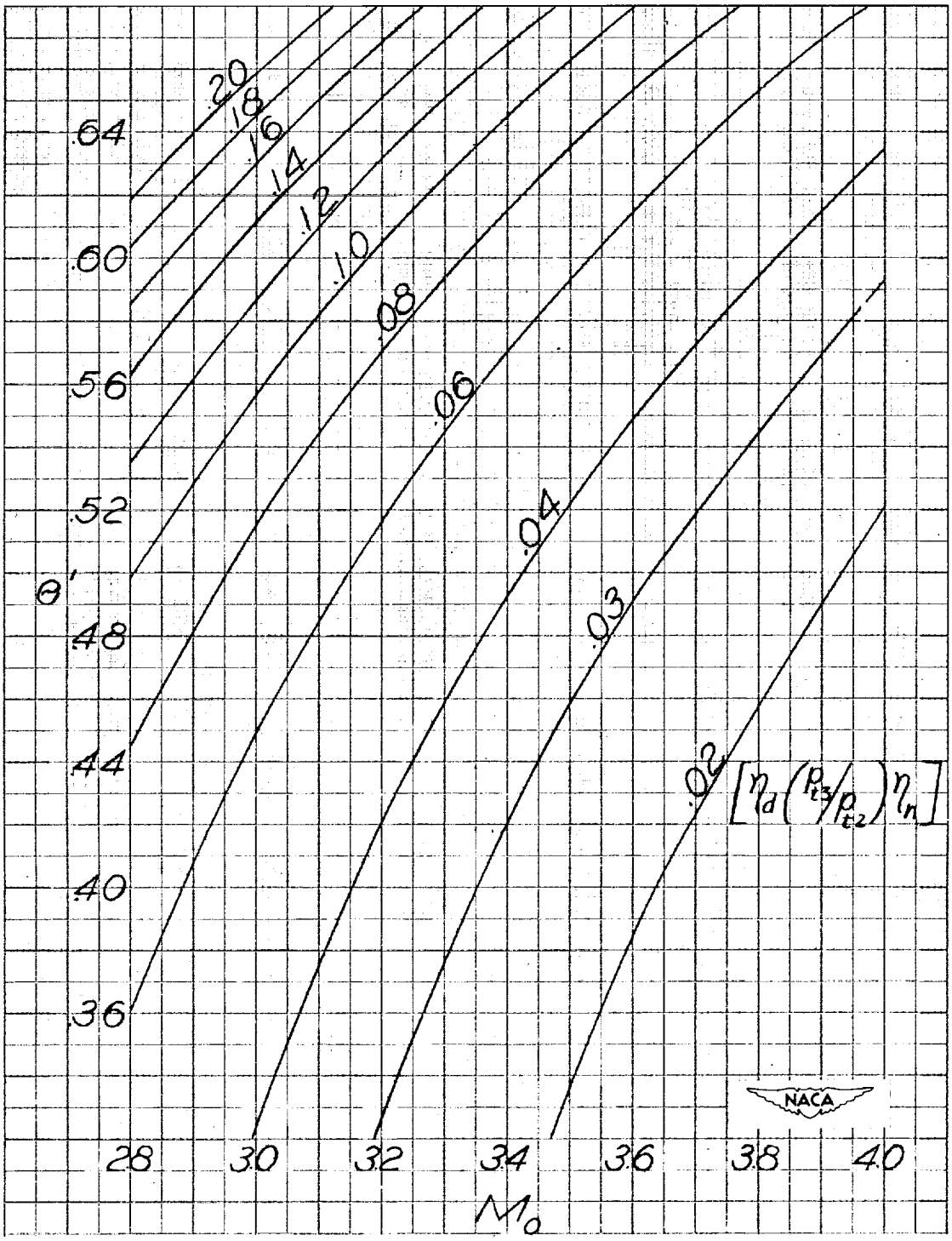

(g) M_0 = 2.80 to 4.00; $\eta_d \left(\frac{p_{t3}}{p_{t2}}\right) \eta_n$ = 0.02 to 0.20; θ' = 0.32 to 0.68.

Figure 4.- Continued.

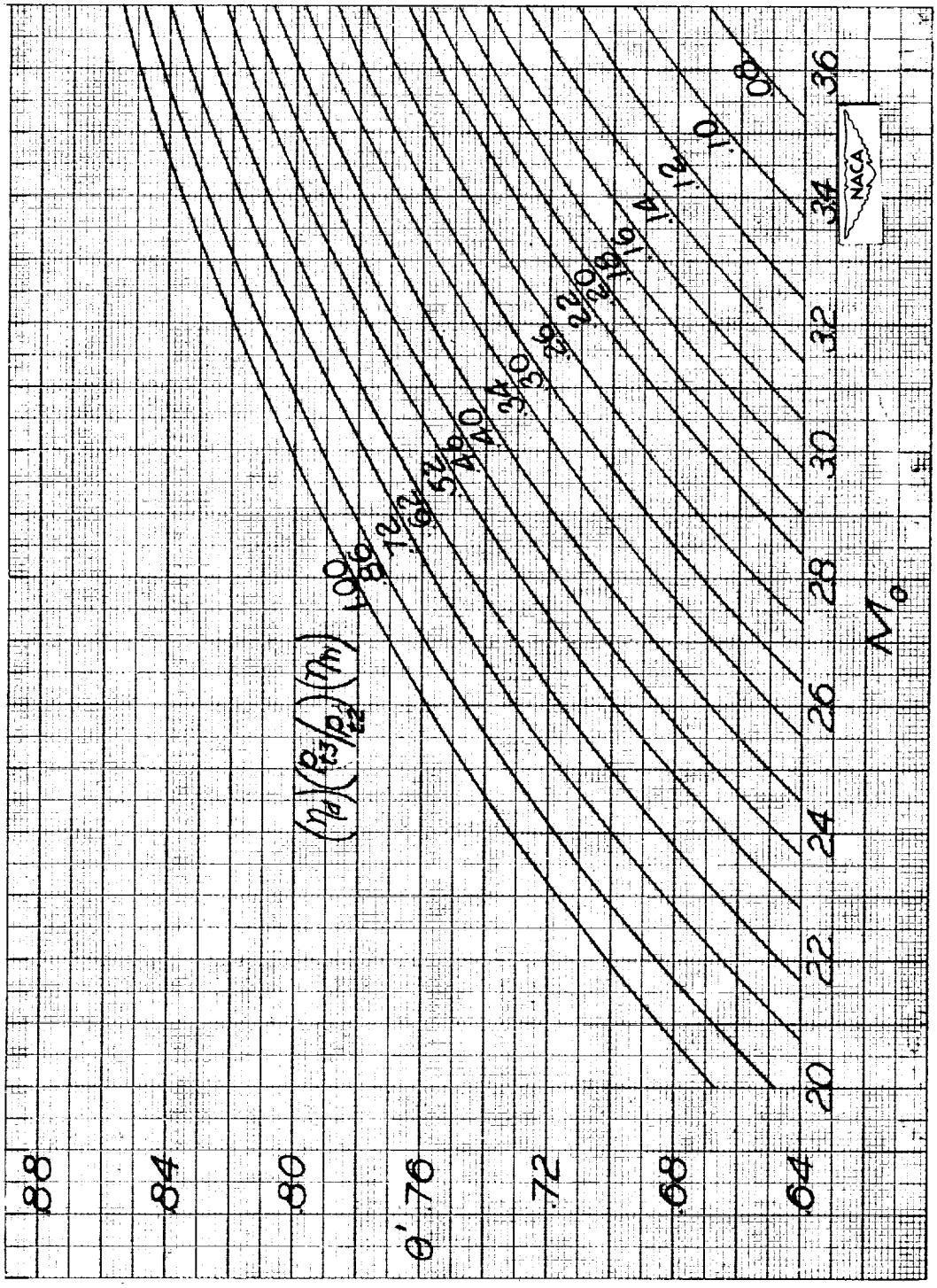

(h) M_0 = 2.00 to 3.70; $\eta_d \left(\frac{p_{t3}}{p_{t2}}\right) \eta_n$ = 0.08 to 1.00; θ' = 0.64 to 0.86.

Figure 4.- Concluded.

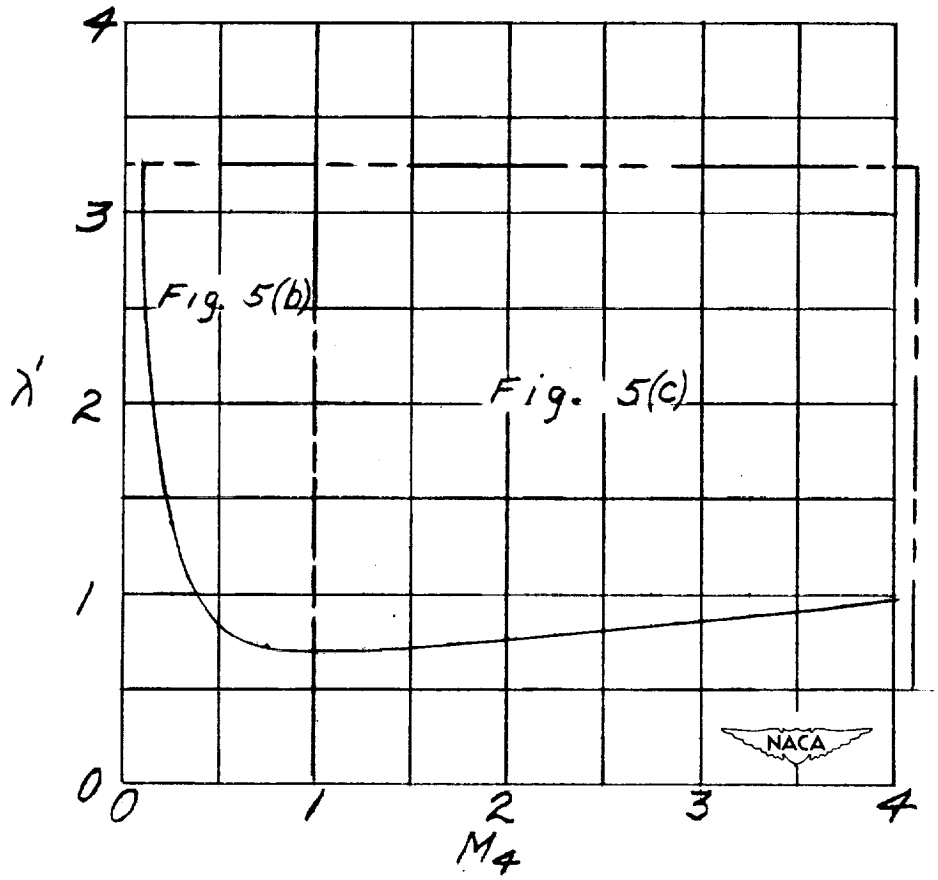

(a) Master plot.

Figure 5.- Pressure-loss parameter λ'.

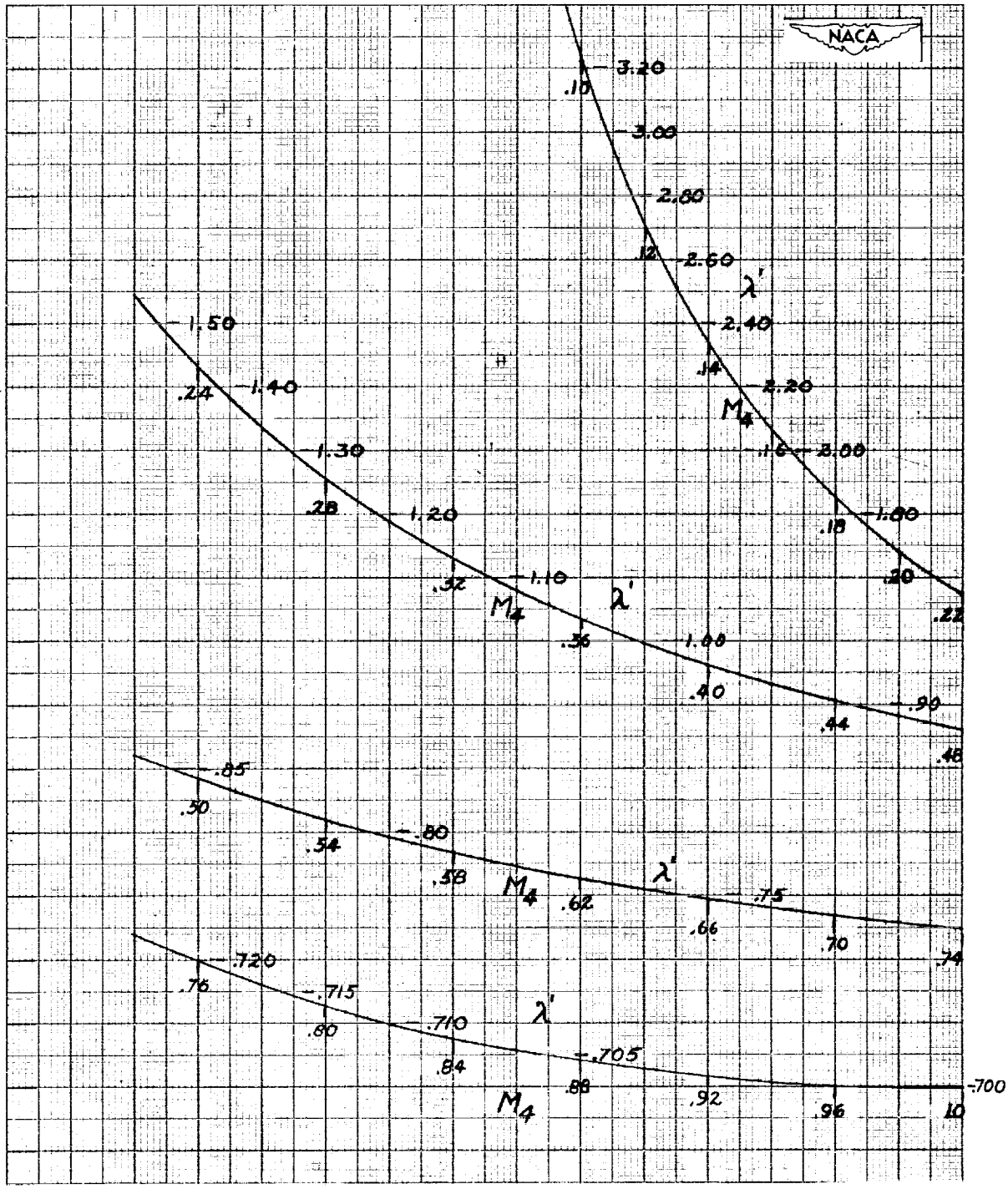

(b) M_4 = 0.10 to 1.00.

Figure 5.- Continued.

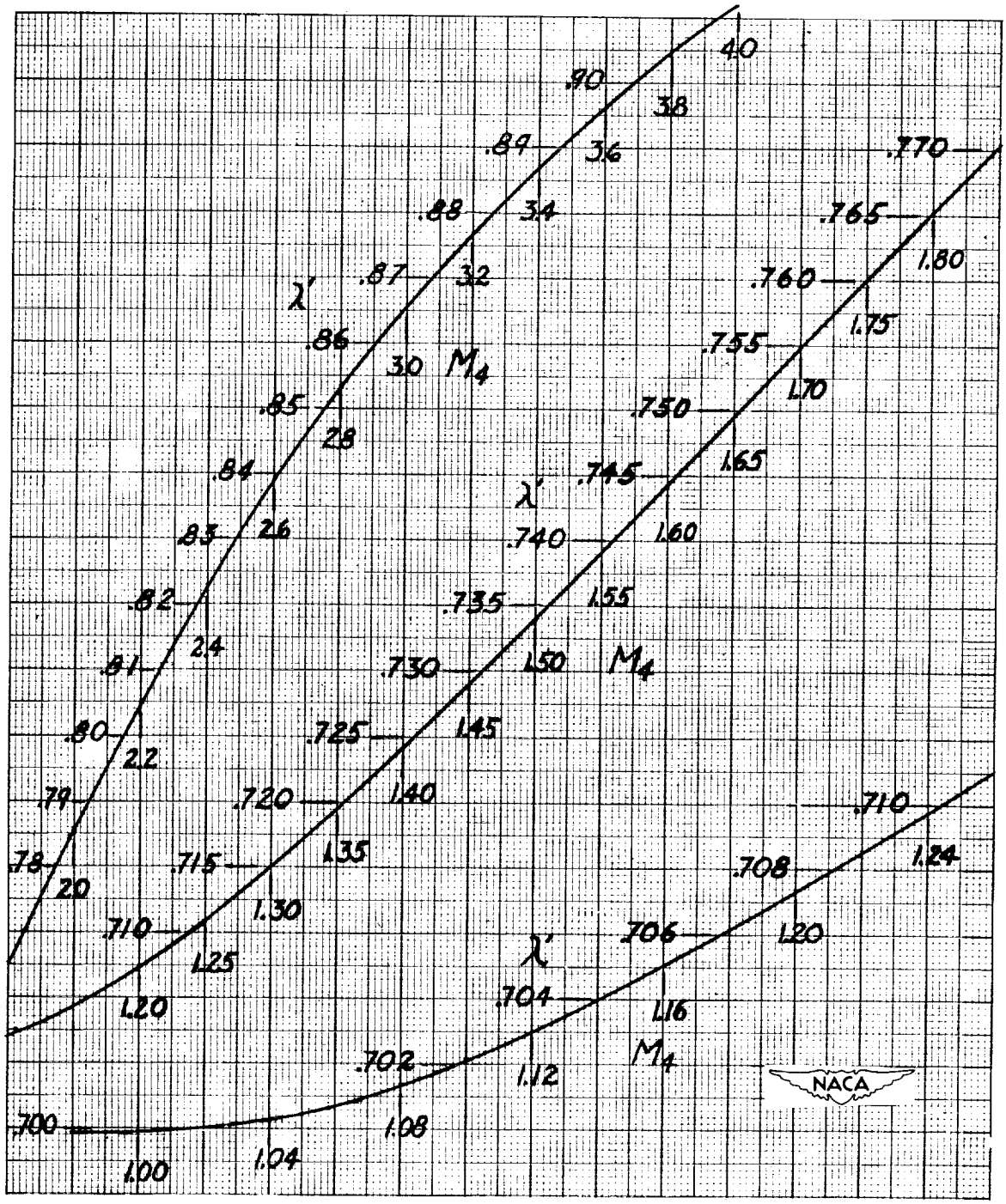

(c) M_4 = 1.00 to 4.00.

Figure 5.- Concluded.

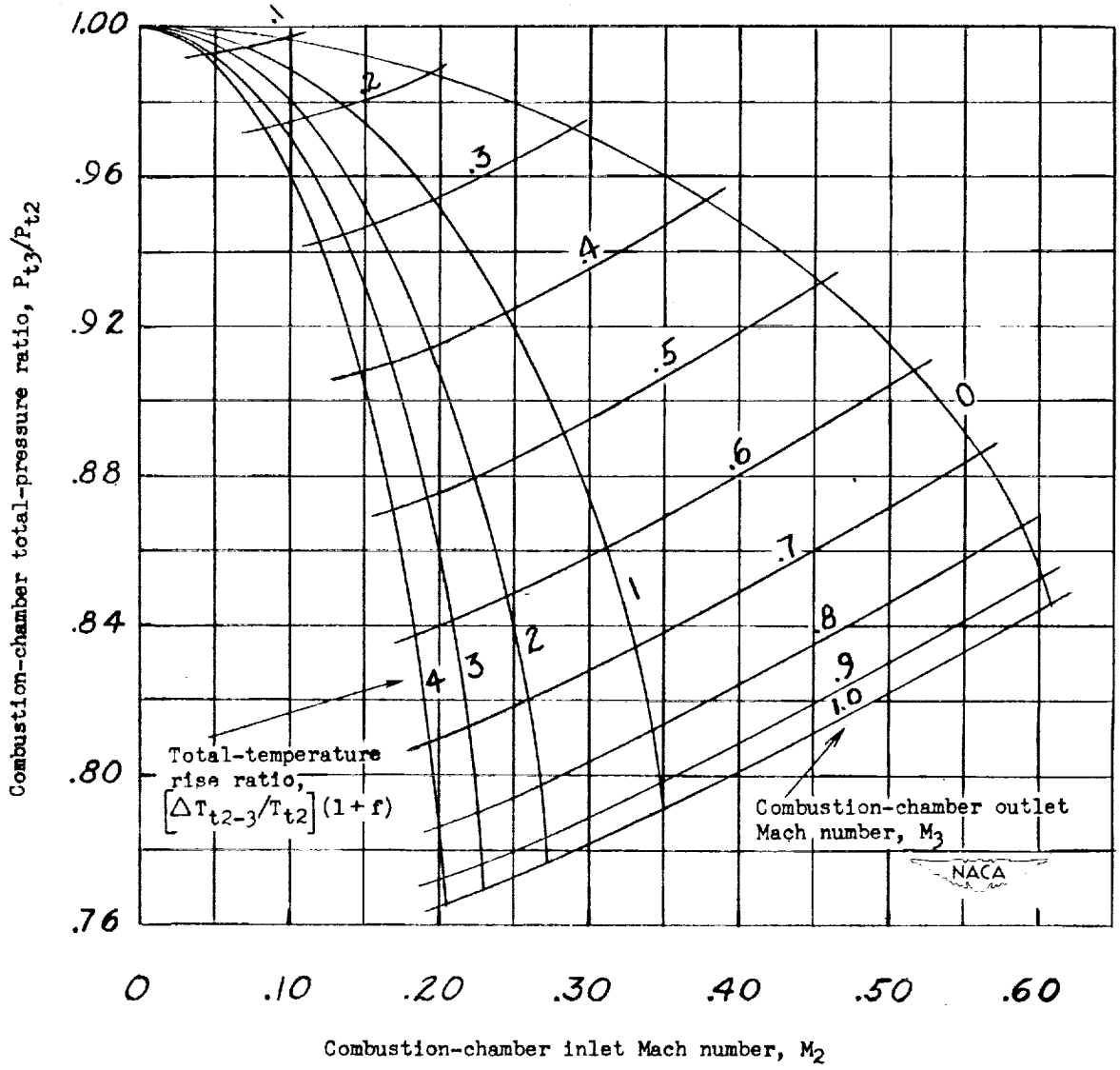

Figure 6.- Example of combustion-chamber performance curve.

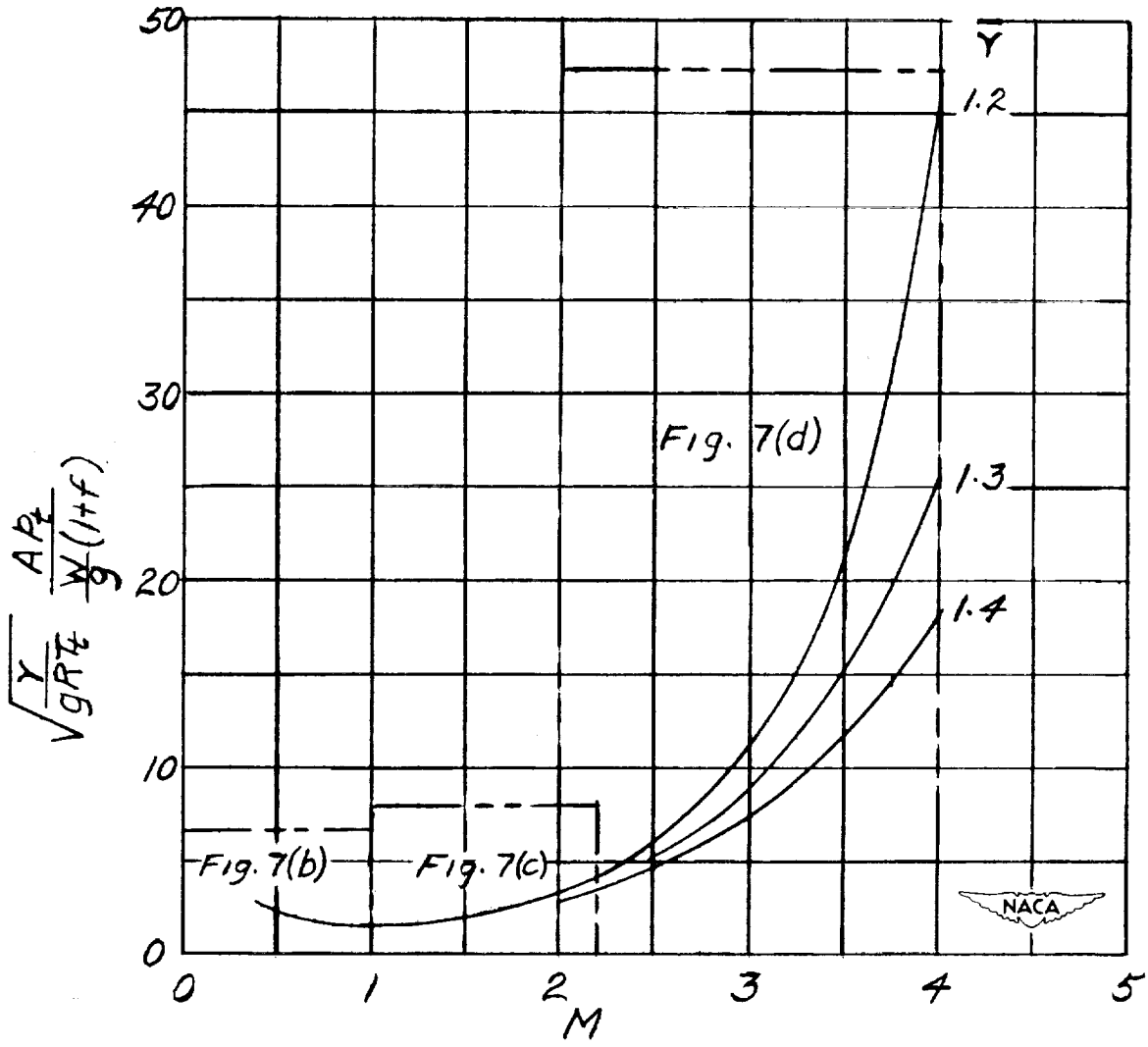

(a) Master plot.

Figure 7.- Chart for converting combustion-chamber exit Mach number to exhaust-nozzle exit Mach number M_3 to M_4.

Multiplying factor; $\frac{A_4}{A_3}\frac{p_{t4}}{p_{t3}}\sqrt{\frac{\gamma_4}{\gamma_3}\frac{R_3}{R_4}\frac{T_{t3}}{T_{t4}}}$

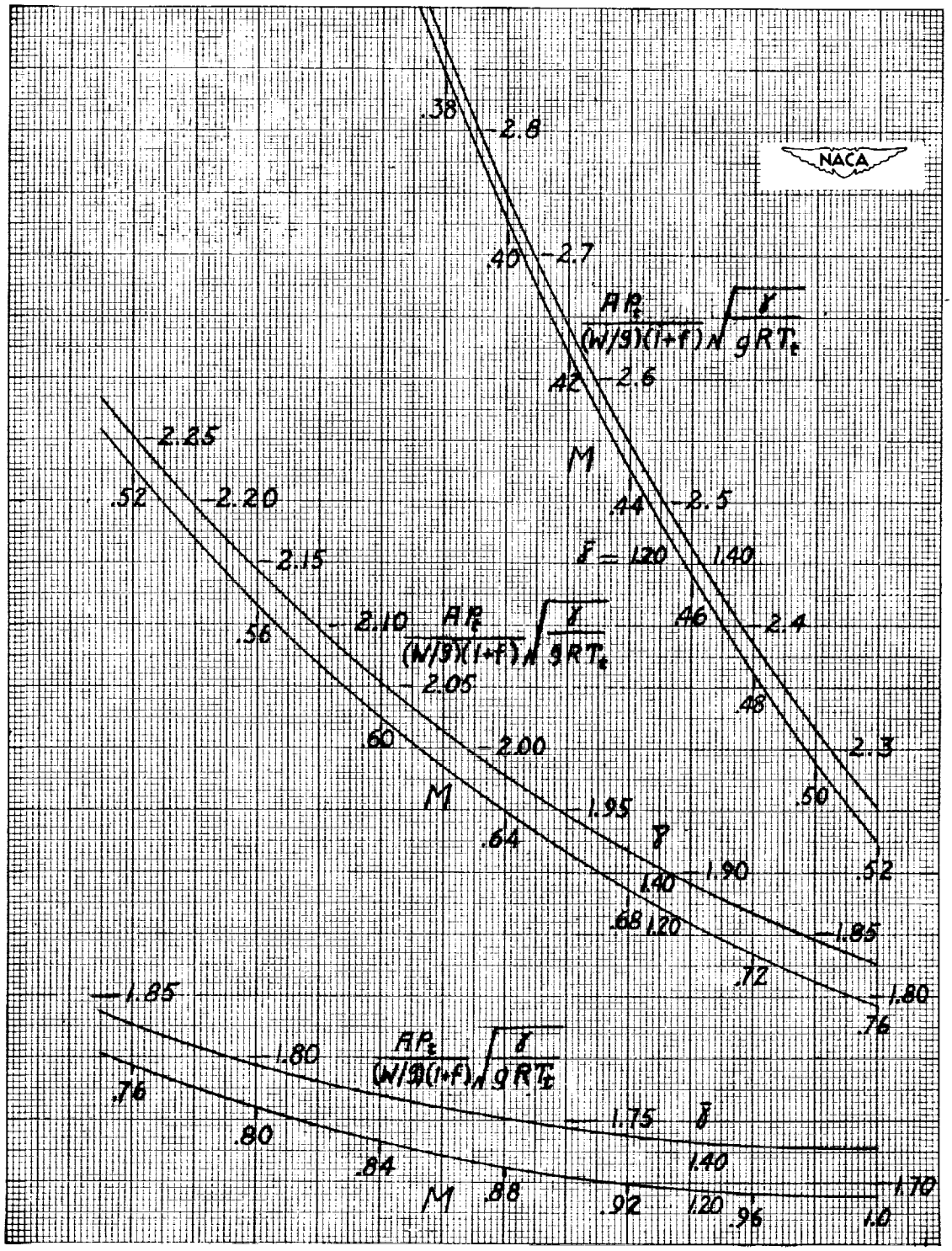

(b) M = 0.38 to 1.00.

Figure 7.- Continued.

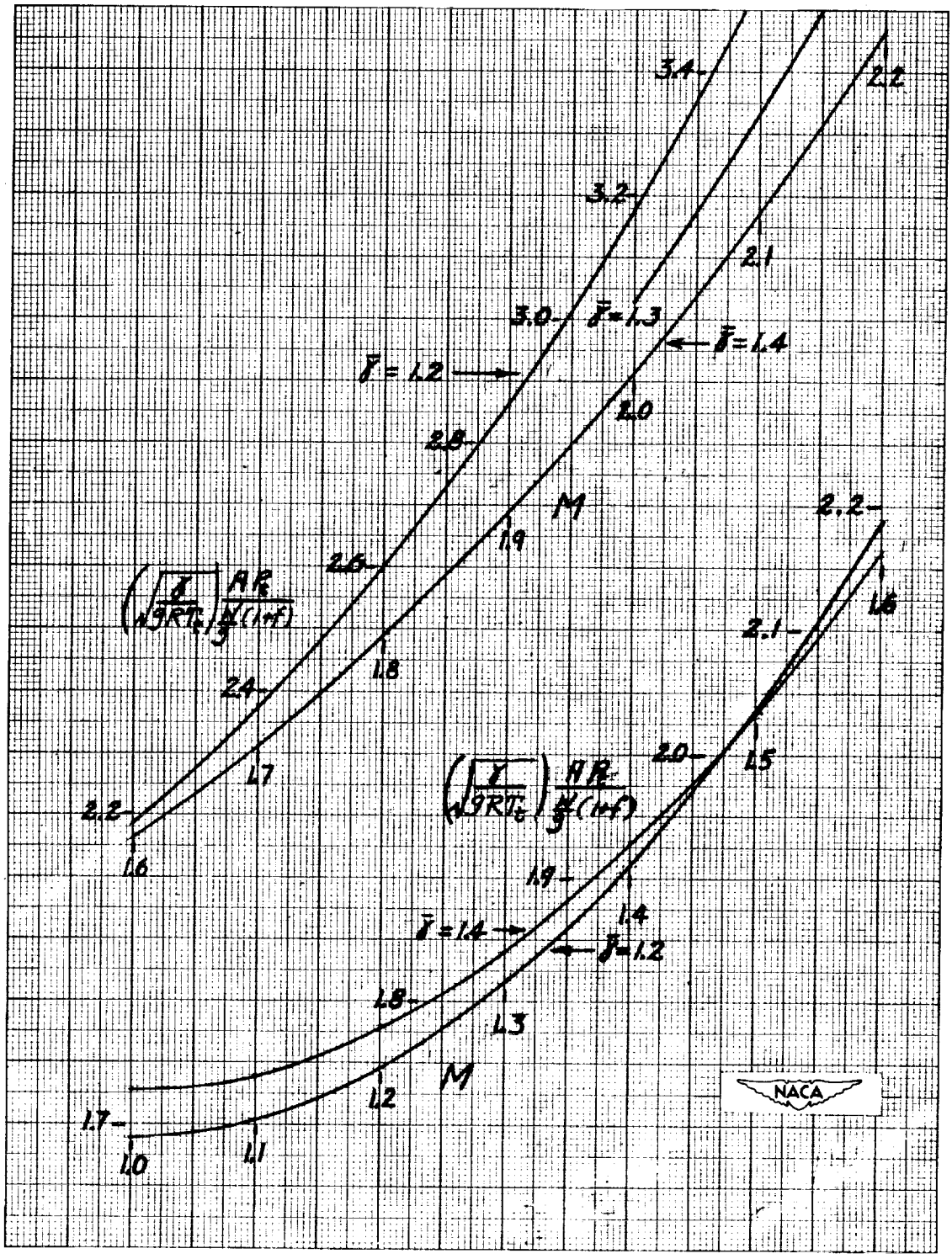

(c) M = 1.00 to 2.20.

Figure 7.- Continued.

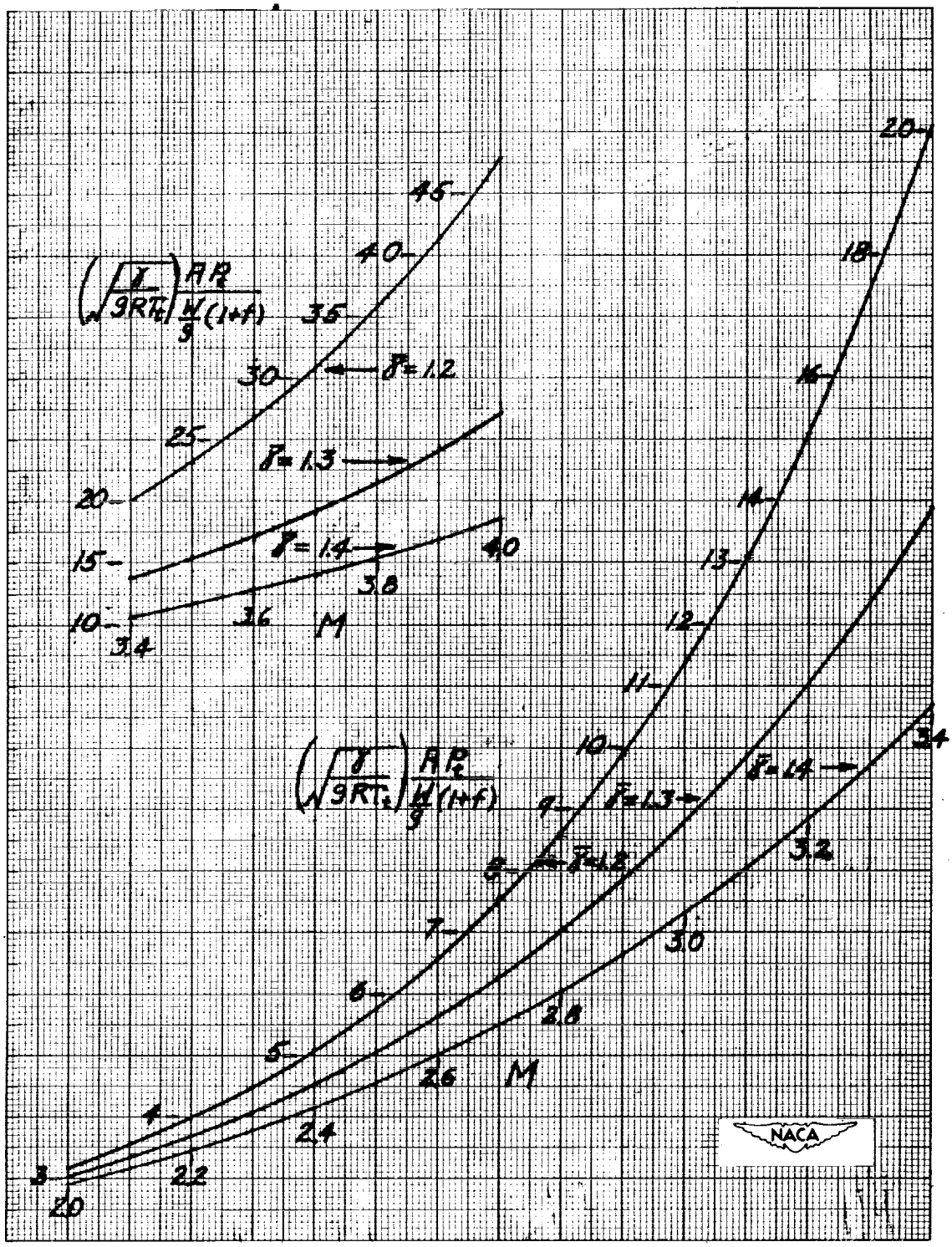

(d) M = 2.00 to 4.00.

Figure 7.- Continued.

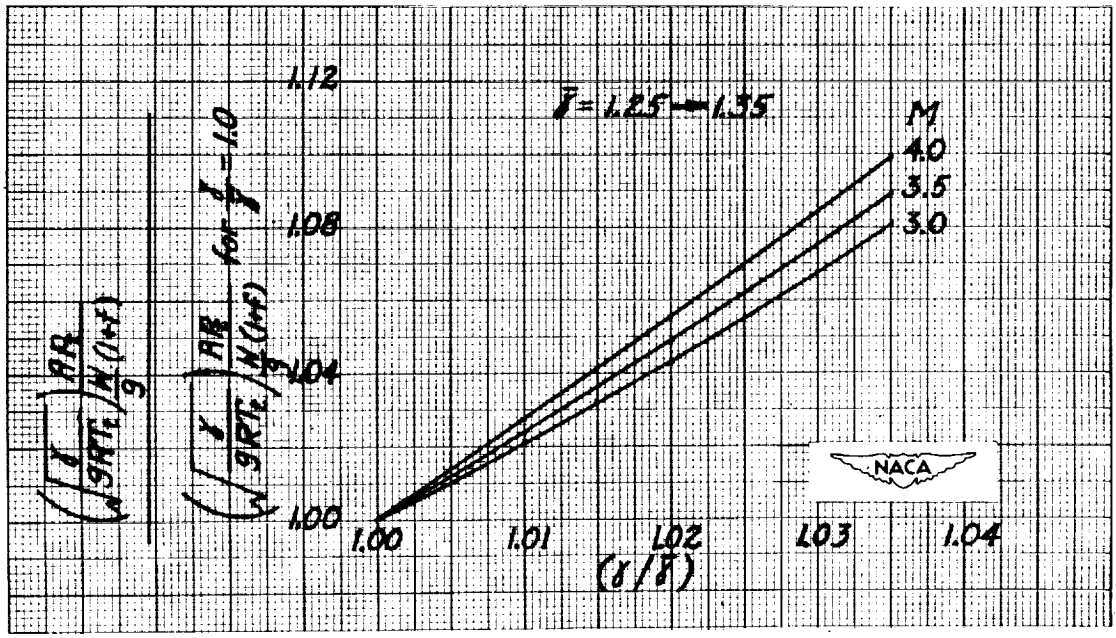

(e) Multiplying factor for correcting the ordinate of figure 7(d) to correspond to values of $\gamma/\bar{\gamma}$ other than 1.0.

Figure 7.- Concluded.

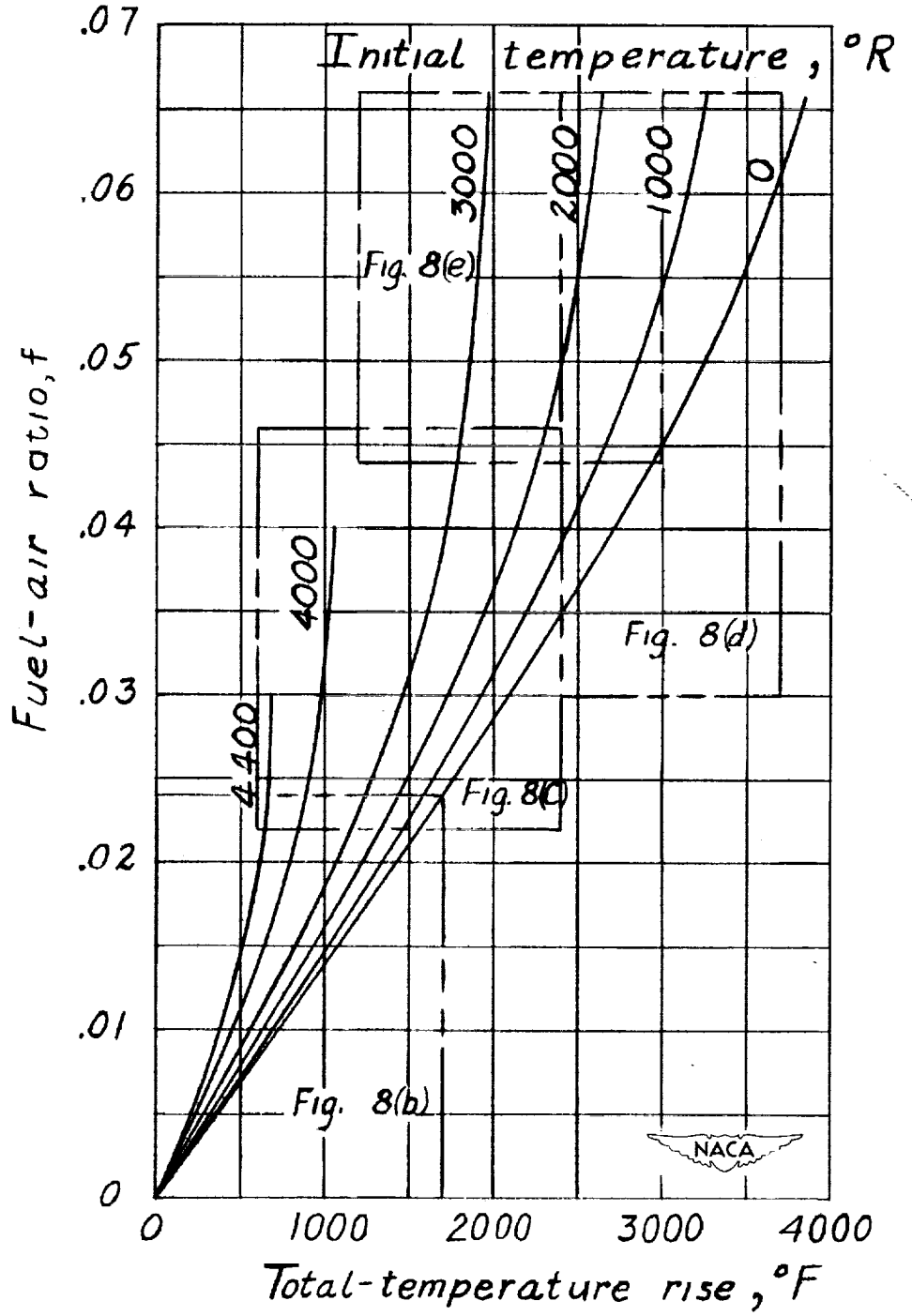

(a) Master plot.

Figure 8.- Relation of theoretical fuel-air ratio to total-temperature rise and initial temperature for combustion of n-octane and air.

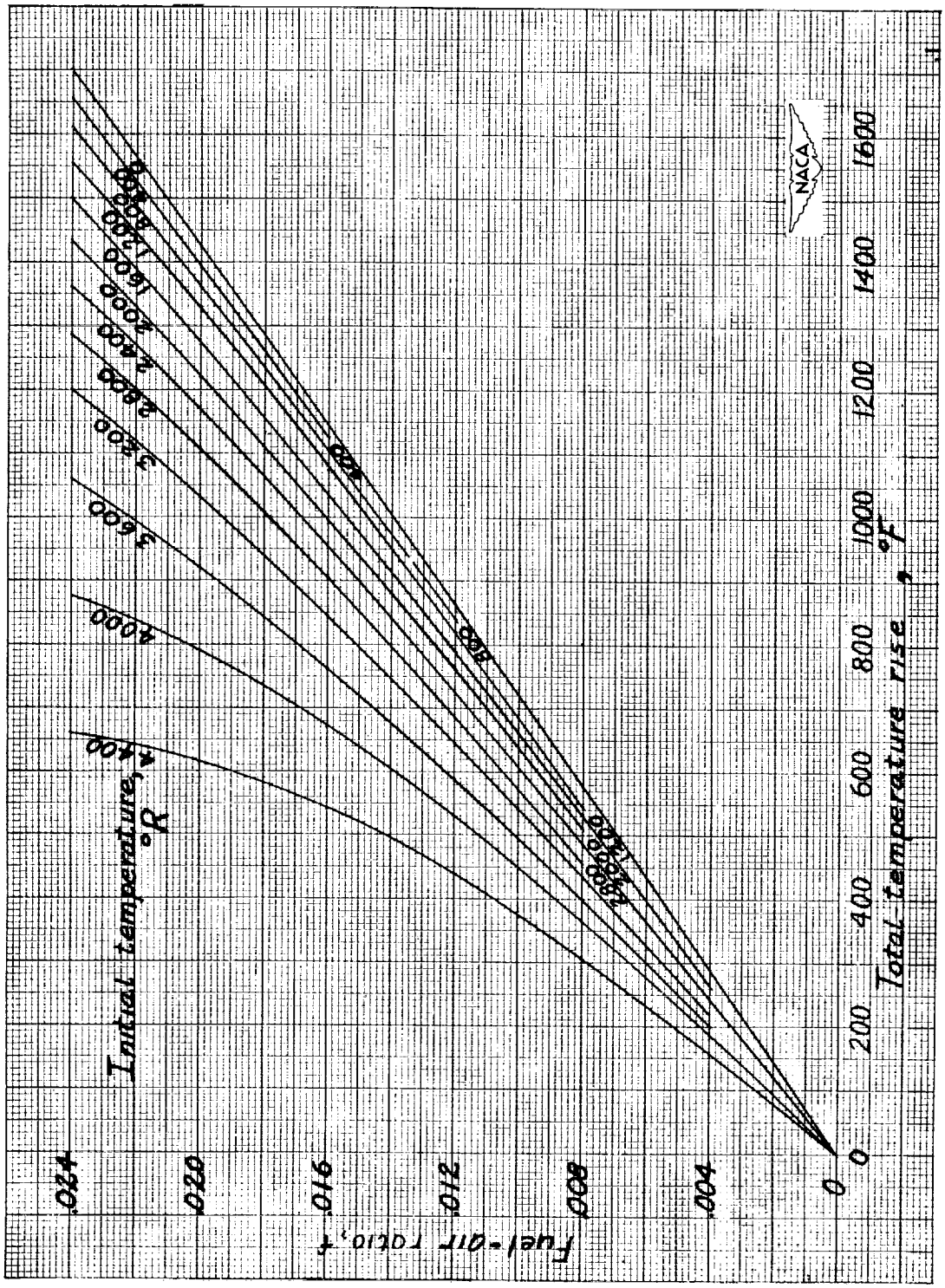

(b) Total-temperature rise = 0° to 1700° F; f = 0 to 0.024.

Figure 8.- Continued.

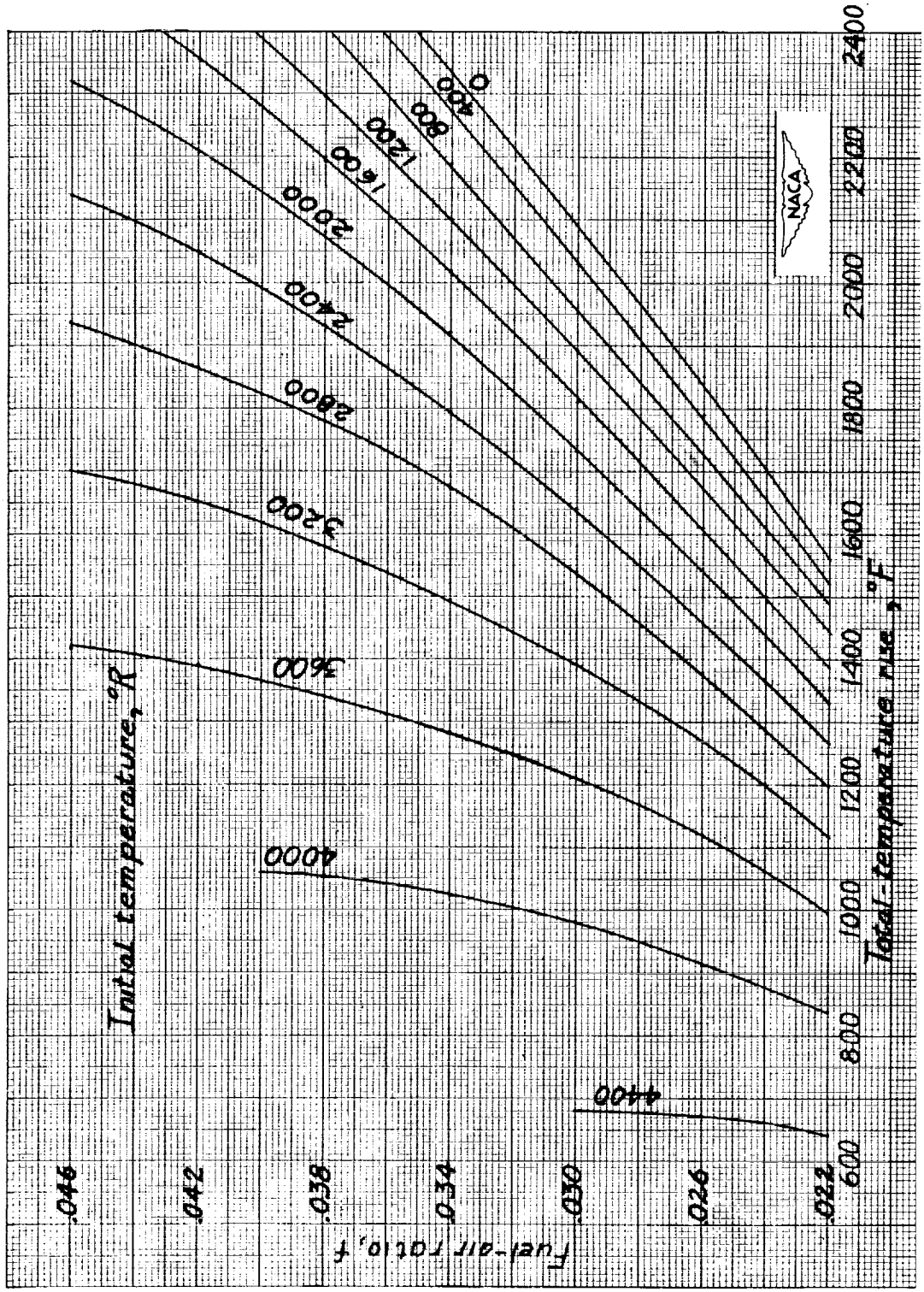

(c) Total-temperature rise = 600° to 2400° F; f = 0.022 to 0.046.

Figure 8.- Continued.

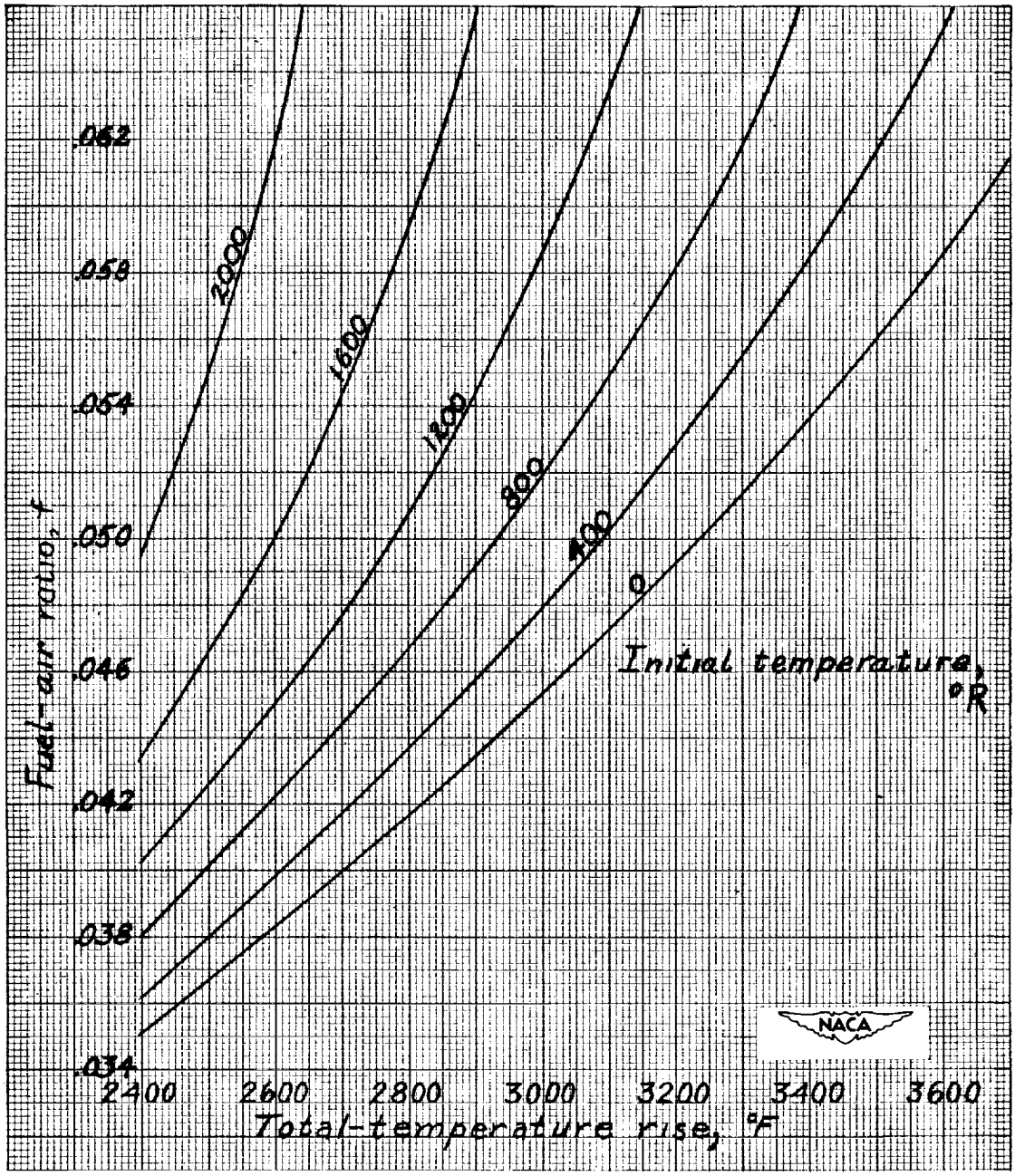

(d) Total-temperature rise = 2400° to 3700° F; f = 0.034 to 0.066.

Figure 8.- Continued.

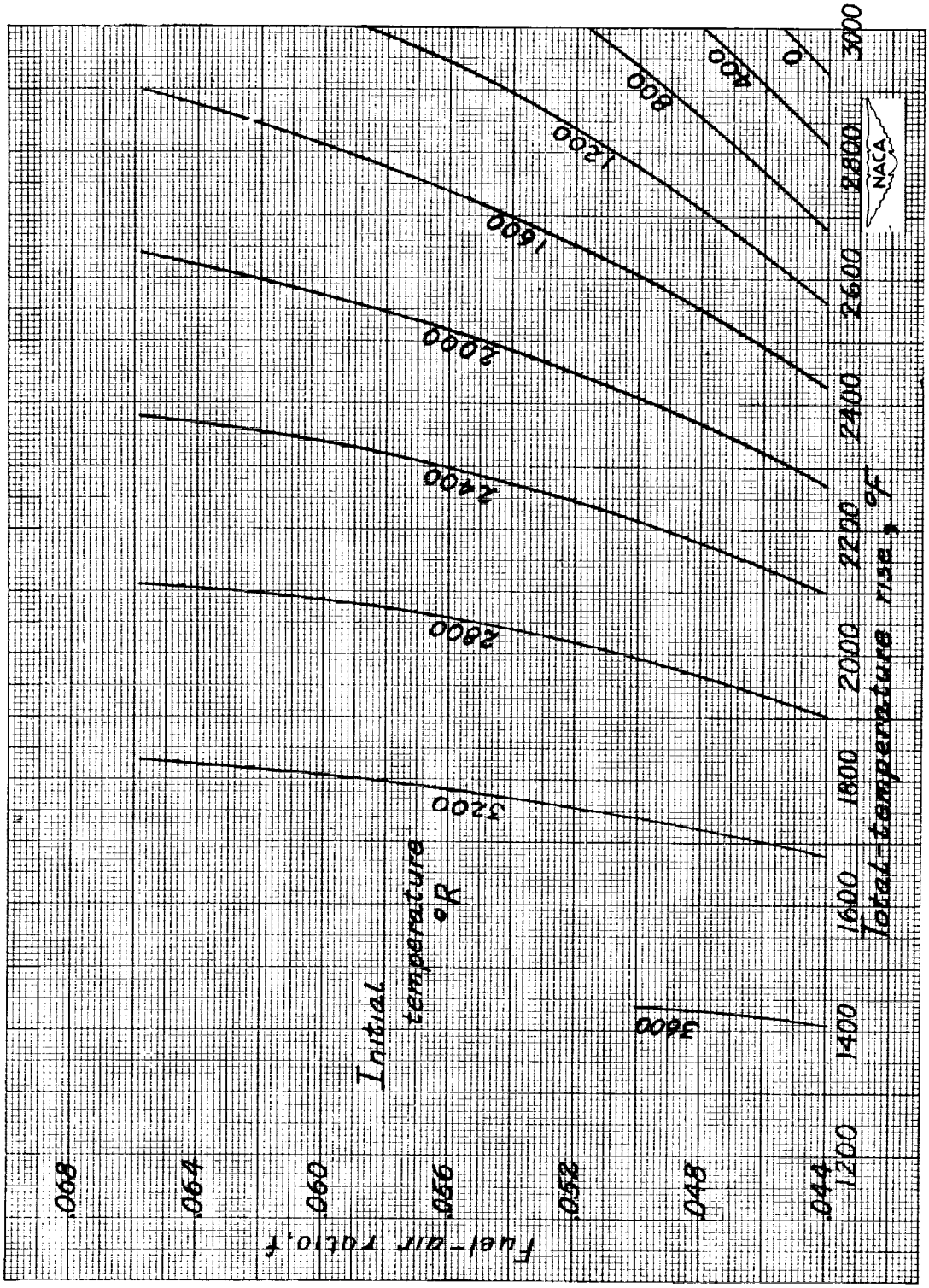

(e) Total-temperature rise = 1400° to 3000° F; f = 0.044 to 0.0658.

Figure 8.- Concluded.

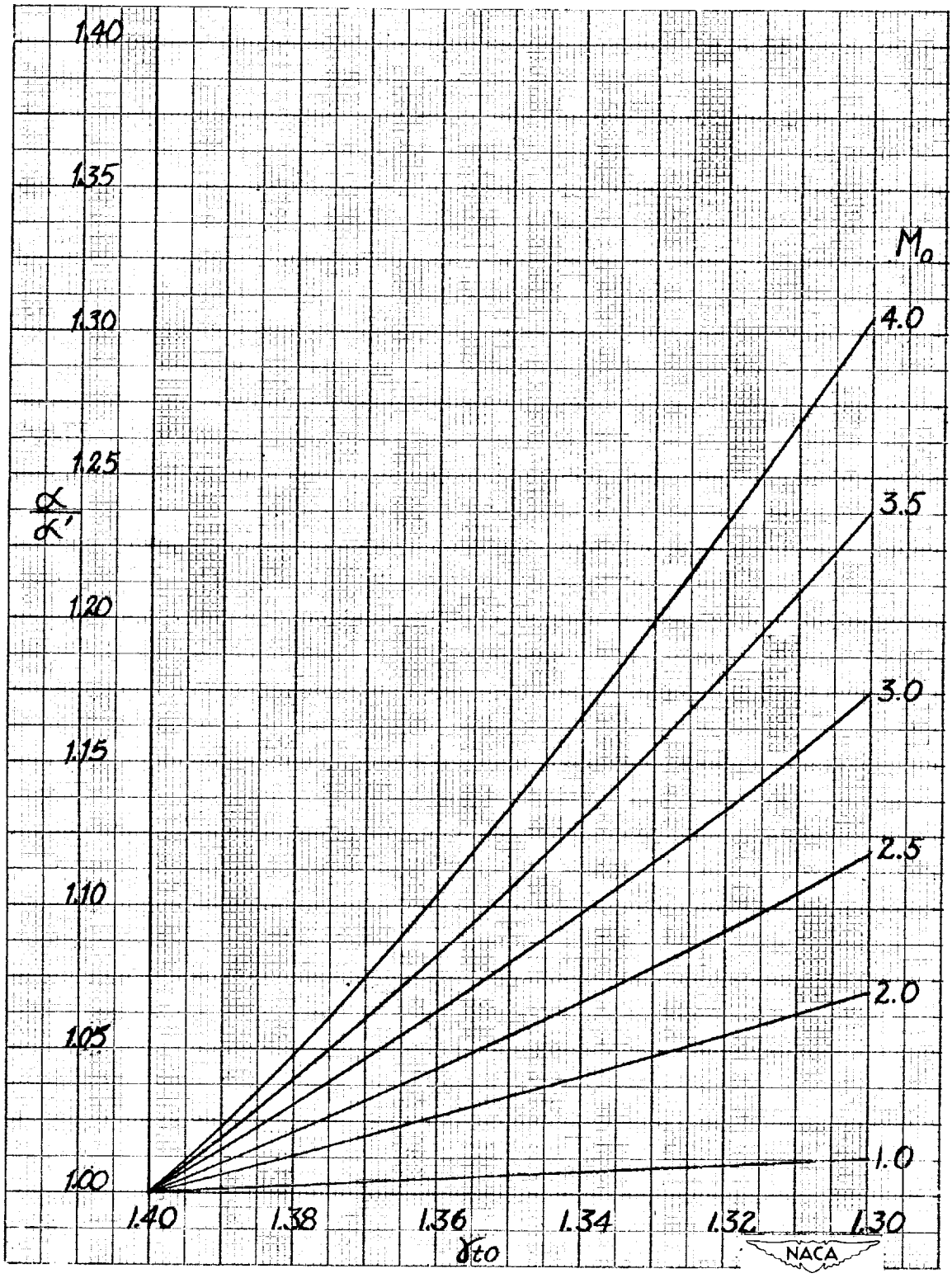

Figure 9.- Mass-flow-parameter correction factor α/α'.

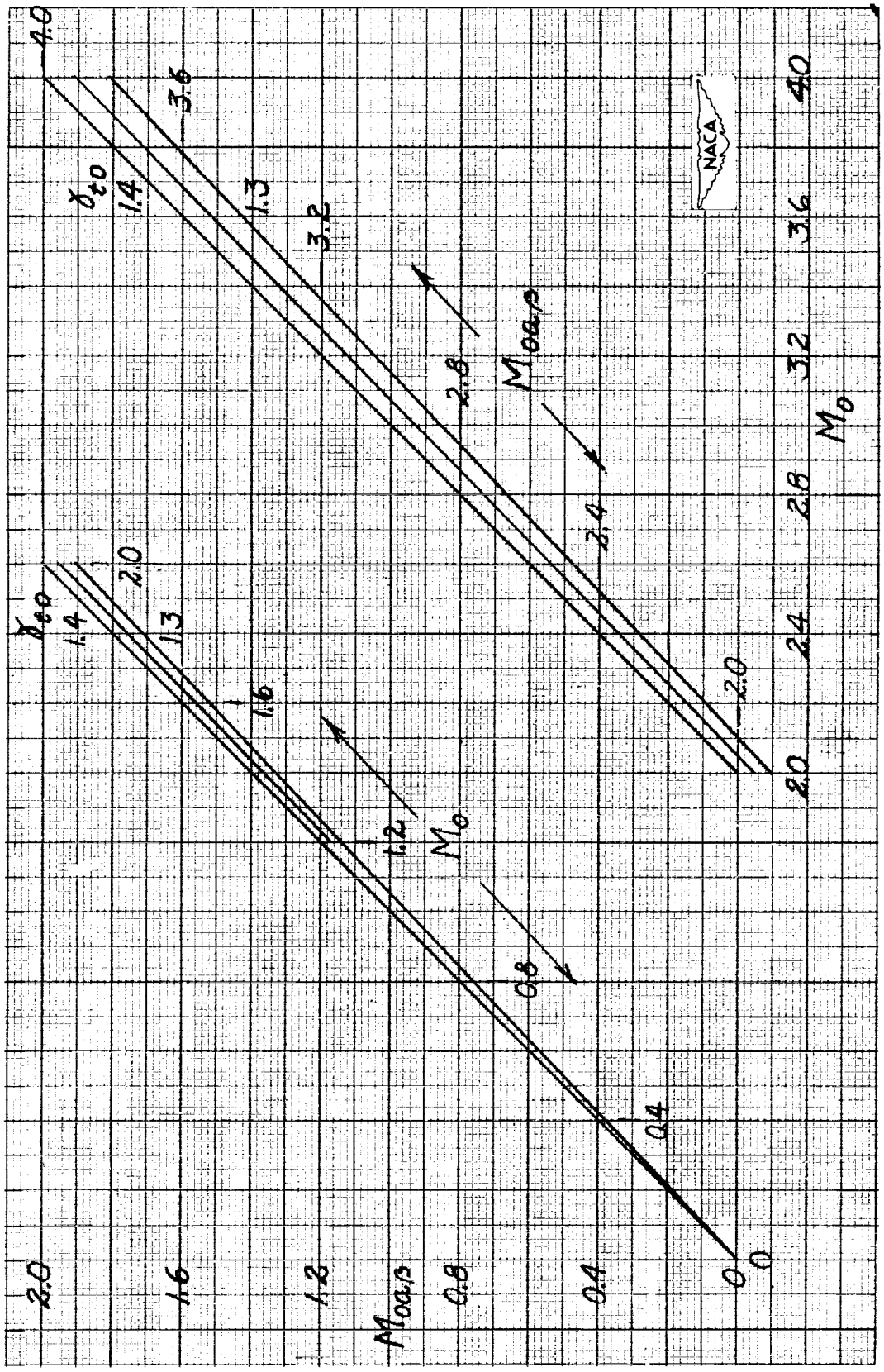

Figure 10.- Adjusted flight Mach number for determining β''.

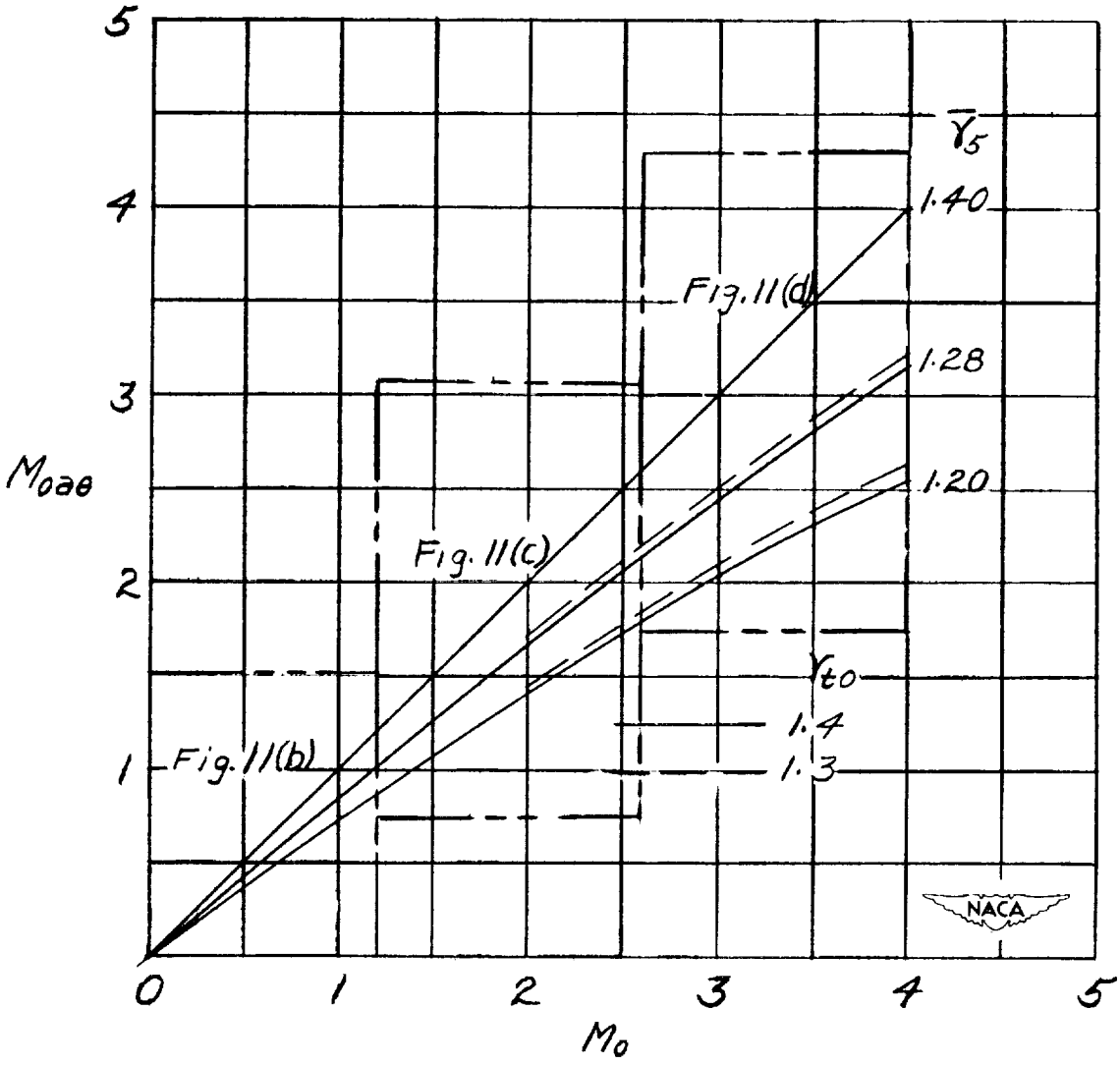

(a) Master plot.

Figure 11.- Adjusted flight Mach number for determining θ''.

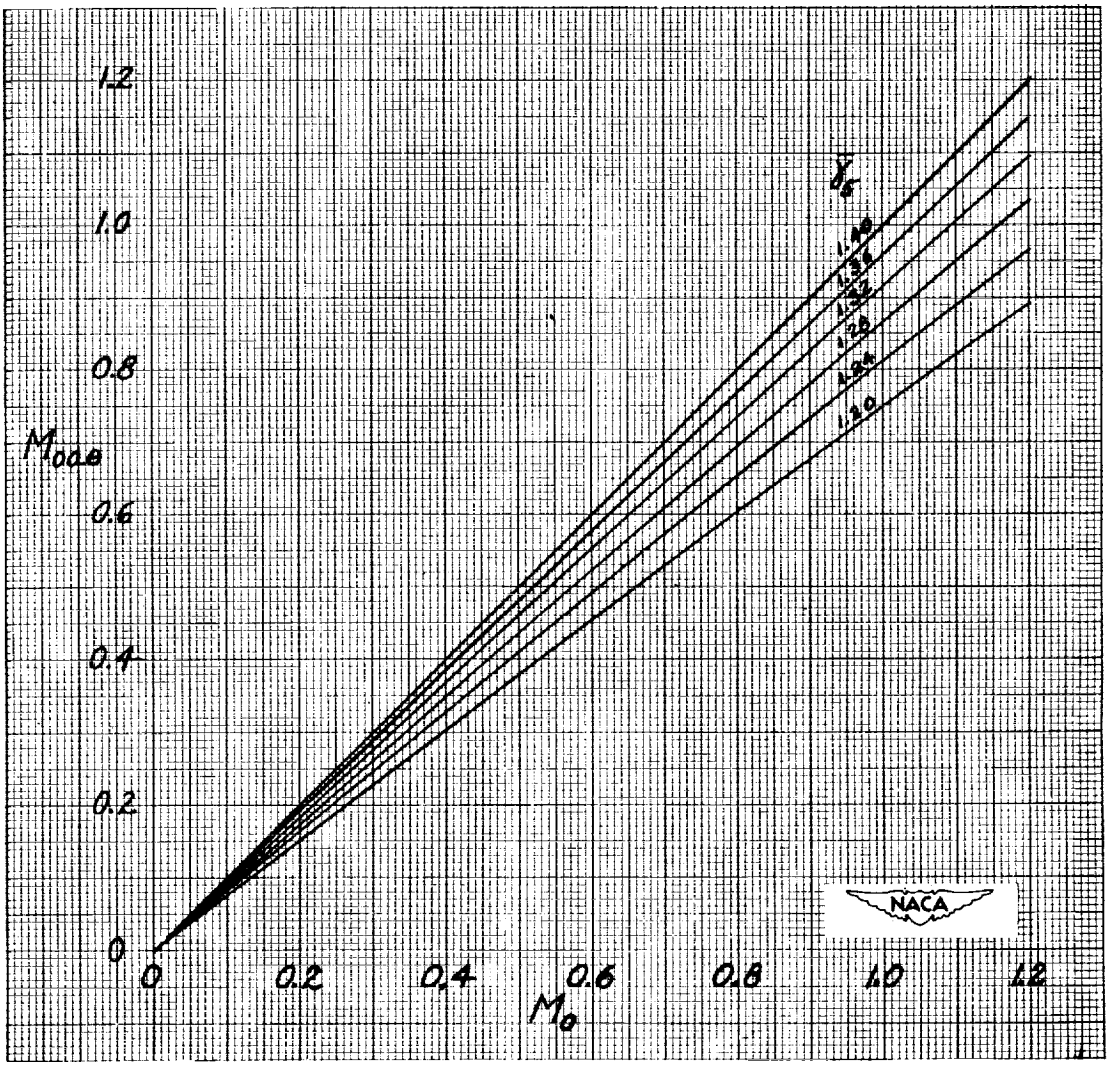

(b) M_0 = 0 to 1.20.

Figure 11.- Continued.

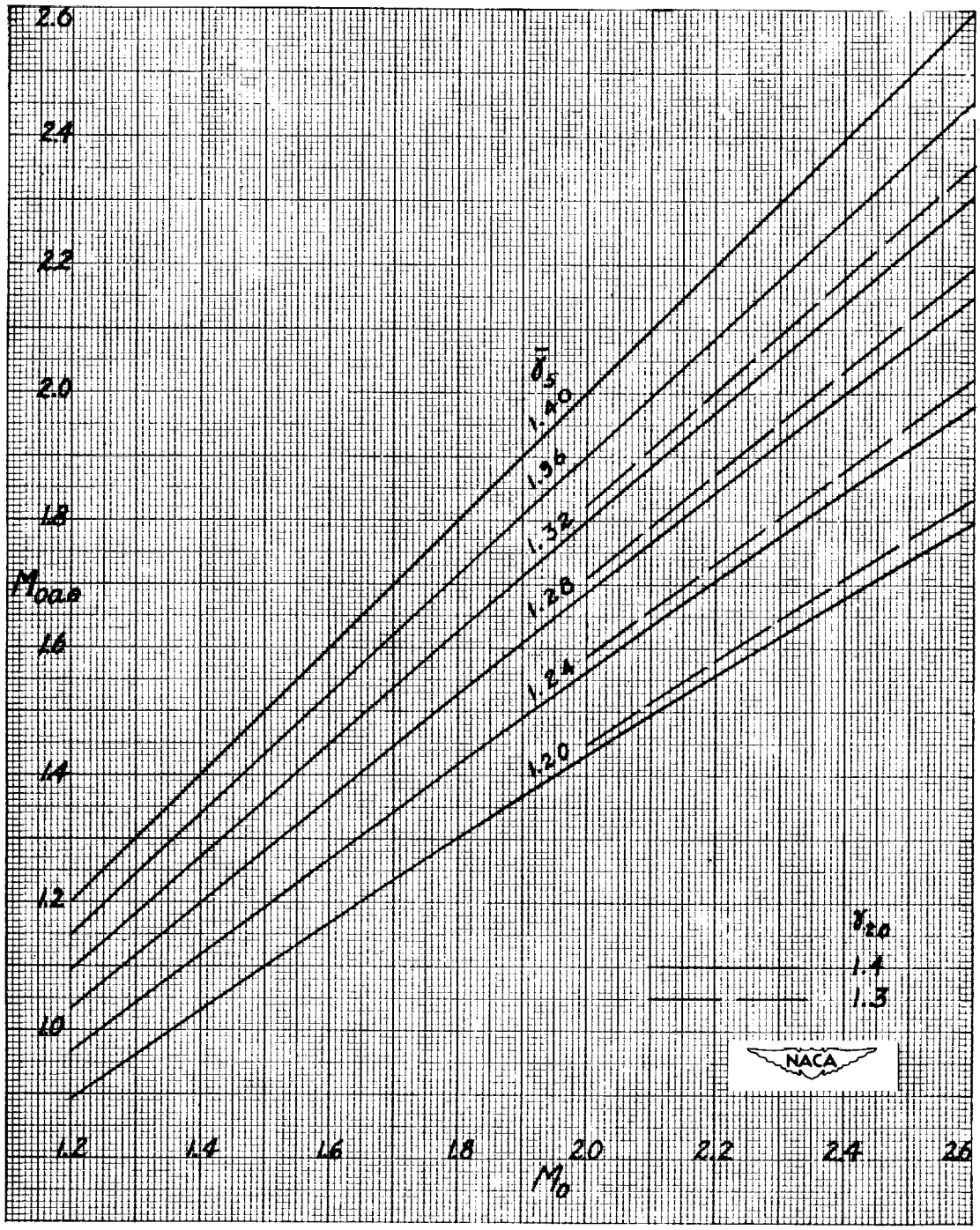

(c) M_0 = 1.20 to 2.60.

Figure 11.- Continued.

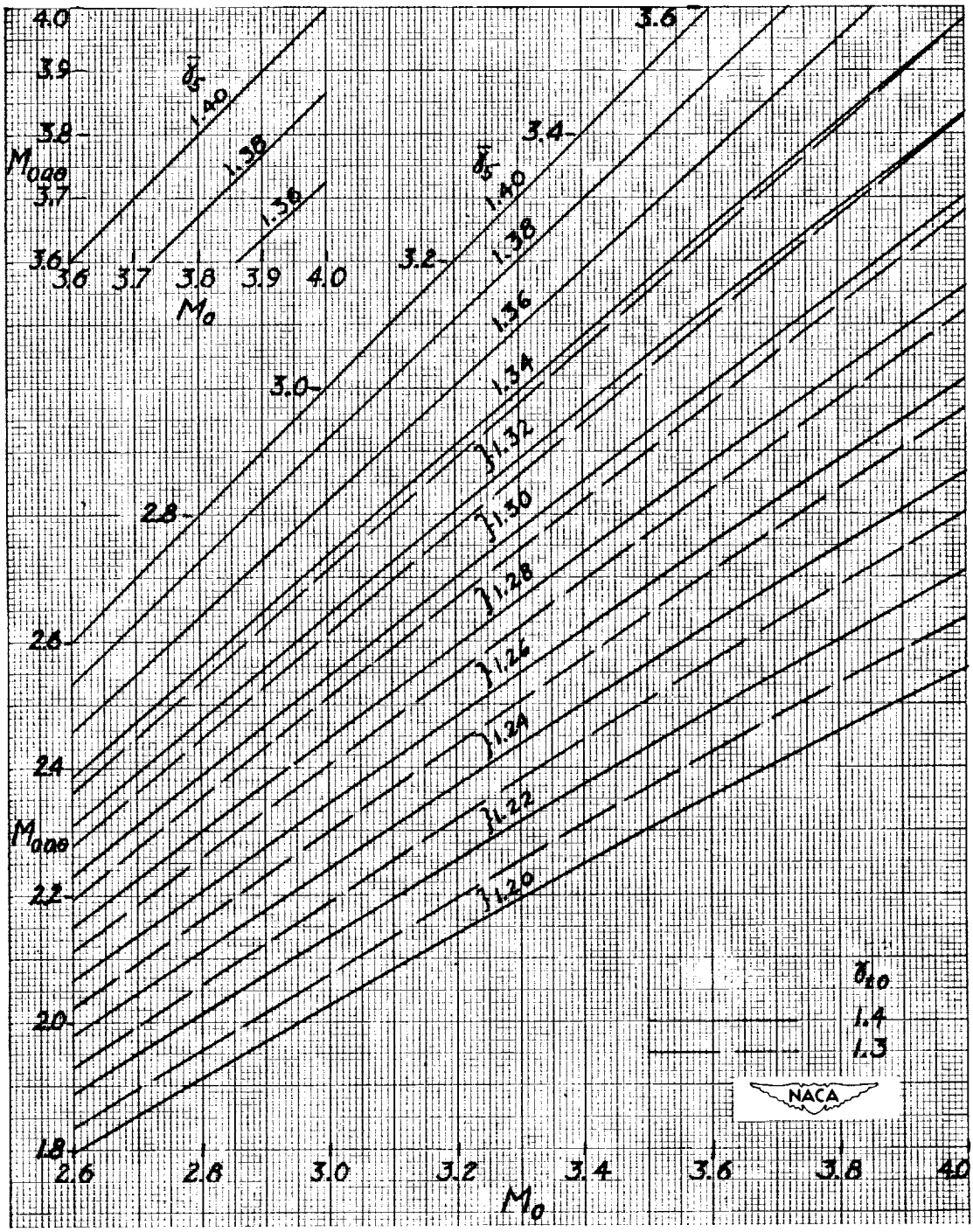

(d) M_0 = 2.60 to 4.00.

Figure 11.- Concluded.

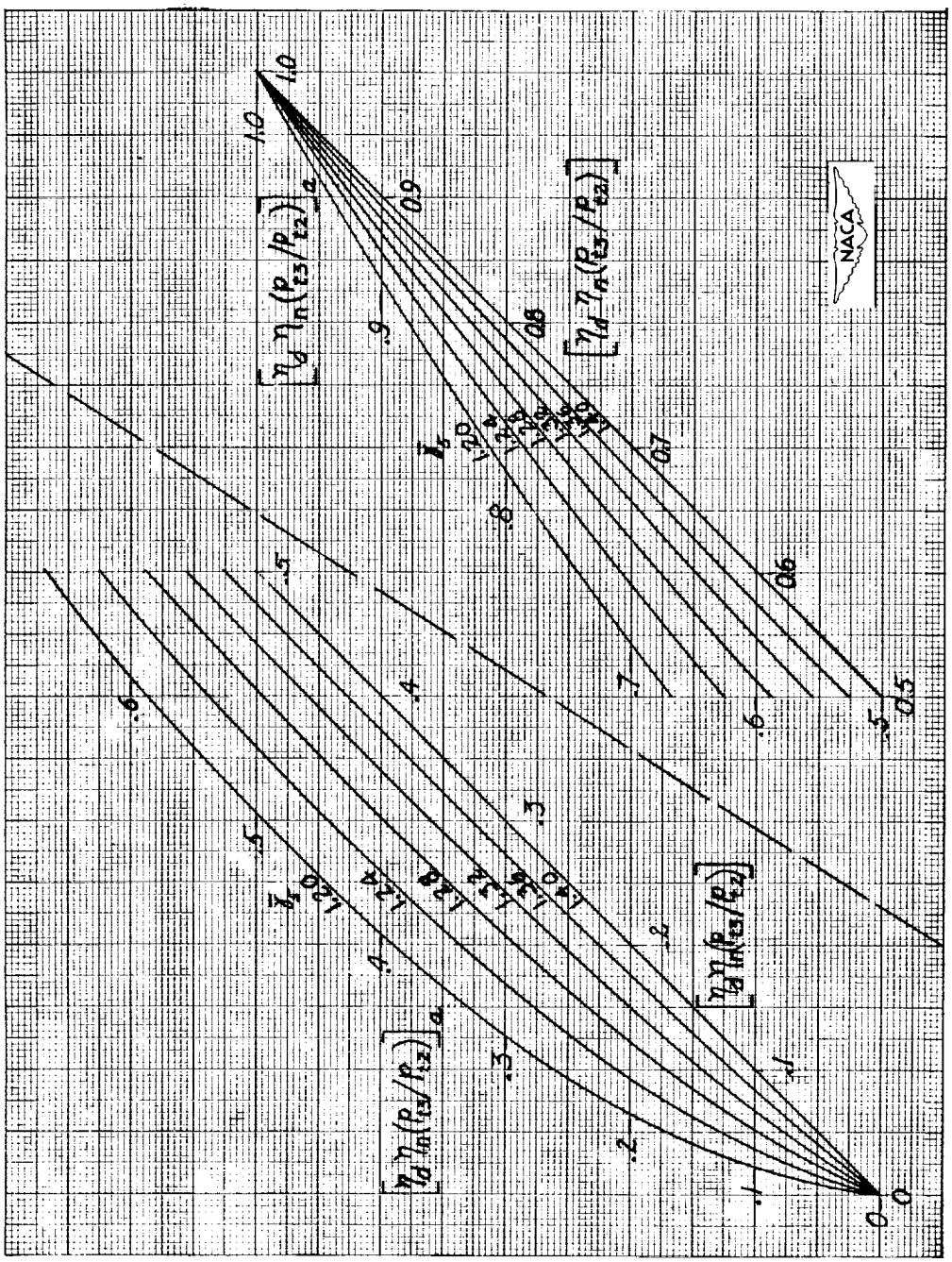

Figure 12.- Adjusted pressure-ratio term $\left[\eta_d \eta_n \left(\frac{p_{t3}}{p_{t2}}\right)\right]_a$ for determining θ.

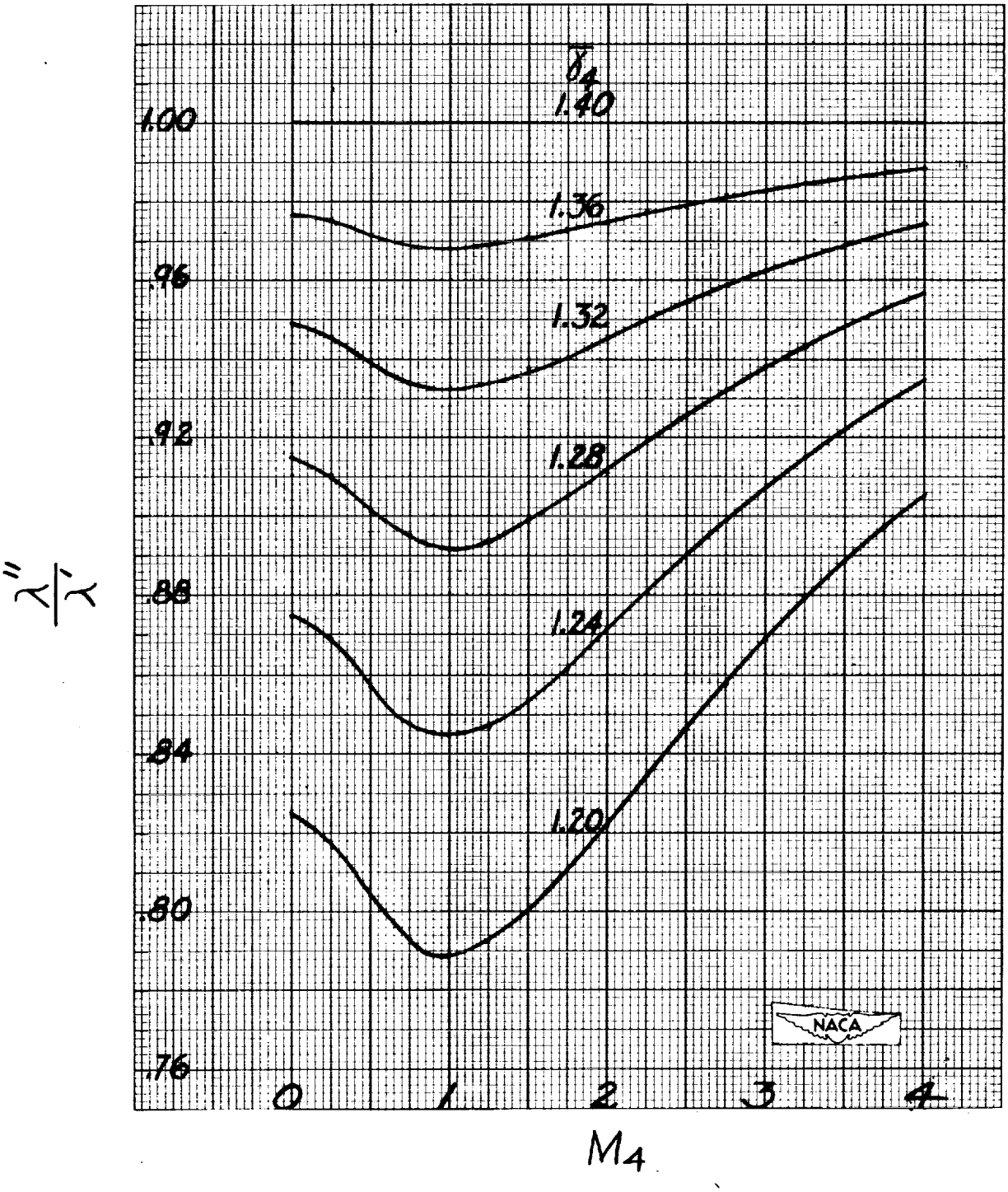

(a) λ''/λ'.

Figure 13.- Pressure-loss parameter λ correction factors.

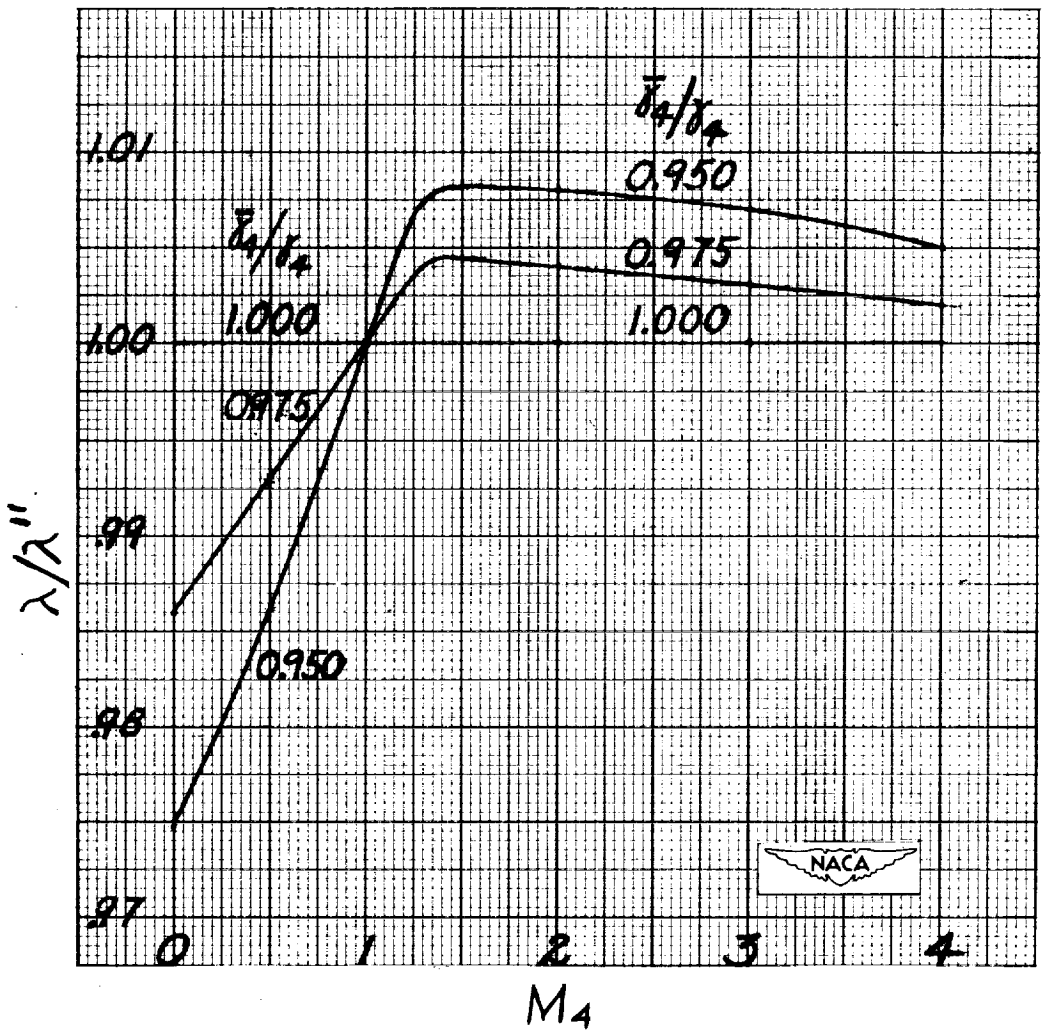

(b) λ/λ''.

Figure 13.- Concluded.

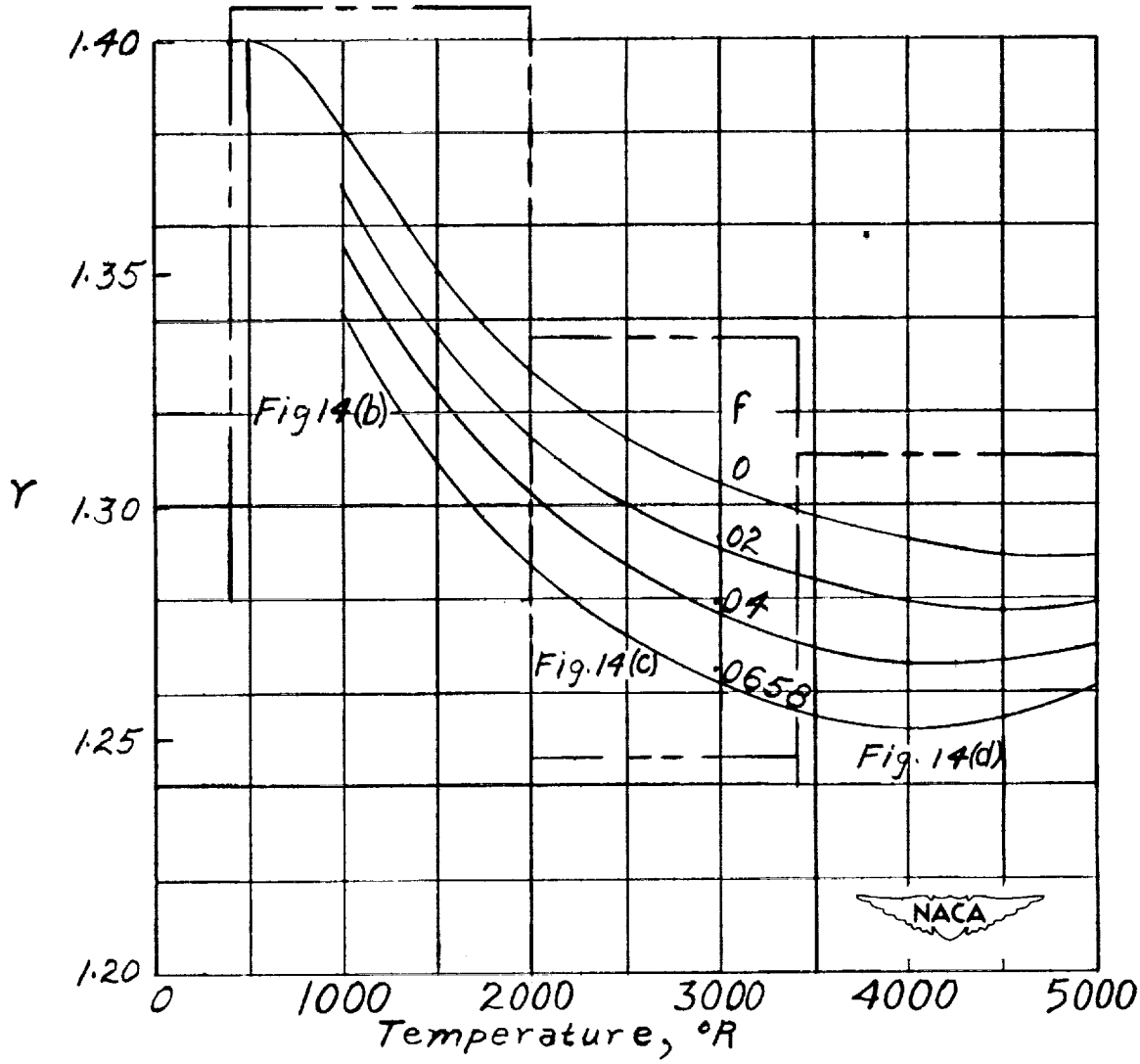

(a) Master plot.

Figure 14.- Relation of the specific-heat ratio γ to temperature for products of combustion of n-octane and air for range of fuel-air ratio from 0 to 0.0658 (stoichiometric).

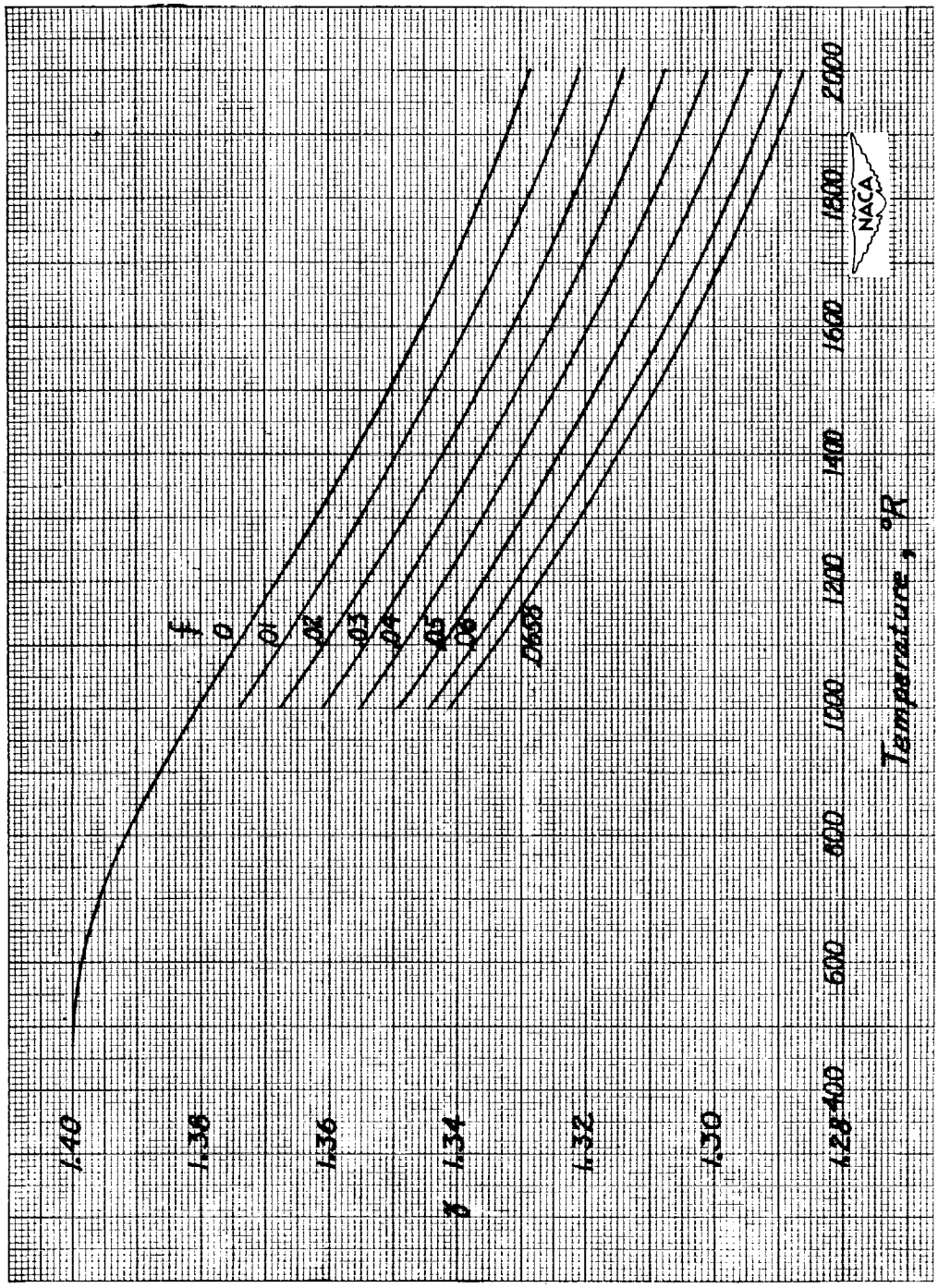

(b) Temperature = 400° to 2000° R.

Figure 14.- Continued.

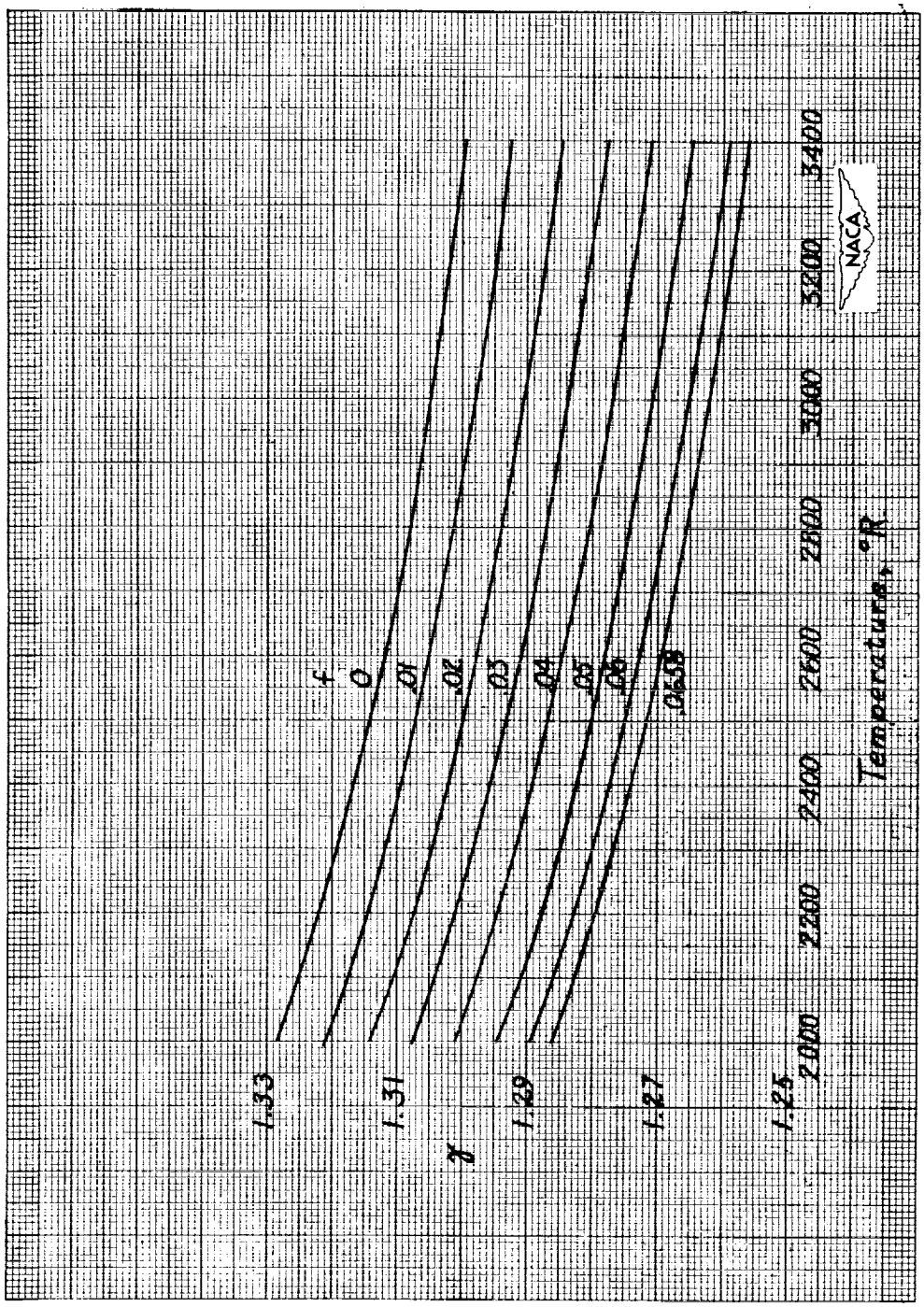

(c) Temperature = 2000° to 3400° R.

Figure 14.- Continued.

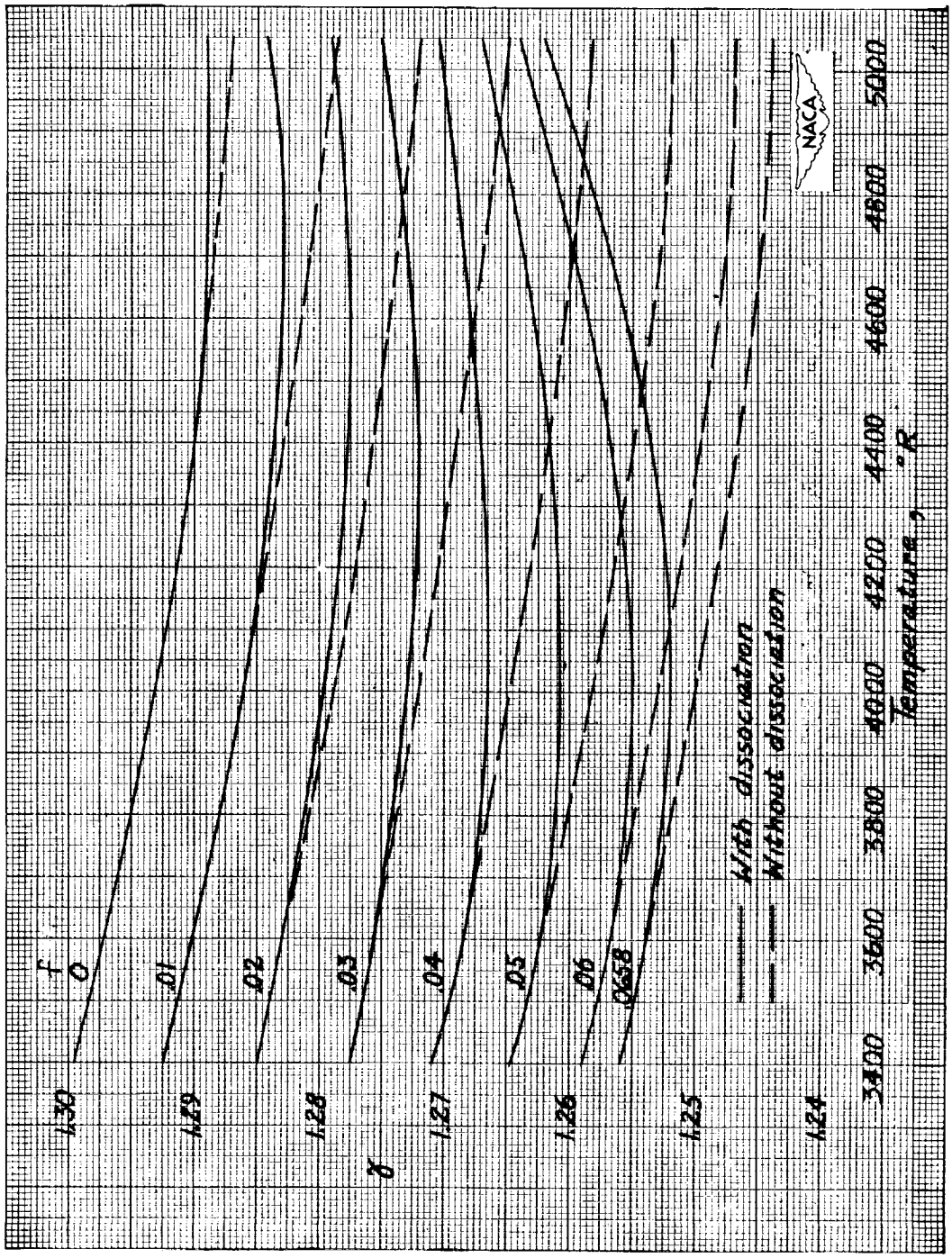

(d) Temperature = 3400° to 5000° R.

Figure 14.- Concluded.

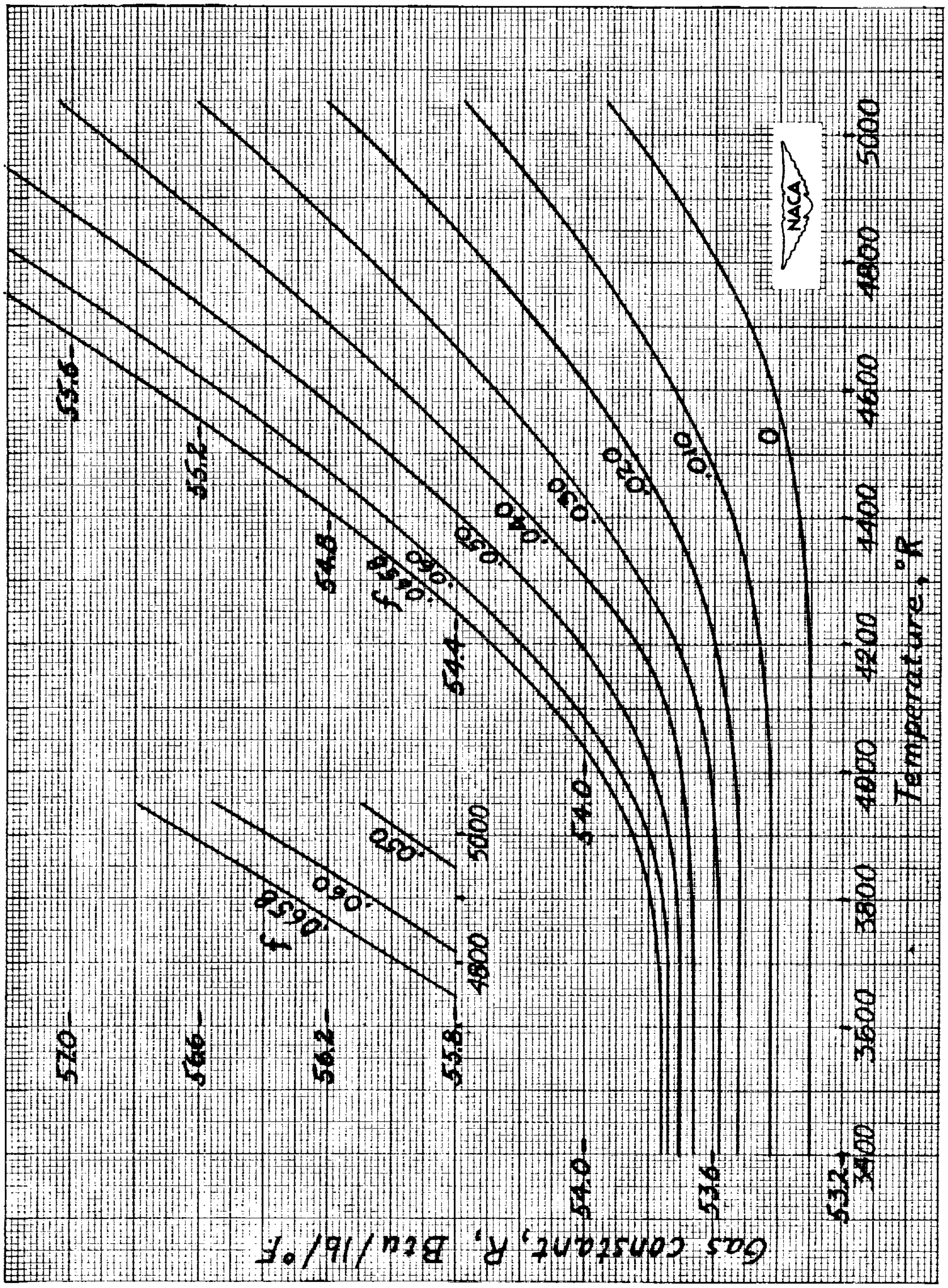

Figure 15.- Relation of gas constant R to temperature and fuel-air ratio for products of combustion of n-octane and air.

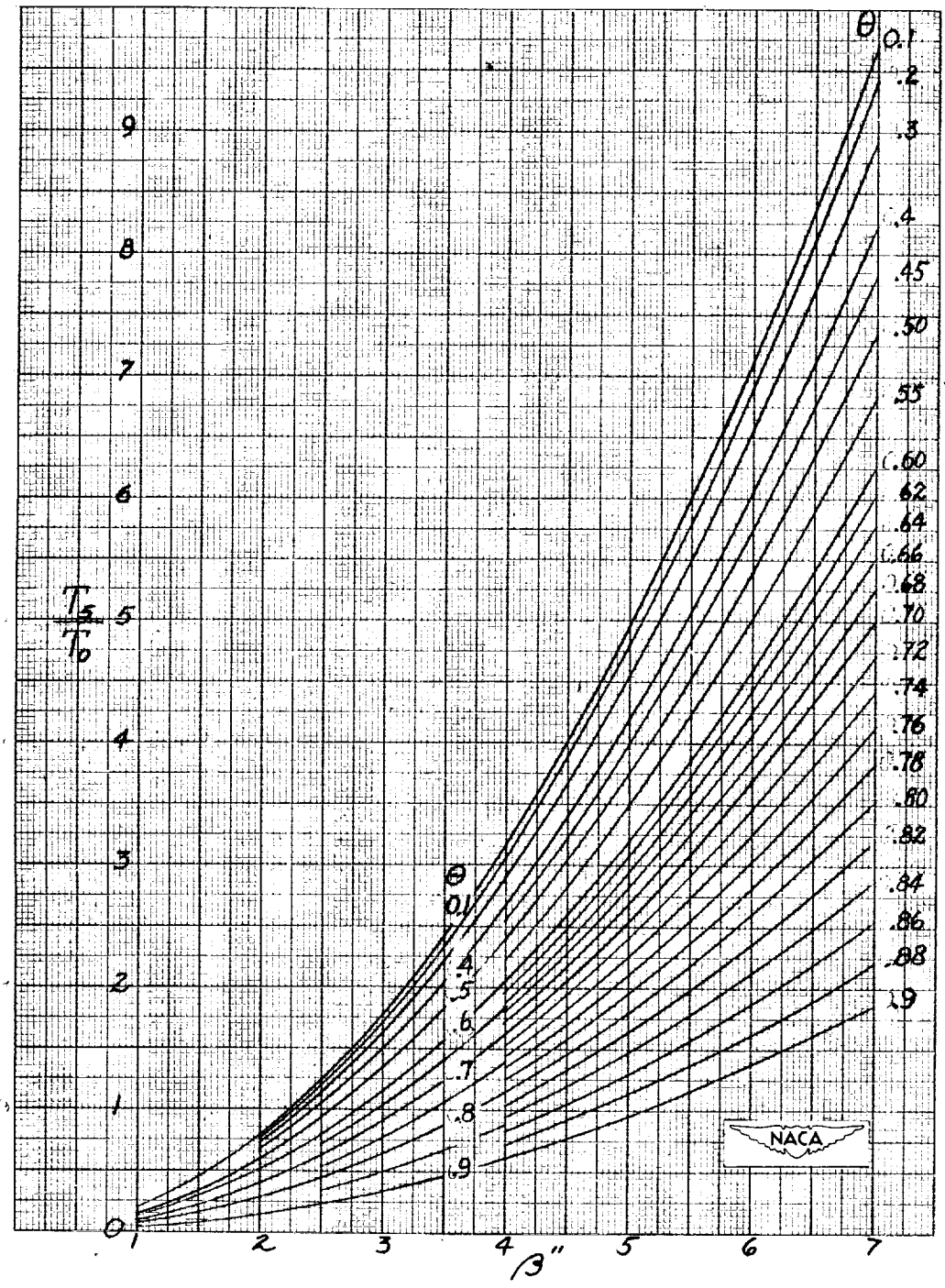

(a) β" = 1.0 to 7.0.

Figure 16.- Relation of nozzle static temperature to heat-addition parameter β" and pressure-loss parameter θ.

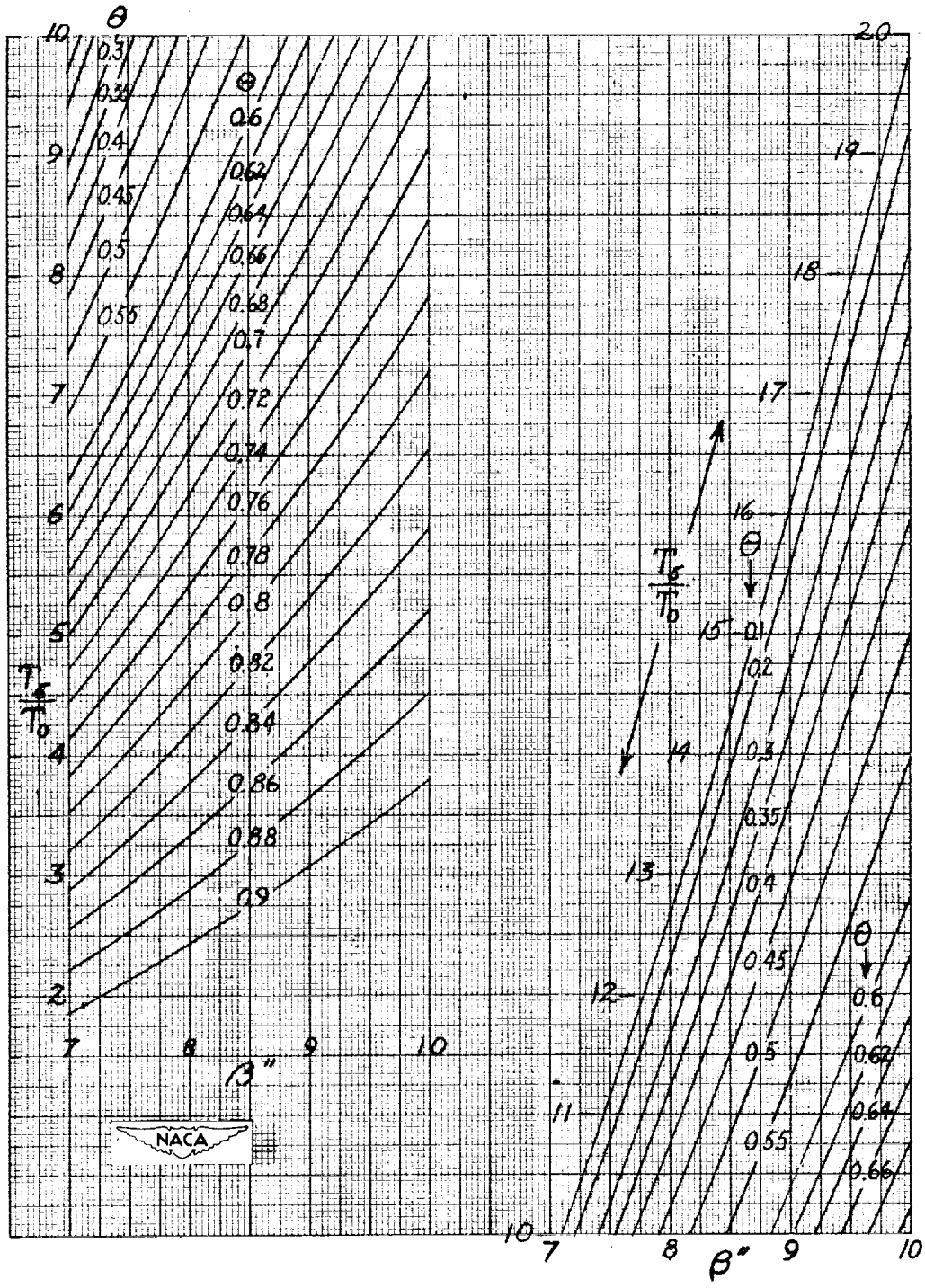

(b) β'' = 7.0 to 10.0.

Figure 16.- Concluded.

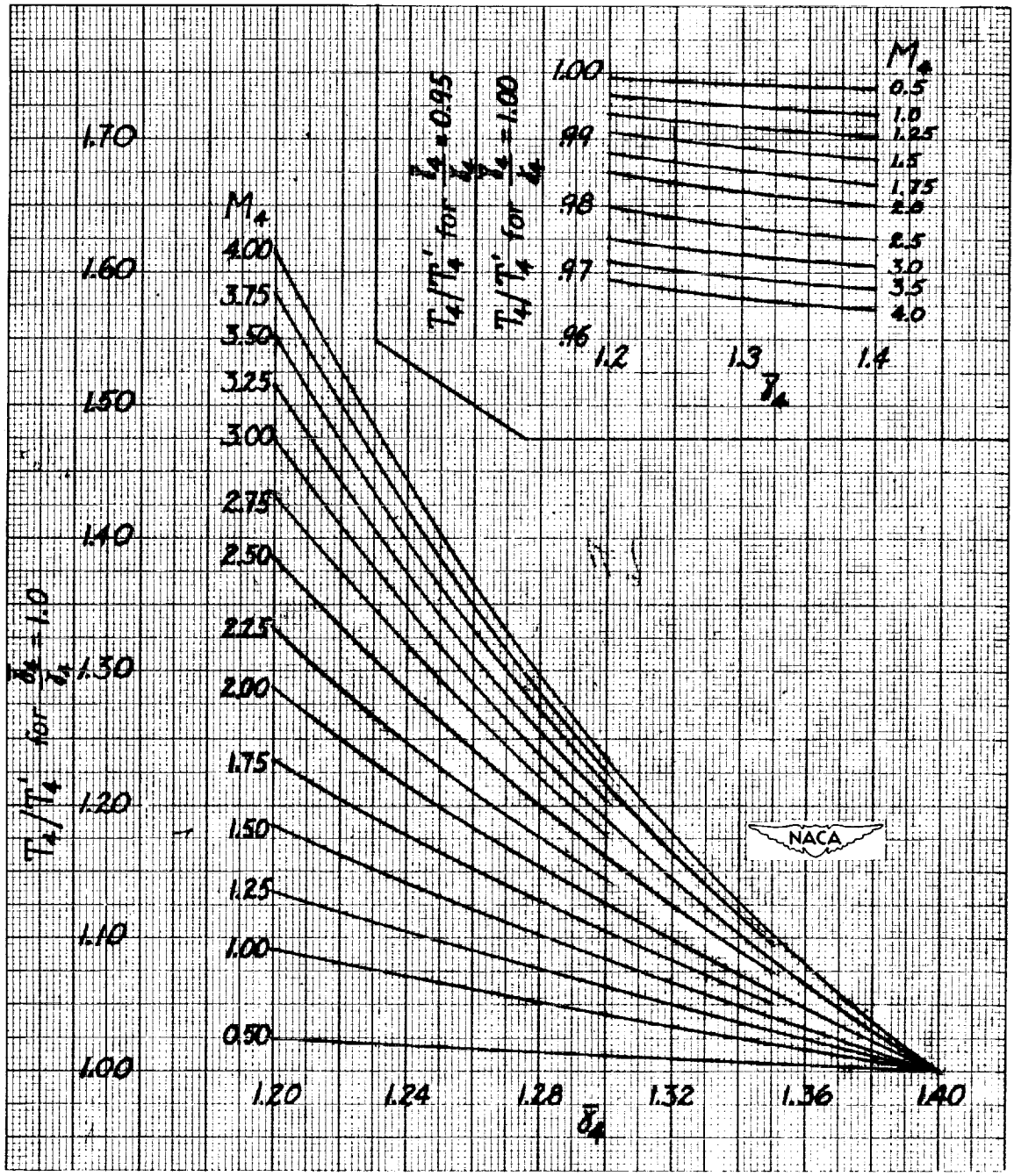

Figure 17.- Correction factors for determining nozzle-exit static temperature for method II.